Optimal Location of New Industries in Existing Industrial Areas Accounting for Environmental and Health Risks

by

Ali Bseibsu

A thesis

presented to the University of Waterloo

in fulfilment of the

thesis requirement for the degree of

Master of Applied Science

in

Chemical Engineering

Waterloo, Ontario, Canada, 2016

AUTHOR'S DECLARATION

I hereby declare that I am the sole author of this thesis. This is a true copy of the thesis, including any required final revisions, as accepted by my examiners.

I understand that my thesis may be made electronically available to the public.

Abstract

Nowadays, a major problem throughout the world is air pollution caused mainly by the fast growth in industry. This growth leads to negative impacts on human health and ecosystems directly or indirectly by chemical reactions in the atmosphere. The gas emissions from industrial plants are a current problem especially on ecosystems close to these sources. These emissions from large industrial complexes have been an increasing concern around the world. Due to the rapid growth of urban areas and the increase in the standard of living, environmental problems in urban areas become particularly critical. Selecting the location of industrial areas has been the traditional way for a community to lower the impact of industrial nuisance such as noise, smoke, odor, dust, dirt, and noxious gases. This growth concern accentuates the need for additional studies of air dispersions and modeling.

The main objective of this thesis is to assess the potential impacts associated with the emissions of toxic air contaminants from new industrial plants in order to select the best location based on human health risk assessment.

Air dispersion models have been widely used to study the patterns of dispersion and air emissions behavior as well as to simulate the dispersion and transport of pollutants. In this work, AERMOD model, which is recommended by the U.S. EPA, has been used to estimate the gas emissions of all significant sources in an industrial complex (taken as a case study), as well as the pollutant concentrations and distributions in the industrial complex area.

In addition, in order to quantitatively assess potential changes in health impacts due to the gas emissions, IRAP View model, which is based on the Human Health Risk Assessment Protocol (HHRAP) for hazardous waste combustion facilities published by the U.S. Environmental Protection Agency (EPA), has been used to estimate the transport and fate of mercury from all proposed industrial plants in the area of concern.

A case study that deals with locating a new industry in an existing complex was considered. Both environmental and health risks are considered in order to determine the best location for a new proposed plant. It is shown that considering both environmental impact as well as health risks leads to different best locations as compared to environmental impact alone.

Acknowledgements

First and foremost, all praise and thanks are due to Almighty Allah for providing me with the strength and patience to accomplish this work.

I am profoundly indebted to my supervisor, Professor Ali Elkamel. There are no words that can express my sincere gratitude to him. I consider myself extremely lucky to have a supervisor who cared so much not only about my work, but also about my personal life. He provided significant help in getting admitted to the University of Waterloo, and provided me with considerable guidance to identify my research topic.

I am grateful to Professor Jesse Thé, who is President of Lakes Environmental Inc. for his continuous guidance, patience and expert advice during the period of my study. He advised me and helped me in various aspects of my research. I am also thankful to Lakes Environmental Inc., Waterloo, Canada for providing a copy of the AERMOD and IRAP-h View software.

I would also like to extend a special acknowledgments to my reviewers and examiners, Professor Ting Tsui and Professor Chandra Mouli R. Madhuranthakam for their time to review this work and the useful suggestions and comments they provided. Also, I would like to thank the University of Waterloo and the department of chemical engineering for providing me the facilities to conduct this research.

I owe my deepest gratitude to my family: my parents, my brothers, and my sisters for their support and encouragement, and unconditional love. I owe a great deal of gratitude to my wife for her continuous understanding, unlimited encouragement, and unending love during the years of my study.

I am a very grateful to all my genuine helpful friends who gave support and encouragement throughout my study and for being great source of motivation and encouragement in many respects during the project and during my day to day life.

I would like also to acknowledge the Libyan Ministry of Higher Education for sponsoring me through this research work.

Ali Bseibsu

April 15th, 2016

Dedication

To my beloved family

Table of Contents

List of Tables

List of Figures

Chapter 1 : Introduction

1.1 General Background

The world has found itself in the clutches of various types of pollution. One of the most dangerous being air pollution. The pure air is a fundamental necessity for the survival of humans, animals, plants, and the earth itself. On the other hand, pollution can be defined as the presence or introduction into the environment of a substance that has harmful or poisonous effects on the environment and even humans and animals. These substances include gases (SO_x, NO_x, CO, HC_s, etc.), particulate matter (smoke, dust, fumes, and aerosols), radioactive materials, and many others. Pollution can ruin the ozone layer, it can prevent plants from growing and even kill animals [1].

Air pollution from industrial sources can be considered as a continuing concern in the recent years, especially on ecosystems close to these sources. Therefore, it is great significance to control and observe all these dangerous emissions.

Industrial activities, including power generation, produce a sizable share of the total flow of air pollution. This thesis sets a particular emphasis on industrial air pollution and the means of abating it. In order to decrease the industrial air pollution, there are three principle methods: 1. Limitations on production, 2. Technological controls of pollution emissions, and (3) land-use controls. Limiting production generally goes against society's goals of economic growth and development; it is not, therefore, recommended as a pollution abatement technique, except perhaps in some unique circumstances. Technology, on the other hand, can be an effective pollution control technique. The third way of regulating air pollution does not affect the levels of pollution emissions, but it does reduce their impacts on receptors by taking advantages of the meteorological characteristics [2].

Air pollution factors were accounted for, if at all, by attempting to locate industries downwind from residential areas. However, as the number of pollution sources grew larger and the air pollution problem grew more severe, it became evident to urban planners that zoning and locational decisions could no longer be made piecemeal and that the overall spatial and temporal arrangement of the urban activities should be considered while designing air quality management policies.

Controlling the location of industrial areas has been the traditional way for a community to diminish the impact of industrial nuisances such as a noise, smoke, odor, dust, dirt, and noxious gases. However, the growing rate of urban and industrial development in recent decades has generated externalities that are difficult to control through zoning alone [3].

The selection of optimal location of a new industrial plant is a complicated problem and a very important decision. In order to identify and find a sufficient solution for this problem, the potential business sustainability such as energy and material supplies, product distribution, labor cost, land availability and community safety and concerns should be taken into account. Before the final decision is made to select the optimal location of a new chemical plant, the air quality standards will be satisfied [3].

The impacts of emission sources to the surrounding area should be evaluated by conducting the health risk assessment before the final decision should be made in order to select the location of new industrial plants. This process should include the pollutant transport in the air, groundwater and surface water. Dispersion modelling is most often use is a part of air company process when a company plan to construct or modify an industrial facility and it is also useful for emergency planning and capital planning.

1.2 Research Objectives

The overall aim of this thesis was to assess the potential impacts associated with the emissions of toxic air contaminants from a new industrial plant in order to select the best location based on human health risk assessment. This required us to first estimate the gas emissions of all significant sources in an industrial complex (taken as a case study), as well as the pollutant concentrations and distributions in the industrial complex area by using AERMOD model. After that, in order to quantitatively assess potential changes in health impacts due to the gas emissions, IRAP-h View model was conducted to predict the maximum health impacts and deposition rates in the area of concern. The main novelty of this work compared to the literature is the taking of health risks into consideration.

1.3 Thesis Outline

The thesis consists of five chapters that are organized as follows:

- Chapter 2 presents a comprehensive literature review on air pollution problem, air quality dispersion models, air quality regulations, industrial location factors, and health risk assessment.
- Chapter 3 describes the air modeling methodology used to achieve the first contribution of this thesis. It also presents and discusses the effects of human exposure from emissions to air from the proposed locations.
- Chapter 4 discusses and analyzes the health risk results estimated from IRAP model, based on the air dispersion modeling estimation of air concentrations and depositions by AERMOD model for the worst-case scenarios emissions generated from all proposed plants.

- Chapter 5 draws some conclusions of this thesis and proposes recommendations for future work.

Chapter 2 : Background Information and Literature Review

2.1 Air Pollution Background

Air pollution maybe defined as the presence of materials into the environment of a substance that has harmful or poisonous effects on the environment and even human and animals [4]. Pollutants are the materials or factors, which cause an adverse effect on the natural quality of any component of the environment. There are five main pollutants: carbon monoxide (CO), hydrocarbons, particulate, sulfur oxides (SO_x), and nitrogen oxides (NO_x) [5].

Industrial activities can be considered as a major cause of air pollution. It produces a high level of chemicals which over time, lead to the formation of holes in the ozone layer. This holes let the ultraviolet rays of the sun reach the earth and thus cause various health problems for habitat.

The pollutant gases, such as nitrogen dioxide, sulfur dioxide and ozone, have impacts on health. In addition, air pollution can affect organisms as well as the environment. The greatest influences occur close to sources of pollution where pollutant concentrations are the highest.
Figure 2.1 summarizes the context of air dispersion models. A problem of air pollution is the result of a chain of different events not the result of isolated events. It results from the formation of air pollutants in a process to the emission, the chemical transformation, and dispersion in the atmosphere, the uptake by a receptor and health effects. In order to have a good understanding of an air pollution problem, a knowledge of all steps in the process is required [1].

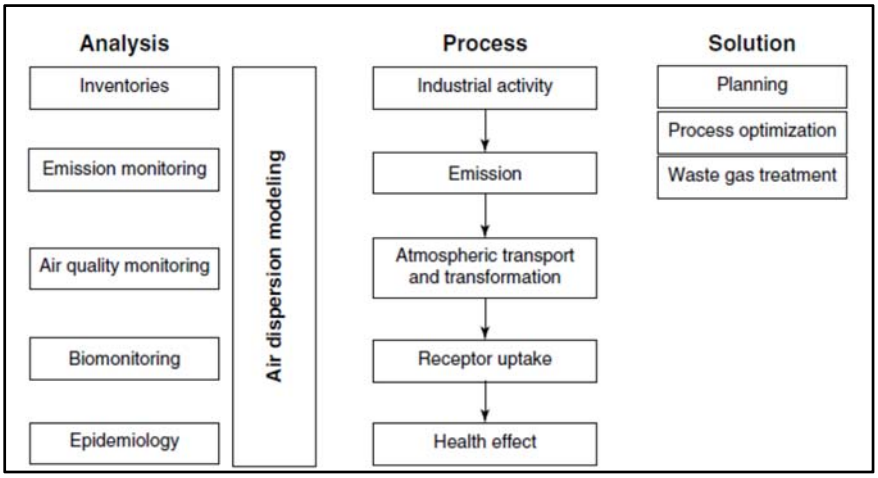

Figure 2.1: The air dispersion modeling context [1].

Figure 2.2 describes the events chain causing air pollution problems and the main factors governing these events. By looking into this figure, it is noted that air pollution is influenced by several factors. These factors include the weather (temperature, wind direction, wind speed, sunshine, rainfall), the terrain (hill, buildings, surface water), the source (stack gas velocity and temperature, stack diameter and height, air pollutant concentration), and the physical and chemical properties of the air pollutant (solubility, reactivity). In air dispersion models, all the above information is needed to be included as input data [1].

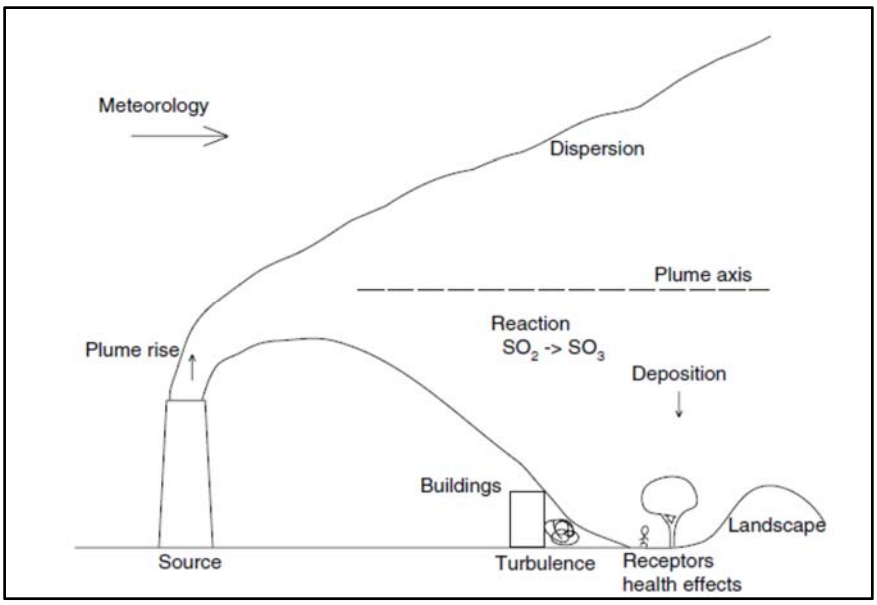

Figure 2.2: Air pollution problem events [1].

2.2 Air Quality Dispersion Model

Some models, called atmospheric dispersion, are used by governmental bureaus in order to investigate the air pollutants emitted from industrial facilities such as petroleum refineries and petrochemical industries. The air quality dispersion models are also used to study the air pollution influences on human health. These models can be used to regulate ambient air quality by predicting and estimating concentrations of pollutants emitted from the industrial plants [5]. In addition, the air dispersion models are used to check and analyze the possibility of new plant establishment taking into account if these new plants are compatible with air quality regulations.

The air dispersion modeling is an effective technique to analyze the emissions impacts from complex industrial sources. It can be considered as the attempt to estimate or simulate, by numerical or physical methods, the ambient concentration of pollutants found within the atmosphere of a domain [1]. The dispersion models are used to predict the contaminant concentrations downwind of various pollution sources. The principle application of air dispersion

modeling is to review air quality scenarios so that the associated environmental impact on the area of study can be quantified and predicted [5]. The main goal of air quality models is to accurately calculate the concentration of pollutants that are downwind of different sources for a wide range of meteorological conditions [1]. They have been widely used to study the behavior of dispersion patterns of air emissions in such areas [6], and also to predict the potential impacts on human health and the environment [7],[8].

Air dispersion modeling involves a computer simulation that predicts the concentration of air pollutants from various emission sources. The United States Environmental Protection Agency (EPA) has developed guidelines on air dispersion models and procedures for model evaluation. Air dispersion modeling incorporates the effects of chemical and physical processes through a set of numerical techniques and mathematical equations which characterize the behavior of pollutants released into the environment [1].

There are many advantages for using the air dispersion models such as:

- Managing existing emission rates
- Planning new facilities
- Calculating the optimal stack height
- Measuring the risk and preparing for emergency situations
- Comparing and evaluating the influences air quality, standards, criteria and guidelines with existing emission rate

The majority of air dispersion models are performed with computer programs. The models follow specific procedures to calculate the pollutants concentrations:

- Topographical data

- Meteorological data
- Characteristics of pollutants source
  - Dimensions of stack (height and diameter)
  - Buildings around stack
- Specifications of emissions
  - Emissions rate
  - Plume temperature
  - Pollutants specifications

This information can be used by atmospheric dispersion models as shown in Figure 2.3.

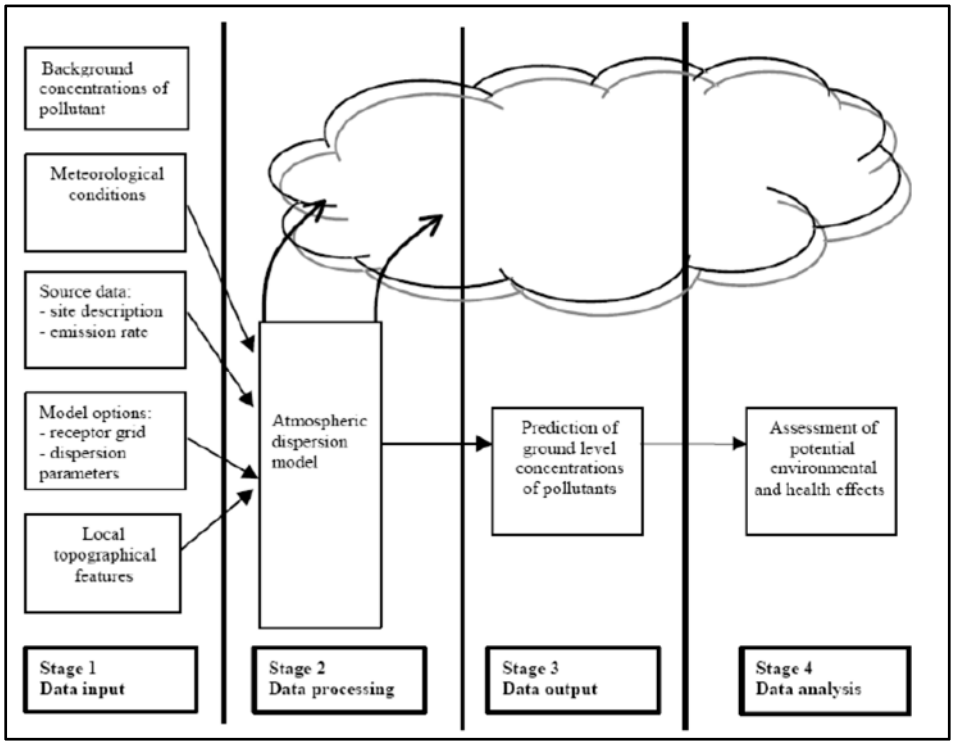

Figure 2.3: Schematic view of air quality model [9].

The air dispersion models are studied and the results indicate that when a model is selected based on the needs and available resources, reliable results can be obtained [1].

Some significant principles that should be followed are stated by [9] in order to decide the best method to model air dispersion:

- The location of modeling domain
- The distance between the emission source and urban area
- Meteorology for the study area

2.2.1 Models Used in Air Dispersion Modeling

Air dispersion models have two main categories: Steady state (Gaussian plume) and non-steady state (advanced) air dispersion models. The suitable method that may use to model air dispersion can be chosen based on many factors. A comprehensive understanding and the accuracy of the needed results are required in order to choose the appropriate model between Gaussian plume models and advanced air quality modeling.

The Gaussian plume model and advanced air dispersion will be presented in following sections.

2.2.1.1 Steady-State Models

Steady-state models are usually called the Gaussian plume models. The Gaussian diffusion model is often referred to as dispersion model. In the early 1920s, the Gaussian diffusion model was developed, and the foundations of statistical theories of diffusion and gradient transport were laid.

The Gaussian plume model can be considered as the most common air pollution model used for solving air pollution problems. It is very old and based on a simple formula that estimates the air pollutant concentrations in the ambient atmosphere at the local scale. The Gaussian plume

models can implement acceptable results if it used in proper conditions. However, there are many limitations in applying these models and are inaccurate sometimes. The Gaussian plume model is the mathematical formulation to show the dispersion of pollutants in the atmosphere from various sources. The computational programs, which simulate the dispersion of pollutant were used to solve the mathematical equations. In addition, the Gaussian plume model can be designed as a standard approach for studying the transport of airborne contaminants because of turbulent diffusion and advection by the wind [10]. The Gaussian plume model deals with particulate pollutants (very light particles) and it does not work for large particle sizes [10]. In addition, the Gaussian plume model can be applied to study the emissions that large industrial operations produce [11].

There are many requirements to apply the Gaussian plume model such as atmospheric turbulence, wind speed, emission release rate, dispersion coefficient, mixing height, effective stack height etc.

The concentration within the plume C(x, y, z) is given by the Gaussian distribution [12]:

$$C(x,y,z) = \frac{Q}{2\pi\sigma_y\sigma_z\bar{u}} exp\left(-\frac{(y-y_s)^2}{2\sigma_y^2}\right) \times \left[exp\left(-\frac{\left(z-z_p\right)^2}{2\sigma_z^2}\right) + exp\left(-\frac{\left(z+z_p\right)^2}{2\sigma_z^2}\right)\right] \quad 2.1$$

Where;

Q = pollutant emission rate (gr/sec).

$\bar{u}$ = wind speed (m/sec).

σ_y = standard deviation, horizontal direction (m).

σ_z = standard deviation, vertical direction (m).

x = downwind distance x (m).

y = cross wind distance y (m).

z = receptor height z (m).

Above equations were originated from the Gaussian Dispersion Model and generated by the mathematical methods of Eulerian and Lagrangian models [12].

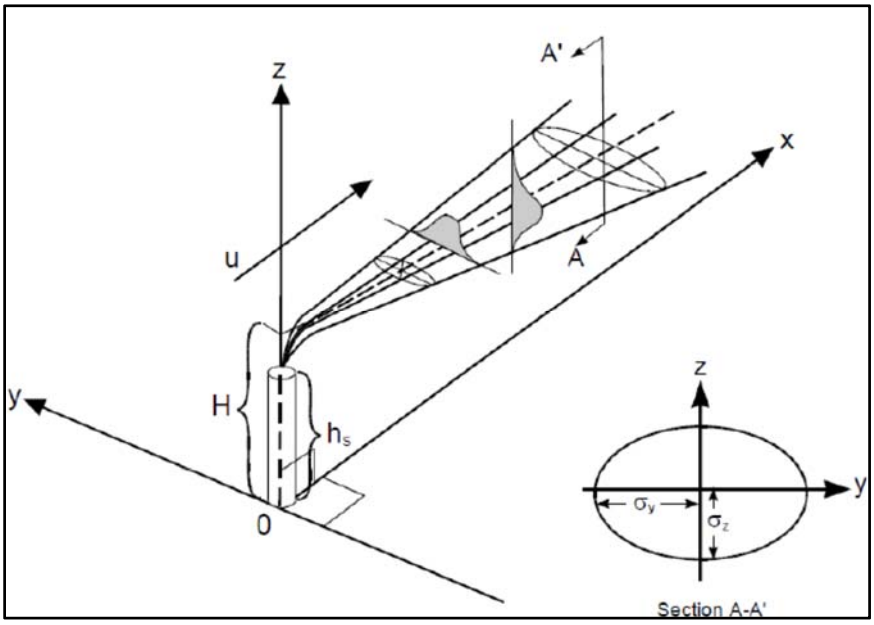

Figure 2.4: Classic Gaussian Plume Model (Adapted from Turner [13]).

The recent dispersion models are using the basic atmosphere characteristics instead of depending on general mathematical calculations in order to better describe the dispersion and dissemination [14]. By using air dispersion models, the possible environmental and health effects due to releases from industrial plants can be estimated [15].

Odor dispersion is affected by many factors that include: 1) meteorological conditions; 2) geography; 3) source of odor release; 4) the position of the receptors to the source including distance and direction; and 5) the odor sensibility and the acceptance of the receptors [15],[16]. However, the weather conditions including, wind direction, wind speed, the topography of the area, atmospheric stability classes and temperature are the dominant factors for air dispersion.

There are different steady-state models that are commercially accessible for air dispersion modelings such as ISCST3, AUSPLUME, and AERMOD.

- **AERMOD Model**

The American Meteorology Society-Environmental Protection Agency developed the AERMOD model, which is applied in this study. It is a software package based on the Gaussian plume equation. The U.S. EPA recommends this model for air quality simulations.

The AERMOD model is a system with three separate components that are showed in Figure 2.5: AERMOD (AERMIC Dispersion Model), AERMAP (AERMOD Terrain Preprocessor) and AERMET (AERMOD Meteorological Preprocessor). AERMOD input data is prepared from output files from AERMET and AERMAP preprocessors [17].

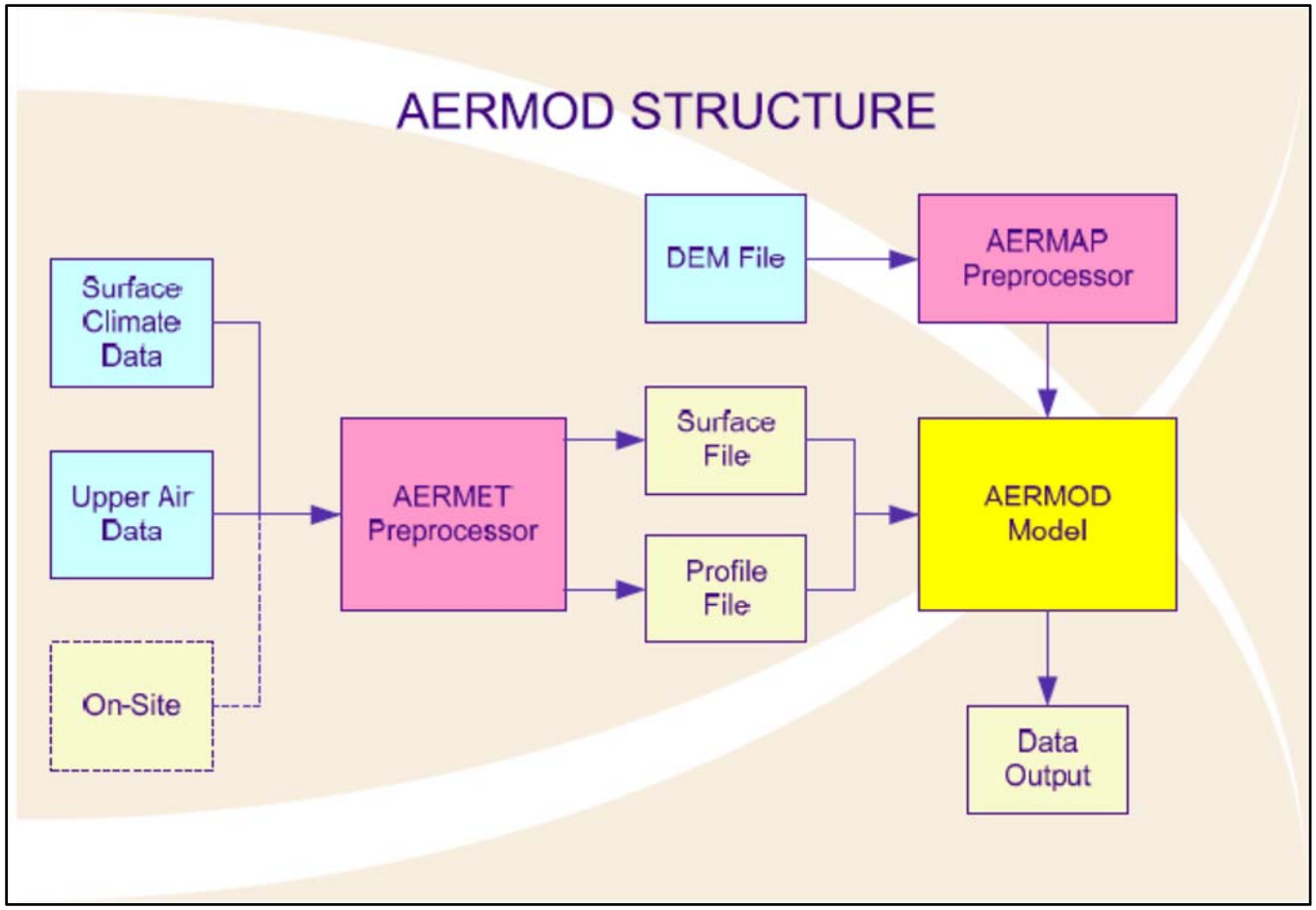

Figure 2.5: Systematic dataflow structure of EPA's AERMOD Model [18].

2.2.1.2 Non-Steady-State Models

Non-steady-state dispersion models are usually called advanced models (unsteady-state models). Puff models can handle the two drawbacks of plume models [19]. In addition, non-steady-state air quality models provide more realistic, accurate, dependable results which can be considered better than Gaussian plume models. Advanced dispersion models are computational and mathematical methods for describing atmospheric dispersion. The results that are obtained from these models are computationally more expensive but more reliable. Many numerical calculations are performed by advanced dispersion models by using high-performance computers. Advanced air dispersion models have main three calculations types; puff, particle, and grid point. It requires three-dimensional meteorological data which increases the complexity of the model and serves as the main difference between the advanced models and Gaussian plume models.

The following are some situations where the advanced dispersion models provide better results [9];

- The importance of chemical reaction between ambient air and pollutants.
- The availability of complete meteorological data.
- Gaussian models cannot be applied for the changing meteorological condition.
- The speed of wind is expected to decrease frequently in different periods.

2.3 Air Quality Regulations

Generally, each province, state or country has its own guidelines and standards, and they periodically change from time to time. As mentioned before, the main objective of this research was to investigate whether or not the proposed industrial plants violate air quality standards.

The Clean Air Act of 1963 was the first federal initiative in the U.S. to regulate the air quality. Air quality was mostly regulated at the municipal level before that time. The Environmental Protection Agency (EPA) is required by the Clean Air Act 1990 to set National Ambient Air Quality Standards (NAAQS) for air pollutants considered harmful to the environment and human health. There are two types of National Ambient Air Quality Standards (NAAQS) identified by the Clean Air Act, primary standards, and secondary standards. Primary standards provide public health protection and secondary standards provide public welfare protection. The Environmental Protection Agency (EPA) has set the National Ambient Air quality for six principle air pollutants. Table 2.1 shows the current National Ambient Air Quality Standards (NAAQS).

The Clean Air Act 1990 revisions also listed about 189 of the most hazardous air pollutants. The EPA has the authority to change this list from time to time. The air pollutants must be regulated in the case of emitting more than 10 tons/year of any of these air pollutants, or 25 tons/year of any combination of air pollutants.

Based on the local industry, conditions, and the like, each state in the U.S. has its own air quality standards. For example, Table 2.2 shows the air quality standards of Ohio State.

Table 2.1: Current National Ambient Air Quality Standards [20].

Pollutant		Primary/Secondary	Average Time	Level	Form
Carbon Monoxide (CO)		Primary	8 hours	9 ppm	Not to be exceeded more than once per year
			1 hour	35 ppm	
Lead (Pb)		Primary and Secondary	Rolling 3 month period	0.15 μ/m^3	Not to be exceeded
Nitrogen Dioxide (NO_2)		Primary	1-hour	100 ppb	98th percentile of 1-hour daily maximum concentrations, average over 3 years.
		Primary and Secondary	1 year	53 ppb	Annual Mean
Ozon (O_3)		Primary and secondary	8 hours	0.070 ppm	Annual fourth-highest daily maximum 8-hour concentration, averaged over 3 years
Particle Pollution (PM)	$PM_{2.5}$	Primary	1 year	12.0 μ/m^3	Annual mean, averaged over 3 years
		Secondary	1 year	15.0 μ/m^3	Annual mean, averaged over 3 years
		Primary and secondary	24 hours	35.0 μ/m^3	98th percentile, averaged over 3 years
	PM_{10}	Primary and secondary	24 hours	150.0 μ/m^3	Not to be exceeded more than once per year on average over 3 years
Sulfur Dioxide (SO_2)		Primary	1-hour	75 ppb	99th percentile of 1-hour daily maximum concentrations, averaged over 3 years
		Secondary	3 hours	0.5 ppm	Not to be exceeded more than once per year

Table 2.2: National Air Ambient Quality Standards of Ohio State [20].

Pollutants	Primary Standards		Secondary Standards
	Level	Average Time	
Carbon Dioxide (CO_2)	9 ppm (10 mg/m^3)	8 hour	None
	35 ppm (40 mg/m^3)	1 hour	None
Lead	0.15 µg/m^3	Rolling three-month average	Same
	1.5 µg/m^3	Quarterly average	Same
Nitrogen Dioxide (NO_2)	0.053 ppm (100 mg/m^3)	Annual (Arithmetic mean)	Same
	100 ppb	1-hour	None
Particulate matter (PM_{10})	150 µg/m^3	24-hour	Same
Particulate matter ($PM_{2.5}$)	12.0 µg/m^3	2012 annual (Arithmetic mean)	Same
	15.0 µg/m^3	1997 annual (Arithmetic mean)	Same
	35 µg/m^3	24-hour	Same
Ozone	0.075 ppm (2008 std)	8-hour	Same
	0.08 ppm (1997 std)	8-hour	Same
	0.12 ppm	1-hour	Same
Sulfur Dioxide	75 ppb	1-hour	None

2.4 Industrial Location Factors

Several factors can be considered as important factors influencing the new location for industries such as economic factors of location such as labor, markets, transportation, and excess of raw material. However, in recent years, several studies have found that the environmental regulations have had an important effect on plant location, especially within a populated area when these industries produce many hazardous gases and wastes.

Several studies have examined the influence of environmental regulations on new plant location decisions. These studies examined the relationship between plant location decisions and environmental regulations. Becker and Henderson used the data from American plants between the years 1963 and 1992 to examine the influence of air quality regulations on polluted plants decisions. They choose about 13 industries with high VOC emissions rates. They found that the later years the polluting industries reduced by 40 – 50% because of the air quality regulations which led to the less polluted areas. During their study, they noticed that the influences were clearer in the seventies in factories large first and then small-sized factories [21].

The influences of pollution regulation across the United States on new manufacturing plants have been studied by Gray [22]. This study used the plant-level data from the Census Bureau`s Longitudinal Research Database in order to classify the new plant births in every state between 1963 and 1987 and examine the manufacturing locations changes in that time. The results indicated that there are fewer new industrial plants in states that have stringent environmental regulations, greater abatement cost, and stronger political support for pollution regulation.

A new mixed-integer nonlinear programming model for the optimal allocation of new Industrial plants that affect the surrounding watersheds has been developed by Lira-Barragán et al. [23] . This model takes into account the minimization of the total annual cost and satisfying the

environmental regulation by wastewater stream treatment as well as decrease the pollution problems in final disposal. This study proposed a model to predict the watershed impacted behavior for the new polluting industries by using the material flow analysis technique. This study combined between the type of treatment selection and the optimal location for a new industrial plant model.

Fliege [24] developed a software package OLAF (Optimal Locating Air Polluting Facilities) for the effects of a low toxic air on the surrounding areas. This software package is able to solve several complex, highly realistic polluted industrial locations. In this study, this software package used an effective optimization process to decide the optimal location for the polluting plants in the region of central Europe, Benelux countries.

The new plant location problem takes into account the environmental restrictions as well as economic issues. Besides that, García-Chan et al. [25] focused on the optimal management of its emissions rate. The combination of the classical weighted sum method and ε-constraint algorithm was used to solve this problem as a multi-objective optimization problem.

Starfford [26] surveyed the most important factors that influence industrial plant location such as markets, labor, raw material availability, and environmental regulation. He collected answers from 162 new branch plants of large U.S. corporations. The results show that the environmental regulations did not consider the most important factors in plant location make decisions but considered it as a secondary importance. This study does not support the idea that the environmental regulations have a significant effect on new plant location decisions. However, if the regulatory costs increase, this evidence will change and he suggested doing more researches on that.

Guldmann and Shefer [27] tested the influences of economical restrictions when deciding on the optimal location of industrial plants as well as the optimal pollution abatement technologies, taking air quality standards into account. In their approach, they developed various optimization models by using the integer and mixed-integer linear programming framework. In this study, the real data of the Haifa region is used to apply the approach.

Murillo-Alvarado et al. [28] discussed the optimal location of new industrial plants taking into consideration the environmental restrictions and gaseous emissions integration by incorporating the networks of reuse and recycle. The new mathematical programming model for the optimal location of the new plant was presented. Three examples of case studies are presented in this study to show the applications of this mathematical model. The outcomes of this study showed the features of this mathematical model and its ability to control the gaseous emissions by classifying several options for it.

Kohn [29] tested the influences of different strategies of emission control for current sources on air quality by applying the connotation from theories of optimization and optimal control.

To avoid costly control measures, to improve public relations, and to prevent litigation, Taylor [30] recommends that site selection takes into account the nature of the air contaminants, the efficiency of available control devices, pertinent meteorological factors, and the potential effects on the surrounding areas.

Jeppesen et al. [31] studied the relationship between new industrial plant location decisions and environmental restrictions. They collected and tested data generated by 11 different studies

that provided more than 365 observations. The main result from their meta-analysis was that the body of received estimates can be affected by the methodological consideration.

Levinson [32] discusses and surveys many previous influences of environmental regulations an industrial locations. He concluded that there is little strong evidence that indicates a relationship between environmental regulations and industrial locations.

McConnell and Schwab [33] used the firm level data between 1973 and 1982 in order to test the location decision determinants for motor vehicles. They found that there are simple effects of the state regulation and environmental regulations on plant locations.

List [34] tested the relationship between the destination choice of relocating plants and air quality regulatory stringency by using an annual (1980 – 1990) county-level panel data set. He had reached the conclusion that more stringent pollution regulations effected siting decisions of relocating plants.

2.5 Health Risk Assessment from Air Toxics

Human activities are considered the main source of air pollution. It suspects to cause harmful impacts on the ecosystem and the environment. The human health impacts of hazardous air pollutants are significant. The study was done by the Puget Sound Area in Washington in 2003 focused on diesel particulate matter between 70% to 85% of the total cancer risk from toxic air from somewhere in that area. The 1990 Clean Air Act Amendments defined hazardous air pollutants as the main source of public health concern because of their relationship with many health outcomes. Animal and occupational studies have found that many of hazardous air pollutants cause, or are suspected to cause, cancer.

Health risk assessment is a scientific process that evaluates potential health impacts associated with the emissions of the toxic air contaminants at proposed industrial plants on the environment, in particular to living organisms and ecosystems. It has become an acceptable technique to identify potential impacts of existing and proposed plants on the surrounding area. Some of the pollutants are largely natural. For example, earthquakes or volcanic eruptions, whilst others may be the result of human activity such as industrialization and urbanization. These pollutants are, therefore, harmful to humans and fish.

Chemical risk can be caused by direct emissions to air, water bodies, soil, or to the atmosphere. There are two types of air risks: short term and long term risks. Short term risks can be caused by accidental releases, explosions, and fire. Long term risks could be in terms of many years of low concentrations, low deposition rates on surfaces, water bodies, and soil. There are three types of long-term risks: Nuisance, cancer risks, and non-cancer risks. Figure 2.6 shows types of air risks.

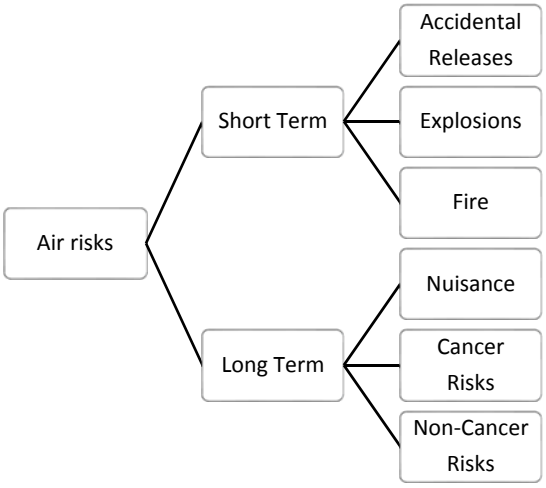

Figure 2.6: Air Risks Types.

The estimate of health risk is dependent upon many factors including the amount of contaminant introduced into the atmosphere, the toxicity of the contaminant, the distance between the emission source and the exposed individuals, weather conditions, and exposure pathways (routes the contaminant can enter the body, such as, inhalation or ingestion).

In July 1998, U.S. EPA Office of Solid Waste and Emergency Response (OSWER) published the Human Health Risk Assessment Protocol (HHRAP). The consolidated information and national guidance previously prepared by the U.S. EPA in other methodology documents and risk assessment are provided by the Human Health Risk Assessment Protocol (HHRAP). The HHRAP was reviewed and found to be based on the same fundamental risk calculations, exposure factors, and exposure pathways and provide the basis for this human risk assessment.

The HHRAP identifies seven recommended exposure scenarios that should be considered for inclusion in the HRA. The seven scenarios are (1) subsistence farmer, (2) subsistence child, (3) adult resident, (4) child resident, (5) subsistence fisher, (6) subsistence fisher child, and (7) acute risk [35].

Exposure assessment incorporates the results of dispersion and deposition modeling with health effects known to be associated with COPCs and potential exposure pathways to produce an estimated health risk.

Table 2.3 shows colored bars that indicate the pollution level and associated health concern. The greater the level of air pollution, the higher the value and the greater the health concern.

Table 2.3: The level of pollution and associated health concern *[36]*.

Air quality index levels of health concern	Numerical Value	Meaning
Good	0 to 50	Air quality is considered satisfactory and air pollution poses little or no risk
Moderate	51 to 100	Air quality is acceptable; however, for some pollutants, there may be a moderate health concern for a very small number of people who are unusually sensitive to air pollution.
Unhealthy for Sensitive Groups	101 to 150	Members of Sensitive groups may experience health effects. The general public is not likely to be affected.
Unhealthy	151 to 200	Everyone may begin to experience health effects. Members of sensitive groups may experience more serious health effects.
Very Unhealthy	201 to 300	Health warnings of emergency conditions. The entire population is more likely to be affected.
Hazardous	301 to 500	Health alert: everyone may experience more serious health effects.

The first Environmental Assessment framework established in governmental legislation worldwide is the 1969 US National Environmental Policy Act (NEPA 1969). NEPA 1969 was developed in response to the controversy surrounding the adverse effects on human health and

natural environment that were occurring as a result of the unregulated emissions of industrial developments that were increased in the period of rapid industrial growth that had followed World War I ([37]; [38]; [39]). The main purposes of 1969 US National Environmental Policy Act (NEPA 1969) were to ensure the reduction of development projects with unacceptable outcomes by interventions at the planning stage.

The U.S. Environmental Protection Agency (EPA) has estimated that the air pollutant concentrations accounted for more than 2500 new cases of cancer annually because of the exposure to pollutant concentrations of 45 of the 188 toxic air pollutants. Burnett et al. [40] found that the mortality increased because of short-term exposure to gaseous pollutants, carbon dioxide, nitrogen dioxide, ozone, sulfur dioxide, and mercury.

Pratt et al. [41] estimated human health risks from air pollution by using three modeling systems: two versions of Minnesota Risk Screening (MNriskS) and the USEPA National Air Toxics Assessment (NATA). In their study, the modeling systems estimated lower air pollutant concentrations than measurements. This led modeled risks to be lower for given pollutants. Although predictions were lower than measurements, and results varied among pollutants, this study showed reasonable agreement between model predictions and available measurements. The results showed that the confidence in describing pathways, pollutants, sources, receptors, and geographic areas of potential concern were increased. This helps to provide a basis for focusing all efforts on specific air pollutants, sources, and geographic areas and informing air pollution reduction strategies.

The US EPA and the World Health Organization have published the unit risk factors for each carcinogen of interest, the upper-bound probability of cancer with continuous exposure to an inhaled of $1\mu g/m^3$ over 70 years. In addition, the Toronto Public Health Unit mentioned that more

than 1,000 precocious death and about 5,500 hospitalizations in Toronto as a result of air pollution [42].

Several models have been used to evaluate potential impacts on the environment and human health from potential emissions such as Industrial Risk Industrial Program-Human Health (IRAP-h) View software package.

IRAP-h View software is used to compare acceptable risk levels to exposure information, either measured or calculated, and to predict a potential risk with safety factors. Typically, reference concentrations and acceptable risk levels can be obtained by regulatory agencies based on scientific evidence available at the time. It typically contains four main components: receptor identification; hazard identification; exposure assessment; and risk characterization.

Chapter 3 Material and Methods

3.1 Case Study

To meet the objective of this thesis, two industrial complexes were selected. One of industrial complex is existing plant and other is proposed plant. The area of study is located in Toledo City in the United States of America (USA). The proposed location for new industrial plant decided to be in the area surrounding the existing plant. This proposed area is primarily agricultural and rural. In this study, the emission database given by Masuraha [43] were used as a hypothetical case study.

In this study, four locations are proposed in order to select the optimal location for the new industrial plant. These four proposed industrial plant locations are listed in Figure 3.1 and Table 3.1. Emissions from each of the proposed industrial plant were simulated separately and evaluated separately for health risk. The detailed information for the existing and proposed locations was obtained from the references [18] and [43] respectively.

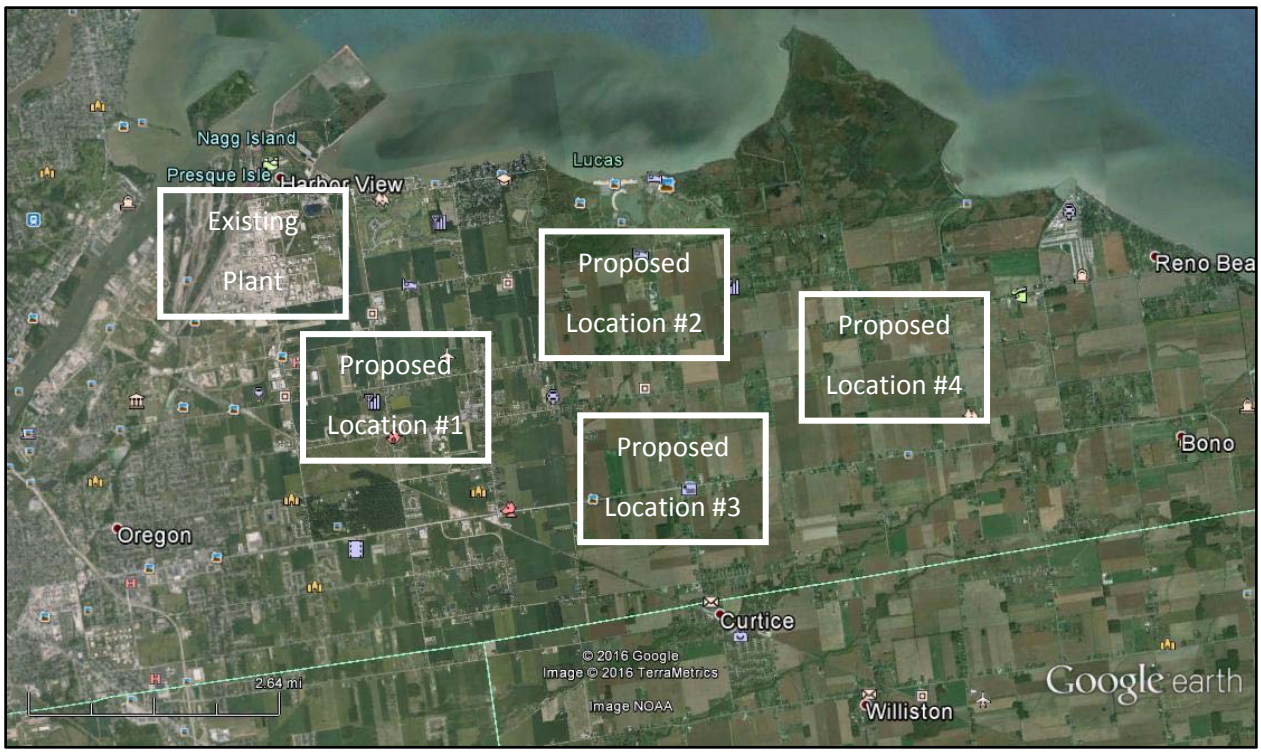

Figure 3.1: The layout of existing and proposed plant locations.

Table 3.1: Location information for proposed industrial plant locations for the year 1990, 1991 and 1992.

ID No.	Proposed Location #1		Proposed Location #2		Proposed Location #3		Proposed Location #4	
	Easting (km)	Northing (km)	Easting (km)	Northing (km)	Easting (km)	Northing (km)	Easting (km)	Northing (km)
1	297.283	4615.649	301.2429	4615.851	301.3412	4613.324	306.133	4614.542
2	297.3569	4615.173	301.3167	4615.376	301.415	4612.848	306.2068	4614.067
3	297.4094	4615.169	301.3693	4615.371	301.4676	4612.844	306.2594	4614.062
4	297.5197	4615.415	301.4796	4615.617	301.5779	4613.09	306.3697	4614.308
5	297.7606	4615.649	301.7205	4615.852	301.8188	4613.324	306.6106	4614.543
6	297.7667	4615.442	301.7266	4615.645	301.8249	4613.118	306.6167	4614.336
7	297.6722	4615.378	301.632	4615.58	301.7303	4613.053	306.5221	4614.271
8	297.6939	4615.369	301.6538	4615.572	301.7521	4613.044	306.5439	4614.263
9	297.6939	4615.369	301.6538	4615.572	301.7521	4613.044	306.5439	4614.263
10	298.5492	4614.643	302.5091	4614.846	302.6074	4612.318	307.3992	4613.537
11	298.458	4614.646	302.4178	4614.848	302.5161	4612.321	307.3079	4613.539
12	298.4573	4614.523	302.4172	4614.726	302.5155	4612.198	307.3073	4613.417
13	298.6326	4615.195	302.5924	4615.397	302.6907	4612.87	307.4825	4614.088
14	298.6403	4615.283	302.6002	4615.486	302.6985	4612.958	307.4903	4614.177
15	298.6323	4615.14	302.5922	4615.343	302.6905	4612.815	307.4823	4614.034
16	298.6403	4615.14	302.6002	4615.343	302.6985	4612.815	307.4903	4614.034
17	298.6783	4615.583	302.6382	4615.786	302.7365	4613.258	307.5283	4614.477
18	298.7083	4615.64	302.6682	4615.843	302.7665	4613.315	307.5583	4614.534

3.2 Existing Industrial Plant Characterization

The study was used the sulfur dioxide database given by Bhardwaj [18].

3.2.1 Sulfur Dioxide (SO_2) Emission Inventory

This study followed up the previous study given by Bhardwaj [18]. It used the same database of sulfur dioxide. A detailed emission inventory for all sources emitting sulfur dioxide (SO_2) was obtained from Bhardwaj [18]. The inventory data contained completed details of the point source as well as the measurement from stack monitors for three years 1990, 1991 and 1992 for all sources emitting sulfur dioxide (SO_2) [18].

The facility, stacks, and the complete information of air pollutant emissions were consisted in the point source report. The facility information includes the Universal Transverse Mercator (UTM) coordinates in which stacks are situated. The stack information includes some stack parameters such as diameter, height, SO_2 emission flow rate, and temperature. The SO_2 pollutant emission includes the annual emission.

There are about 123 stacks emit SO_2 in Lucas County. The SO_2 emissions from the stacks range from 1 ton/year to 6655 tons/year [18]. In order to analyze these emission rates, stacks were classified based on the amount of emission per year into three groups as shown in Table 3.2. In addition, Table 3.3, Table 3.4 and Table 3.5 summarize the properties of main stacks for years 1990, 1991 and 1992 respectively. Stacks are divided into three groups, main stacks, and superstacks, depended on the emission percent causing the pollution. Stacks that have low emission contribution considered as superstacks [18].

A superstack is defined as an imaginary stack that is positioned over the grid containing the major stacks. It is assumed that the superstack produces a similar effect on the pollutant

concentration as all the comprising stacks do. The properties of super stacks are summarized in Table 3.6, Table 3.7and Table 3.8 [18].

Table 3.2: Specifications of stacks for years 1990, 1991 and 1992.

Group	Number of stacks	Emission percent (%)	Emission rate (ton/year)	Comments
Year 1990				
First Group	16	96	210	Main Stacks
Second Group	28	3.7	5	Super Stacks
Third Group	79	0.24	Less than 5	
Year 1991				
First Group	15	95.79	200	Main Stacks
Second Group	40	3.9	10	Super Stacks
Third Group	68	0.31	Less than 10	
Year 1992				
First Group	16	96.71	200	Main Stacks
Second Group	37	3.12	10	Super Stack
Third Group	70	0.14	Less than 10	

Table 3.3: Ohio EPA emission inventory system point source report for sulfur dioxide for the year 1990 [18].

No	Stacks information	Height (ft)	Diameter (ft)	Temperature (F°)	Flow rate (ft^3/min)	Horizontal UTM (km)	Vertical UTM (km)	Emission rate (tons/year)
1	BP Oil Company: Flare Stack & Burner Tip M.W. Kellog	343	0.5	3000	-	295.7	4616.8	260
2	BP Oil Company: 55000 BPD UOP FCC Unit with new B & W Co. Boiler	250	11	400	130619	295.7	4616.8	1659.84
3	Sun Refining: Babcock & Wilcox Heater	100	9.5	390	100000	291.7	4611.8	1099.31
4	Sun Refining: Fluid Catalytic Cracking Unit	249	9.7	450	186844	291.4	4611.8	2238.6
5	Sun Refining: Amine Class Sulfur Recovery Plant	150	3.5	1200	16700	291.4	4611.8	553.92
6	Toledo Coke Corporation: Battery Coke Ovens and Auxiliaries	200	7.5	200	-	292.8	4616.1	259.85
7	Toledo Edison Co: Acme Station: 802 MM BTU/Hr B & W Coal Fired Boiler W/ESP ACME #16 Boiler	246	11	327	295000	290.5	4614.3	668.39
8	Toledo Edison Co: Acme Station: 649 MM BTU/Hr B & W Coal Fired Boiler W/ESP ACME #91 Boiler	298	22	352	133300	290.52	4614.3	554.01
9	Toledo Edison Co: Acme Station: 649 MM BTU/Hr B & W Coal Fired Boiler W/ESP ACME #92 Boiler	298	22	352	133300	290.5	4614.3	461.02
10	Toledo Edison Co: Bayshore Station: Babcock & Wilcox Custom Built Boiler	469	23	300	467000	297.1	4518.3	5065.3
11	Toledo Edison Co: Bayshore Station: Babcock & Wilcox Custom Built Boiler	469	23	300	490000	297.1	4618.3	6642.24
12	Toledo Edison Co: Bayshore Station: Babcock & Wilcox Custom Built Boiler	469	23	300	467000	297.1	4618.3	6655.51
13	Toledo Edison Co: Bayshore Station: Babcock & Wilcox Custom Built Boiler	469	23	300	710000	297.1	4618.3	8225.43
14	Coulton Chemical Corp: Contact Type Sulfuric Acid Plant	120	4	100	25000	295.6	4617.1	294.25
15	LOF CO Rossford plant: Float Glass Melting Furnace	252	8	1310	155300	287.9	4610.3	307.64
16	LOF CO Rossford plant: Float Glass Melting Furnace	212	8	1200	179000	287.9	4610.3	210.35

Table 3.4: Ohio EPA emission inventory system point source report for sulfur dioxide for the year 1991[18].

No	Stacks information	Height (ft)	Diameter (ft)	Temperature (F°)	Flow rate (ft^3/min)	Horizontal UTM (km)	Vertical UTM (km)	Emission rate (tons/year)
1	BP Oil Company: Flare Stack & Burner Tip M.W. Kellog	343	0.5	3000	-	295.7	4616.8	1509
2	BP Oil Company: 55000 BPD UOP FCC Unit with new B & W Co. Boiler	250	11	400	130619	295.7	4616.8	1659.84
3	Sun Refining: Babcock & Wilcox Heater	100	9.5	390	100000	291.7	4611.8	659.02
4	Sun Refining: Fluid Catalytic Cracking Unit	249	9.7	450	186844	291.4	4611.8	2238.6
5	Sun Refining: Amine Class Sulfur Recovery Plant	150	3.5	1200	16700	291.4	4611.8	553.92
6	Toledo Coke Corporation: Battery Coke Ovens and Auxiliaries	200	7.5	200	-	292.8	4616.1	259.85
7	Toledo Edison Co: Acme Station: 802 MM BTU/Hr B & W Coal Fired Boiler W/ESP ACME #16 Boiler	246	11	327	295000	290.5	4614.3	397.96
8	Toledo Edison Co: Acme Station: 649 MM BTU/Hr B & W Coal Fired Boiler W/ESP ACME #91 Boiler	298	22	352	133300	290.52	4614.3	431.68
9	Toledo Edison Co: Acme Station: 649 MM BTU/Hr B & W Coal Fired Boiler W/ESP ACME #92 Boiler	298	22	352	133300	290.5	4614.3	331.04
10	Toledo Edison Co: Bayshore Station: Babcock & Wilcox Custom Built Boiler	469	23	300	467000	297.1	4518.3	5822.67
11	Toledo Edison Co: Bayshore Station: Babcock & Wilcox Custom Built Boiler	469	23	300	490000	297.1	4618.3	5213.87
12	Toledo Edison Co: Bayshore Station: Babcock & Wilcox Custom Built Boiler	469	23	300	467000	297.1	4618.3	6255.02
13	Toledo Edison Co: Bayshore Station: Babcock & Wilcox Custom Built Boiler	469	23	300	710000	297.1	4618.3	7275.41
14	Coulton Chemical Corp: Contact Type Sulfuric Acid Plant	120	4	100	25000	295.6	4617.1	294.25
15	LOF CO Rossford plant: Float Glass Melting Furnace	252	8	1310	155300	287.9	4610.3	263.64
16	LOF CO Rossford plant: Float Glass Melting Furnace	212	8	1200	179000	287.9	4610.3	216.92

Table 3.5: Ohio EPA emission inventory system point source report for sulfur dioxide for the year 1992 [18].

No	Stacks information	Height (ft)	Diameter (ft)	Temperature (F°)	Flow rate (ft^3/min)	Horizontal UTM (km)	Vertical UTM (km)	Emission rate (tons/year)
1	BP Oil Company: Flare Stack & Burner Tip M.W. Kellog	343	0.5	3000	-	295.7	4616.8	1509
2	BP Oil Company: 55000 BPD UOP FCC Unit with new B & W Co. Boiler	250	11	400	130619	295.7	4616.8	1659.84
3	Sun Refining: Babcock & Wilcox Heater	100	9.5	390	100000	291.7	4611.8	688.41
4	Sun Refining: Fluid Catalytic Cracking Unit	249	9.7	450	186844	291.4	4611.8	2238.6
5	Sun Refining: Amine Class Sulfur Recovery Plant	150	3.5	1200	16700	291.4	4611.8	553.92
6	Toledo Coke Corporation: Battery Coke Ovens and Auxiliaries	200	7.5	200	-	292.8	4616.1	259.85
7	Toledo Edison Co: Acme Station: 802 MM BTU/Hr B & W Coal Fired Boiler W/ESP ACME #16 Boiler	246	11	327	295000	290.5	4614.3	397.96
8	Toledo Edison Co: Acme Station: 649 MM BTU/Hr B & W Coal Fired Boiler W/ESP ACME #91 Boiler	298	22	352	133300	290.52	4614.3	425.07
9	Toledo Edison Co: Acme Station: 649 MM BTU/Hr B & W Coal Fired Boiler W/ESP ACME #92 Boiler	298	22	352	133300	290.5	4614.3	331.04
10	Toledo Edison Co: Bayshore Station: Babcock & Wilcox Custom Built Boiler	469	23	300	467000	297.1	4518.3	5443.99
11	Toledo Edison Co: Bayshore Station: Babcock & Wilcox Custom Built Boiler	469	23	300	490000	297.1	4618.3	5213.87
12	Toledo Edison Co: Bayshore Station: Babcock & Wilcox Custom Built Boiler	469	23	300	467000	297.1	4618.3	6455.55
13	Toledo Edison Co: Bayshore Station: Babcock & Wilcox Custom Built Boiler	469	23	300	710000	297.1	4618.3	7750.42
14	Coulton Chemical Corp: Contact Type Sulfuric Acid Plant	120	4	100	25000	295.6	4617.1	294.25
15	LOF CO Rossford plant: Float Glass Melting Furnace	252	8	1310	155300	287.9	4610.3	257.09
16	LOF CO Rossford plant: Float Glass Melting Furnace	212	8	1200	179000	287.9	4610.3	210.37

Table 3.6: Properties of super stacks for 1990 [18].

No	Stack No.	Height (m)	Temp. (K)	Diameter (m)	Flow rate (m^3/sec)	Exit Velocity (m/sec)	Emission (g/sec)	Horizontal UTM (km)	Vertical UTM (km)	Description of the Source
1.	SS01	39.99	547.00	2.90	1300.58	7.02	2.71	290.7	4614.5	Superstack 1 for SO_2 emission
2.	SS02	32.76	544.10	2.00	407.95	9.54	42.97	289.1	4614.3	Superstack 2 for SO_2 emission

Table 3.7: Properties of super stacks for 1991 [18].

No	Stack No.	Height (m)	Temp. (K)	Diameter (m)	Flow rate (m^3/sec)	Exit Velocity (m/sec)	Emission (g/sec)	Horizontal UTM (km)	Vertical UTM (km)	Description of the Source
1.	SS03	37.30	555.24	3.03	53.1426	7.37	3.05	289.2954	4612.94	Superstack 1 for SO_2 emission
2.	SS04	33.11	617.026	1.93	38.2074	13.06	38.89	289.0679	4613.45	Superstack 2 for SO_2 emission

Table 3.8: Properties of super stacks for 1992 [18].

No	Stack No.	Height (m)	Temp. (K)	Diameter (m)	Flow rate (m^3/sec)	Exit Velocity (m/sec)	Emission (g/sec)	Horizontal UTM (km)	Vertical UTM (km)	Description of the Source
1.	SS05	43.37	540.737	2.97	1197.28	7.20	1.68	292.5762	4615.93	Superstack 1 for SO_2 emission
2.	SS06	34.45	574.154	2.01	516.806	10.71	31.25	288.638	4613.29	Superstack 2 for SO_2 emission

3.2.2 Monitoring Data

In this area of study, two air monitoring locations were used to record data for the period of 1990, 1991, and 1992. The two air monitoring data has been obtained from the US EPA's air quality system. The UTM coordinates of these two air monitoring stations are (293889, 4615115) and (289304, 4613488) [18].

3.2.3 Location of Stacks, Superstacks, and Monitoring Stations

The stacks, superstacks, and the air monitoring stations are plotted on a Cartesian Grid represented by Figure 3.2, Figure 3.3 and Figure 3.4 for the period of 1990, 1991 and 1992 respectively [18].

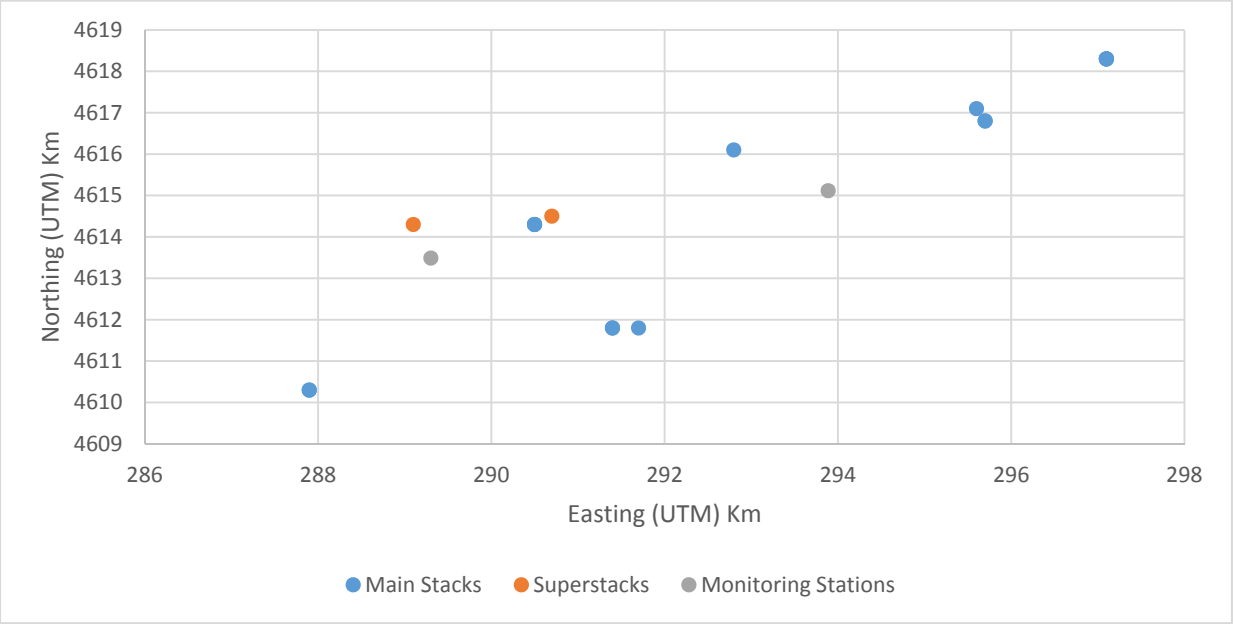

Figure 3.2: Main stacks, superstacks and monitorring stations locations for 1990 [18].

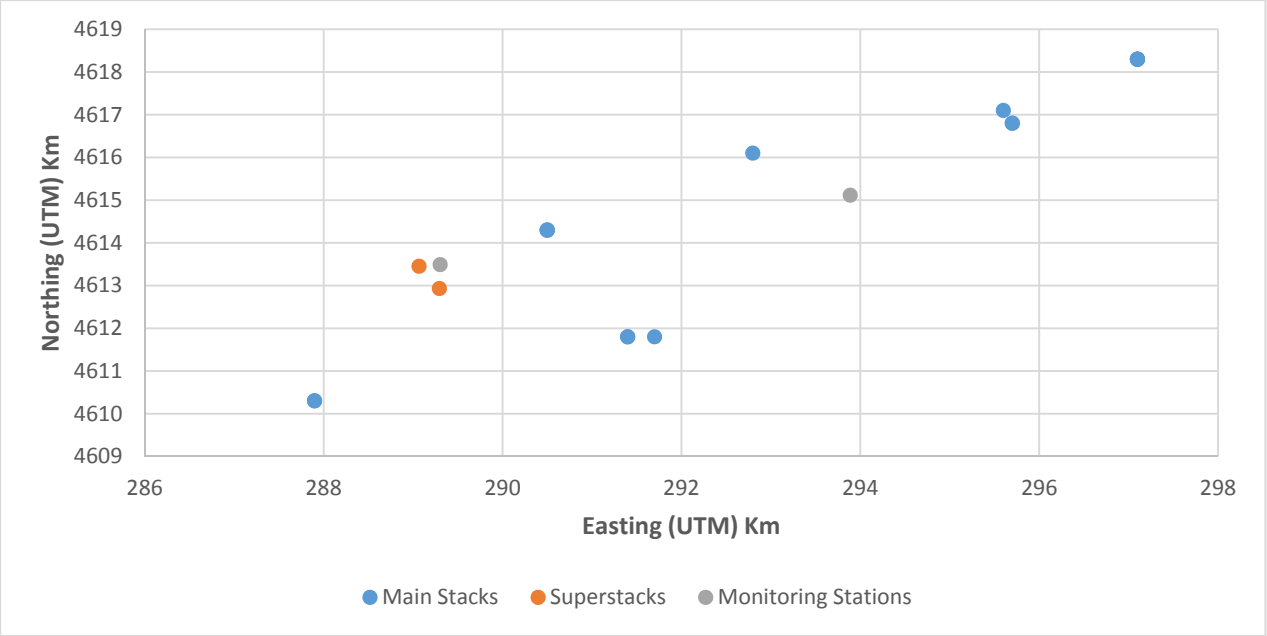

Figure 3.3: Main stacks, superstacks and monitorring stations locations for 1991 [18].

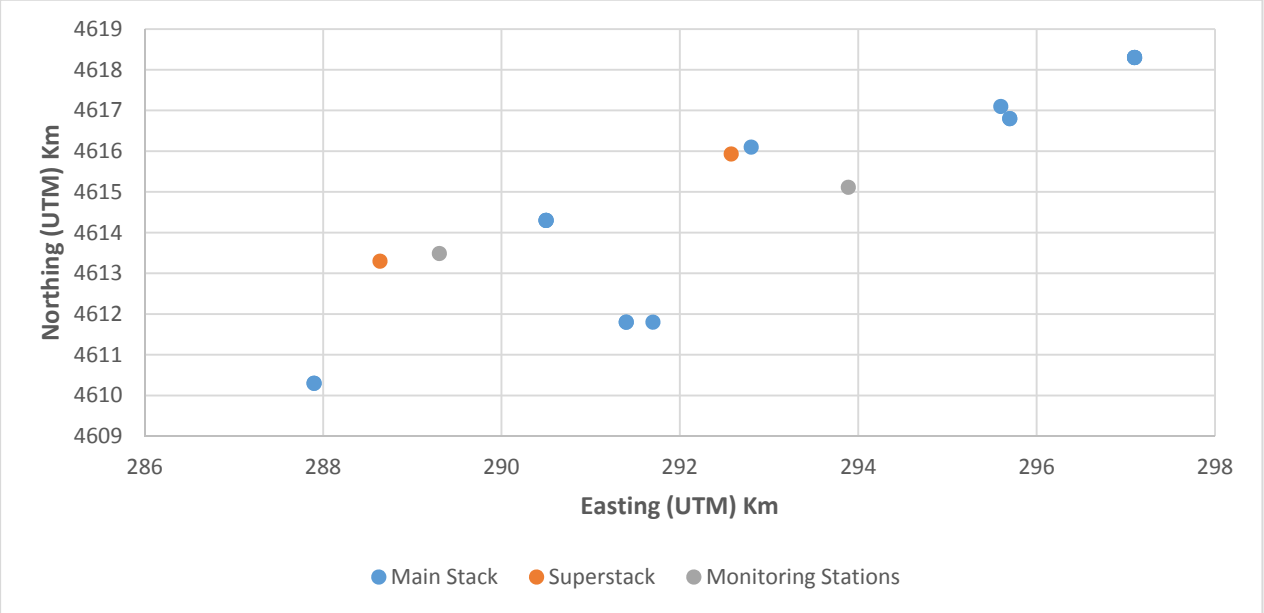

Figure 3.4: Main stacks, superstacks and monitorring stations locations for 1992 [18].

3.3 Proposed Industrial Plants Characterization

3.3.1 Mercury Emission Inventory

Mercury emissions from various combustion and industrial sources pose a serious problem in many locations across the world. The study used the mercury database given by [43] as a database for the proposed plant as a hypothetical case study. In this case study, there are 18 stacks considered as major sources of mercury emissions [43].

The detailed emission inventories of all the proposed stacks for the period of 1990, 1991, and 1992 consist of stack parameters for all 18 sources. These parameters including stack height, stack diameter, and stack velocity and stack exit temperature, and yearly emission rates and the source ID for all 18 point sources. The details of the stacks for years 1990, 1991, and 1992 are showed in Table 3.9 [43].

Table 3.9: Stack parameters for mercury for the period 1990, 1991 and 1992 *[43]*.

Stack-Parameter and Emissions information for year 1990, 1991 and 1992.												
Stack Description												
ID No.	Height (m)	Diameter (m)	Velocity (m/sec)			Temperature (K)			Mercury Emission(g/sec)			
			1990	1991	1992	1990	1991	1992	1990	1991	1992	
1	103.20	2.59	20.46	20.46	20.46	437.67	437.67	394.11	1.36E-02	3.32E-02	2.03E-02	
2	117.35	3.73	45.15	45.15	45.15	420.78	420.78	420.78	2.68E-08	1.49E-07	3.97E-08	
3	129.54	3.91	48.75	48.75	48.75	433.00	433.00	433.00	5.44E-03	3.89E-03	3.04E-03	
4	170.39	4.42	42.69	42.69	42.69	433.00	433.00	433.00	1.41E-05	6.11E-06	1.78E-06	
5	171.60	4.88	42.70	42.70	42.70	410.78	410.78	410.78	8.98E-06	1.29E-06	1.52E-06	
6	245.37	8.53	39.04	39.04	39.04	405.22	405.22	405.22	2.55E-02	2.57E-02	1.32E-02	
7	245.37	8.53	39.04	39.04	39.04	402.44	402.44	402.44	2.57E-02	2.62E-02	1.42E-02	
8	245.37	8.53	39.04	39.04	39.04	405.22	405.22	405.22	4.62E-06	1.29E-06	1.03E-06	
9	245.37	8.53	39.04	39.04	39.04	405.22	405.22	405.22	1.15E-04	8.87E-05	4.18E-05	
10	201.17	7.77	27.47	27.47	27.47	416.33	416.33	416.33	1.55E-02	1.50E-02	6.67E-06	
11	201.17	7.77	27.47	27.47	27.47	416.33	416.33	416.33	1.57E-02	1.54E-02	6.19E-06	
12	88.39	1.37	22.75	22.75	22.75	588.56	588.56	588.56	1.23E-05	1.23E-05	5.32E-05	
13	182.58	4.06	27.39	27.39	27.39	438.56	438.56	438.56	3.29E-03	2.66E-03	2.89E-09	
14	182.58	4.06	27.39	27.39	27.39	438.56	438.56	438.56	3.00E-03	2.27E-03	4.80E-09	
15	182.58	4.06	27.39	27.39	27.39	438.56	438.56	438.56	3.23E-03	2.85E-03	3.89E-07	
16	182.58	4.06	27.39	27.39	27.39	438.56	438.56	438.56	3.36E-03	3.09E-03	4.51E-07	
17	129.54	4.04	39.96	39.96	39.96	421.89	421.89	421.89	4.78E-06	5.53E-06	5.98E-06	
18	182.58	4.98	42.74	42.74	42.74	425.78	425.78	425.78	6.72E-06	1.97E-06	4.22E-06	

3.3.2 Location of Stacks and Monitoring Stations

The stacks and the air monitoring stations are plotted on a Cartesian Grid represented by Figure 3.5, Figure 3.6, Figure 3.7 and Figure 3.8 for the period of 1990, 1991 and 1992 respectively.

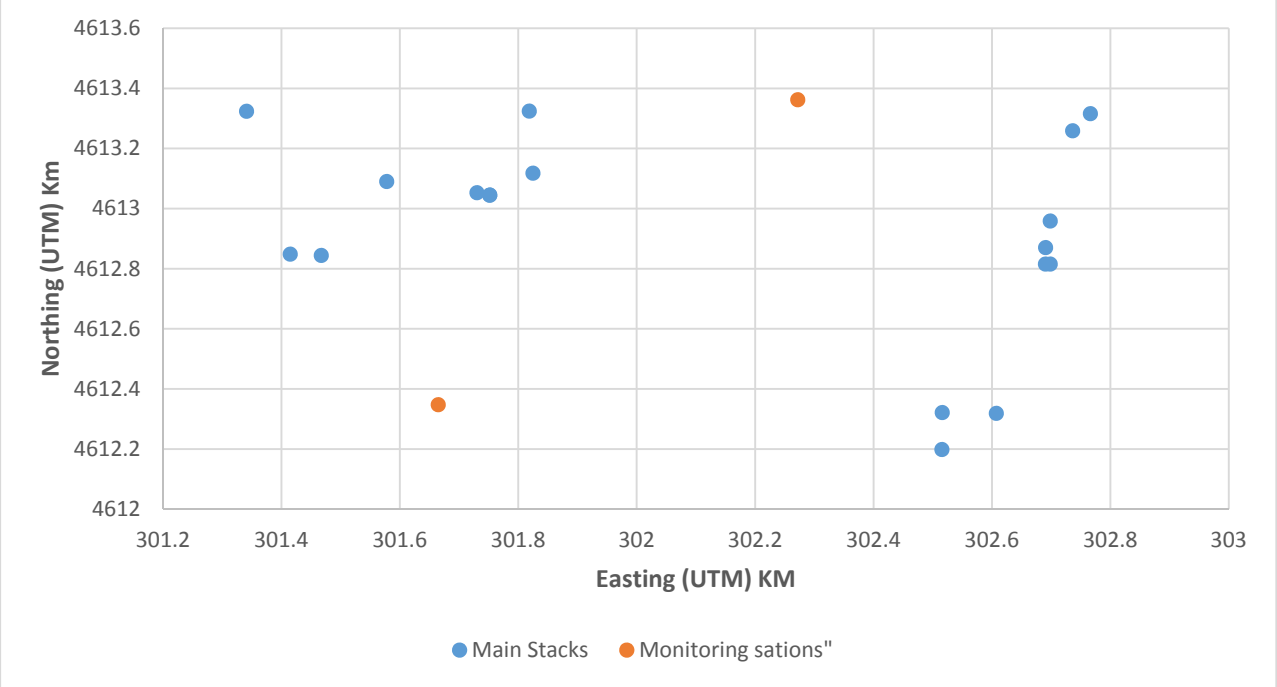

Figure 3.5: Main stacks and monitoring stations for the first proposed location for the period 1990, 1991 and 1992.

.

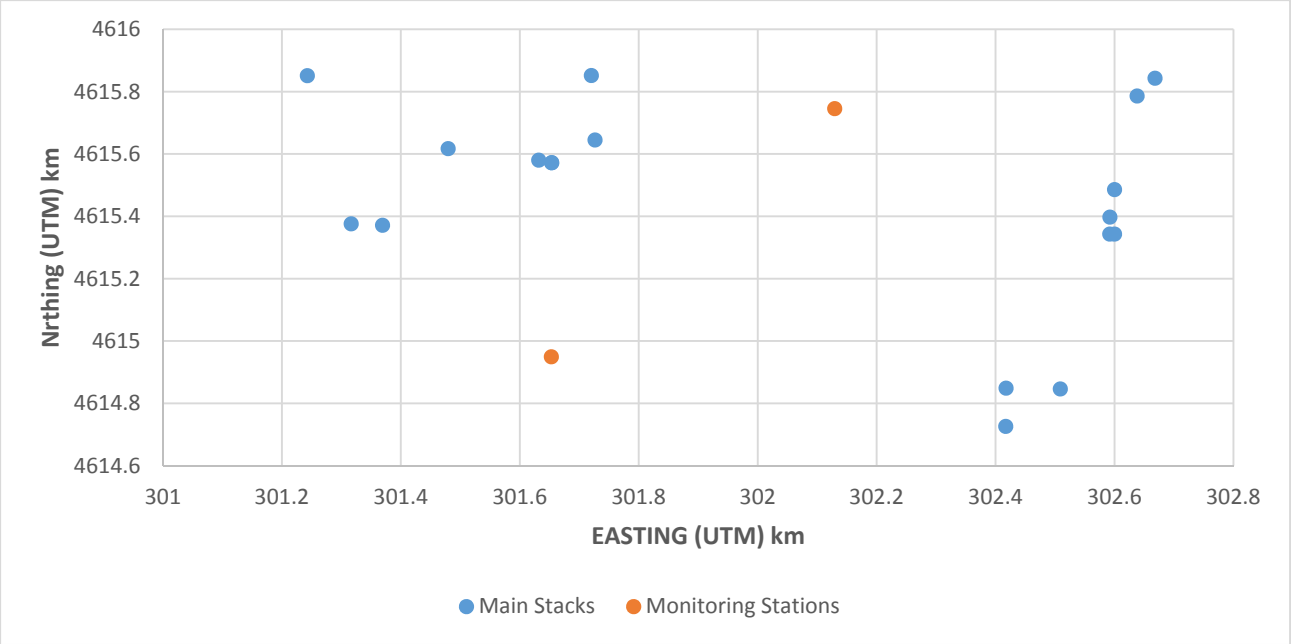

Figure 3.6: Main stacks and monitoring stations for the second proposed location for the period 1990, 1991 and 1992.

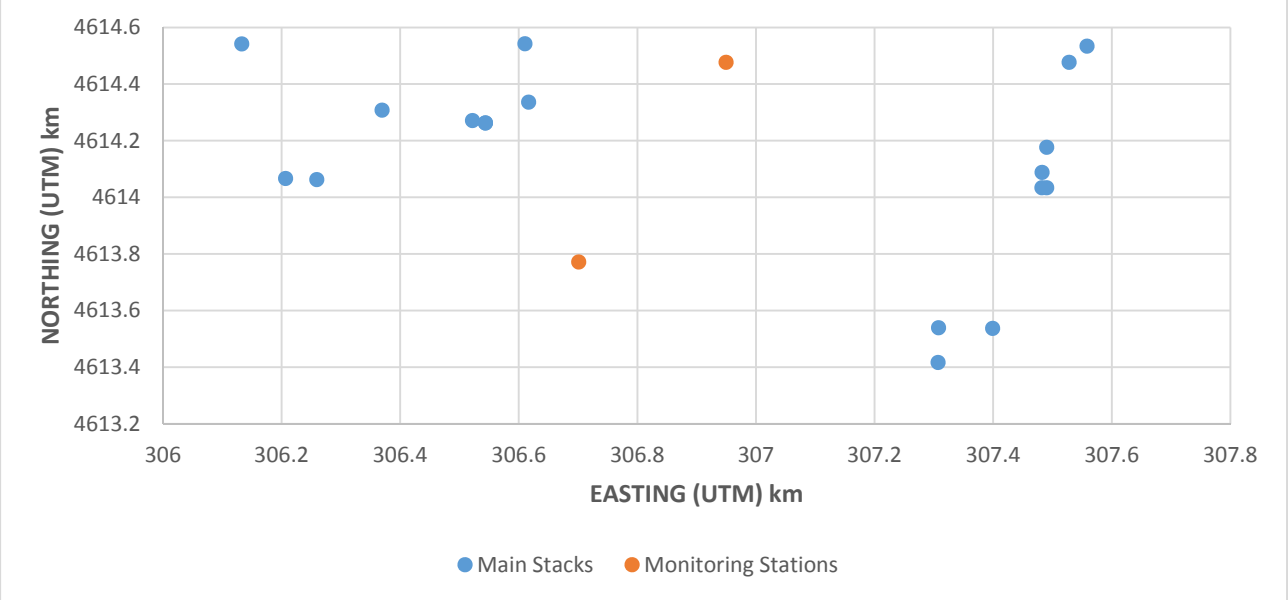

Figure 3.7: Main stacks and monitoring stations for the third proposed location for the period 1990, 1991 and 1992.

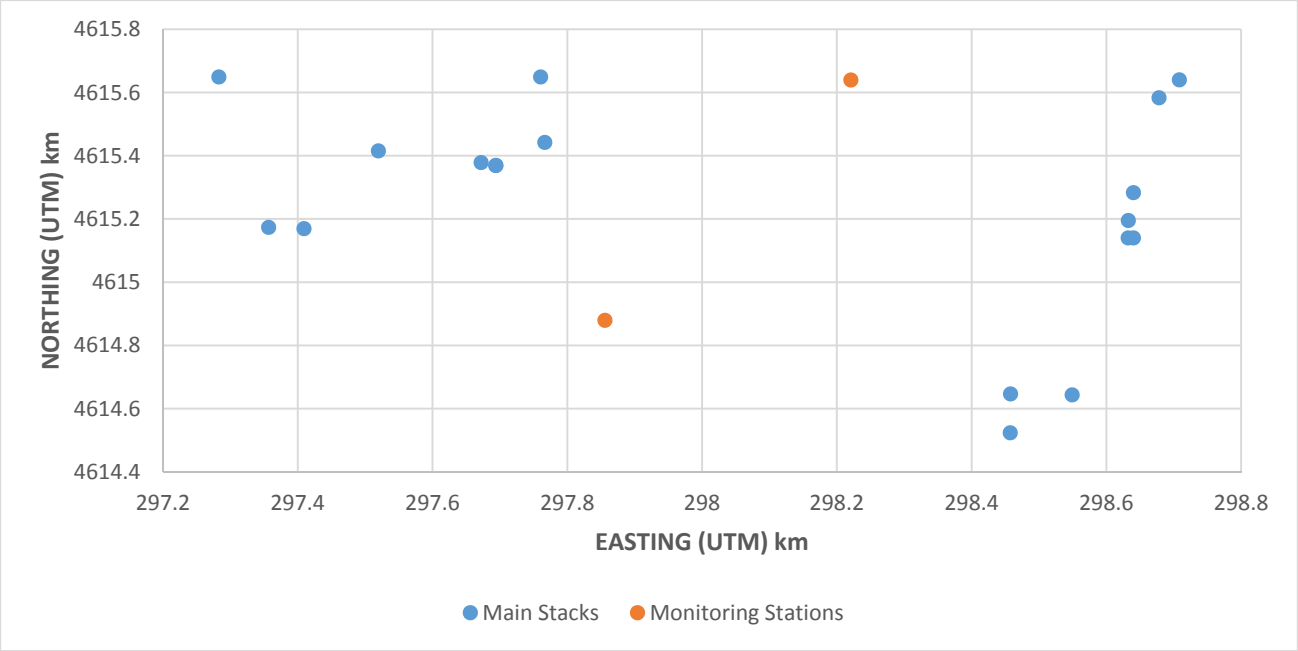

Figure 3.8: Main stacks and monitoring stations for the fourth proposed location for the period 1990, 1991 and 1992.

3.4 Model Description

3.4.1 AERMOD Dispersion Model

AERMOD is a steady-state plume model designed to calculate the near-field (less than 50 km) concentration and run with a minimum of observed meteorological parameters. The AERMOD model a system with three separate components: AERMOD (AMS EPA Regulatory Dispersion Model), AERMAP (AERMOD Terrain Preprocessor) and AERMET (AERMOD Meteorological Preprocessor). AERMOD input data is prepared from output files from AERMET and AERMAP preprocessors [44].

3.4.1.1 AERMET

The AERMET program is a meteorological data preprocessor that accepts surface meteorological data, upper air soundings, or data from on-site instrument towers, then calculates atmospheric parameters needed by the dispersion model [44]. Hourly surface data (Samson surface

met data format) and upper air data (TD 6201 format) both were obtained from WEBMET database (www.webmet.com) for Toledo International Airport [18].

Processing the data following three main steps. In the first step, meteorological data will be extracted and a serious of quality assessment checks will be used to assess data quality. In the second step, all data available for 24-hour periods will be merged and written together in a single intermediate files. In the final step, the merged meteorological data will be read and the necessary boundary layer parameters will be calculated by AERMOD model for dispersion calculations [44].

The AERMET preprocessor generates two files to be used by AERMOD: Surface file and profile file. The AERMAP preprocessor calculates a representative terrain-influence height associated with each receptor by using gridded terrain data for the area of study.

In this study, analyzing the three-kilometer area around the meteorological site using 12 pie-shaped sectors were used to calculate the land use parameters. For each sector, surface parameters, namely Albedo, Bowen Ratio, and Surface Roughness were specified by the sectors that were no smaller than a 30-degree arc. The value of anemometer height was taken as 21 ft (6.4 meters). The AERMET model was run on a short regional domain extending westward to 83.75-degree longitude and Northward to 42.96-degree latitude. Results generated by the AERMET preprocessor were used by AERMET to generate two meteorological files, which used in AERMOD meteorological pathway.

3.4.1.2 AERMAP

The AERMAP program is a terrain preprocessor that provides a physical relationship between terrain features and the behavior of air pollution plumes [44]. The AERMAP preprocessor has been developed to facilitate the generation of hill height scales and elevation for AERMOD

and to process the terrain data in conjunction with a layout of receptor and sources to be used in AERMOD control files. The AERMAP was run after the AERMET data was complied. The gridded data is supplied to AERMAP in the format of a Digital Elevation Model (DEM), from which elevations for both discrete receptors and receptor grids are computed.

In this study, the AERMAP was run using two separate 1 degree DEM Toledo East and Toledo West to cover the area of concern. The geographical data, including land use and terrain, were obtained from the Geographic Information System Resource website (www.webgis.com). Table 3.10 shows the details of DEM files. The AERMAP was run using NAD27 datum (North American Datum of 1927). These two files were used same for all AERMOD runs.

Table 3.10: List of USGS DEM 1-degree files used for AERMAP run.

Name	Half	Min Longitude	Max Longitude	Min Latitude	Max Latitude
Toledo	West	-84°00′00′′	-83°00′00′′	41°00′00′′	42°00′00′′
Toledo	East	-83°00′00′′	-82°00′00′′	41°00′00′′	42°00′00′′

3.4.2 Air Dispersion and Deposition Modelling

3.4.2.1 Control Pathway

Control Pathway contain options that effectively control the AERMOD dispersion model to predict impacts based on several options such as dispersion options, averaging time options and terrain options (Elevated). In Control Pathway, the overall control options are specified Mercury (Hg). These options include dispersion options where concentration, dry deposition, wet deposition, and total deposition were selected. The AERMOD dispersion model was run for short-

term averaging time period option (1-hr) and long-term averaging time period option (annual) in order to calculate the human health risk. This human health risk assessment.

According to U.S. EPA recommendations, urban dispersion coefficient and mixing are recommended when the area of study is greater than 50 percent; otherwise, rural coefficient and mixing heights will be applied. In this study based on the land use evaluation of the study area, dispersion coefficient was taken for the urban area for the existing plant and, as an input, urban population for Lucas 436,393 was taken. In addition, the dispersion environment was classified as rural for proposed plant locations. Elevated terrain height option was used for this study.

3.4.2.2 Source Pathway

In Source Pathway, the source input parameters and source group information such as source type, building downwash, and variable emissions were specified. AERMOD air modeling was performed based on a unit emission rate of 1.0 g/s, instead of compound-specific emission rates. The unitized air modeling outputs based on a unit emission rate were multiplied by a compound-specific emission rate prior to use in the risk assessment. The AERMOD dispersion model was run one by one using 3 years for the period 1990, 1991 and 1992 by using base emission inventories.

Table 3.11 lists the source parameters for gas and particle deposition for mercury entered into AERMOD. In the AERMOD dispersion model, since the mercury particle density is unknown, a particle density of 1 g/cm^3 is assumed for the sources as recommended in the HHRAP.

Table 3.11: Source parameters for gas and particle deposition for mercury.

Source Parameter	Mercury
Diffusivity in air *(cm^2/sec)*	1.09E-02
Diffusivity in water *(cm^2/sec)*	3.01E-05
Cuticular resistance *(s/cm)*	1.0E+5
Henry's law constant *($Pa.m^3/mol$)*	7.19E+2

The AERMOD model requires input of particle size distribution and density data for completion of the particle phase and particle-bound phase modeling. Site-specific data for these parameters are not available. Since this study deals with proposed plants, we assumed some particle size distribution to input to AERMOD. Table 3.12 lists the assumed values for particle size distribution.

Table 3.12: Assumed values for particle size distribution.

Particle	Method	Particle Diameter (microns)	Mass Fraction (0 to 1)	Particle Density (g/cm^3)
Particle - Dry	Method 1: 10% or more has a diameter ≥ 10 microns	2.5	0.45	1
		10	0.55	1
Particle Bound - Dry	Method 1: 10% or more has a diameter ≥ 10 microns	2.5	0.766	1
		10	0.234	1

3.4.2.3 Receptor Pathway

Discrete Cartesian grid receptor monitoring networks option were utilized for the area of study. In order to predict the concentration and depositions at Lucas County, two monitoring stations are used for every proposed location.

3.4.2.4 Meteorology Pathway

The meteorological data files generated by AERMET preprocessor for mercury are utilized for AERMOD run. Wind speed was taken from model default values. For Lucas Country, the average base elevation 180 m above MSL was taken.

3.4.2.5 Output Pathway

The averaging results were obtained for short term, 1 hour, and annual time period options. The short term averaging results were obtained for the highest second highest 1 hour, 3 hr, 8 hr,

3.5 IRAP-h View Model

The IRAP-h View, applied is this study, is designed to accept output files of annual average concentrations and annual average deposition rates from AERMOD dispersion model. The annual average concentrations is the mean concentration over a year to which a receptor may be exposed at ground level. The annual average deposition rate is the average transfer of air pollutants from the air to ground surfaces. The IRAP-h View uses these output files to predict human exposure to pollutants emitted to environment media from proposed plants. In addition, IRAP-h View uses risk output files processed by Risk Mode post-processor in the AERMOD software.

The human health risk assessment (HHRA) is required in this study because mercury emissions emitted from the proposed plant cannot be evaluated in terms of its effects on human health simply reference to National Ambient Air Quality Standards (NAAQS). In addition, mercury has appreciable potential to accumulate in the environment harmful concentrations that could affect human and other ecosystems.

As discussed in section 2.5, the human health risk assessment process is based on the application of the U.S. EPA Human Health Risk Assessment Protocol (HHRAP). IRAP-h View

software has been used for assessing health risks arising from exposure to air pollutants emitted by proposed industrial plants.

The Mercury Study Report to Congress [45] reported that there are three forms of mercury in the environment: elemental, divalent, and methylated.

3.6 Methodology for Estimating Exposure to Emissions

Exposure to mercury occurred when exposure pathway from the source to receptors is completed. The exposure to mercury or other Chemicals of Potential Concern (COPCs) can occur direct or indirect exposure pathways.

Exposure to mercury can be evaluated by different exposure pathways. Inhalation pathway is used to evaluate the exposure to elemental mercury. Direct and indirect exposure pathways both are used to evaluate the exposure to divalent mercury [35].

In order to do health risk assessment, the following exposure pathways were considered [35]:

- Direct exposure pathway, including:
  - Inhalation (including acute inhalation);
- Indirect exposure pathways, including:
  - Deposition on soil;
  - Consumption of fruit and vegetables;
  - Consumption of poultry and eggs;
  - Consumption of meat (beef, pork and fish);
  - Consumption of cow's milk and human breast milk; and
  - Consumption of drinking water.

Figure 3.9 shows more elaborate definition of the exposure pathways.

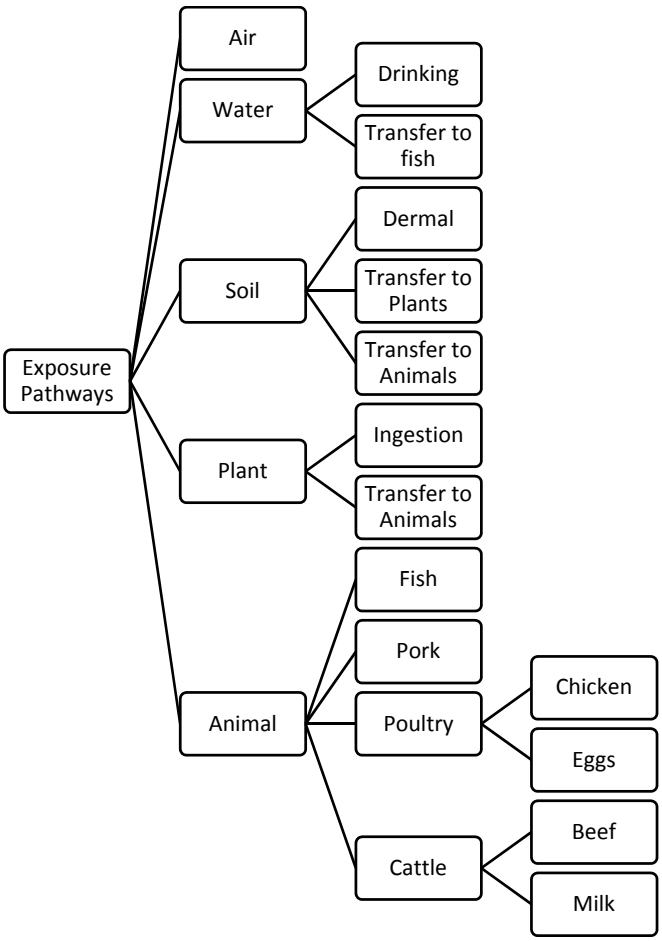

Figure 3.9: Exposure pathways.

3.6.1 Exposure Scenario Selection

Exposure scenarios are identified to predict the potential health impact of proposed industrial plants on the surrounding area. Each exposure scenario defines a particular combination of exposure pathways and the parameter values used to characterize risk and hazards [35].

As discussed in section 2.5, the HHRAP identifies seven recommended exposure scenarios that should be considered for inclusion in the health risk assessment. The seven scenarios are: resident adult, resident child, farmer adult, farmer child, fisher adult, fisher child, and acute risk

[35]. Since the area of study is located in rural, urban, grassland and water (fresh and sea), the seven exposure scenarios were selected for health risk assessment.

The locations of exposure scenarios are the grid nodes (i.e., the actual geographic positions). The locations of exposure scenarios were selected based on the air concentrations and deposition fluxes estimated by AERMOD and land uses within the area of concern.

Proposed locations were eliminated as a parameter used to define exposure scenarios by utilizing the maximum off-site impact (based on air dispersion modeling) of all receptors in the evaluated off-property assessment area. This technique effectively maximizes the estimated exposure to every individual regardless of the actual location of the resident/farmer/fisher.

Receptor polygons were drawn around each land use area of interest within the area of concern. To estimate the grid nodes within each polygon, the IRAP-h View receptor identification tool was used. These grid nodes were estimated by IRAP-h View where the utilized air concentrations and depositions were maximized.

Table 3.13 presents the chronic and acute exposure pathways and exposure scenarios considered in this study.

3.6.2 Exposure Scenario Locations

The current and reasonable potential future land use surrounding the proposed plants is considered when evaluating potential risk. The locations associated with the exposure scenarios include occupational, residential, and sensitive receptors. Sensitive receptors include community centers, hospitals, nursing homes/retirement homes, schools, and day-care centers. In this study, receptor grids total 264 receptor locations are used for the risk assessment around every proposed plant location. In addition, the receptor locations are automatically identified by IRAP every 5000 m as a worst-case scenario as shown in

Figure ***3.10***.

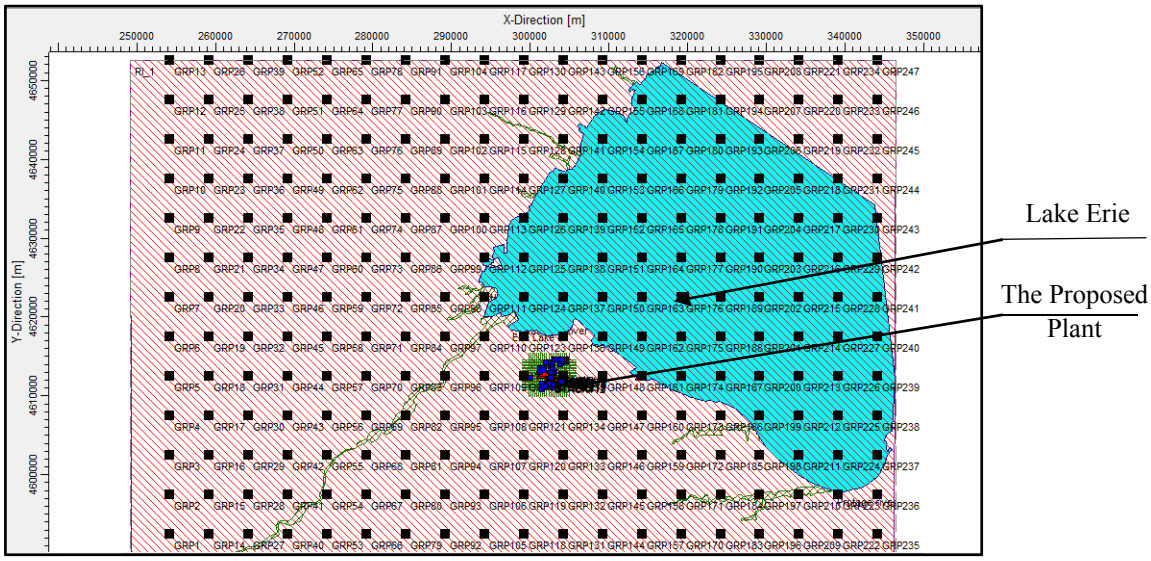

Figure 3.10: Receptor location identified by IRAP-h View model.

Table 3.13: Selected Exposure Scenarios and Associated Exposure Pathways *[35]*.

Exposure Pathways	Exposure Scenarios						
	Farmer	**Farmer Child**	**Adult Resident**	**Child Resident**	**Fisher**	**Fisher Child**	**Acute Risk[a]**
Inhalation of Vapors and Particulates	X	X	X	X	X	X	X
Incidental Ingestion of Soil	X	X	X	X	X	X	
Ingestion of Homegrown Produce	X	X	X	X	X	X	
Ingestion of Homegrown Beef	X	X					
Ingestion of Milk from Homegrown Cows	X	X					
Ingestion of Homegrown Chicken	X	X					
Ingestion of Eggs from Homegrown Chickens	X	X					
Ingestion of Homegrown Pork	X	X					
Ingestion of Fish					X	X	
Ingestion of Breast Milk[b]	X		X		X		

Notes:

[a] The acute risk scenario evaluates short-term 1-hour maximum pollutant air concentrations based on hourly emission rates.

[b] COPC estimated concentrations in the three exposure scenarios indicated are utilized to model exposure to infants. Infant exposure to COPC via the ingestion of their mother's breast milk is evaluated as an additional exposure pathway, separately from the recommended exposure scenario.

3.6.3 Water Bodies and Watersheds

The drinking water and fish consumption pathways require site-specific data regarding water bodies and their watersheds. Water bodies and watersheds were selected for evaluating in order to estimate mercury concentrations in surface water and sediment. These water bodies and watersheds were drawn in IRAP-h View by drawing receptor polygon around the corresponding water bodies.

Lake Erie is the fourth largest lake in North America. It is bounded by the Canadian province of Ontario, with Ohio, Pennsylvania, and the New York States on its southern and easternmost shores and Michigan on the west. It is approximately 3 km south of the proposed industrial plant location. The average depth of the Lake Erie is 18.9 meters.

In this study, one water body, Lake Erie, and nine watersheds: Maumee River, Portage River, Raisin River, Toussaint River, Ottawa River, Halfway Creek, Plume Creek, Otter Creek, and Swan Creek. Figure 3.11 shows water body and watersheds polygons drawn in the IRAP-h View.

Figure 3.11: Water body and watersheds polygons.

3.6.3.1 Drinking Water Ingestion Pathway

The exposure to mercury emissions from the proposed industrial plants that are deposited on surface water bodies used for drinking purposes is considered by the drinking water ingestion pathway. The contributions from deposition onto surface water are considered by the HHRAP equations used to estimate Chemical of Potential Concern (COPC) concentrations in surface water. The Lake Erie water body and watersheds polygons are shown in Figure 3.11.

3.6.4 Estimating Media Concentrations

The methodology of estimating COPC concentrations in environmental exposure media are provided in this section. As a result, the potential contribution of these COPC concentrations can be evaluated.

The COPC concentration will be estimated based on air concentrations and deposition fluxes, calculated using the AERMOD model. It uses equations and parameters described in Appendices B and C of the HHRAP [35].

3.6.4.1 Calculation of COPC Concentrations in Air

The HHRAP [35] recommended that the concentration of COPC in air can be estimated by summing the vapor phase and particle phase air concentrations of COPC depending on the equations described in Appendix B of the HHRAP [35].

3.6.4.2 Calculation of COPC Concentrations in Soil

The HHRAP [35] recommended that COPC concentrations in soil can be estimated by summing the vapor and particle phase COPC deposition to the soil [35]. In addition, both wet and dry depositions of vapors and particles are considered to calculate COPC concentrations in soil.

The cumulative soil concentrations for carcinogenic COPCs can be calculated by using equations 3.1-A and 3.1-B recommended by the HHRAP [35]. In addition, equation 3.1-C was recommended to estimate the annual average concentration of soil for non-carcinogenic COPCs [35].

For Carcinogens:

For $T_2 \leq tD$

$$Cs = \frac{Ds}{Ks.(tD-T_1)}.\left[\left(tD + \frac{\exp(-Ks.tD)}{Ks}\right) - \left(T_1 + \frac{exp(-Ks.T_1)}{Ks}\right)\right] \quad \text{3.1-A}$$

For $T_1 < tD < T_2$

$$Cs = \frac{\left(\frac{Ds.tD-Cs_{tD}}{Ks} + \left(\frac{Cs_{tD}}{Ks}\right).(1-exp[-Ks.(T_2-tD)])\right)}{(T_2-T_1)} \quad \text{3.1-B}$$

For Non-carcinogens:

$$Cs_{tD} = \frac{Ds.[1-exp(-Ks.tD)]}{Ks} \quad \text{3.1-C}$$

Site-specific data was obtained for evapotranspiration, irrigation, runoff, watershed area, impervious watershed area, depth of water bodies, rainfall factor and volumetric flow of water bodies.

Table 3.14: Summarizes site-specific data used in IRAP-h View model.

Site-specific Parameters	Value	Unit
Average annual runoff	73.25	cm/year
Average annual precipitation [a]	86.9696	cm/year
Average annual irrigation [b]	0	cm/year
Average annual evapotranspiration	86.36	cm/year
USLE Rainfall Factor [d]	100	($year^{-1}$)
Depth of water column	18.9	m
Average volumetric flow rates through water body	175E9	m^3/year
USLE Cover and Management Factor [c]	0.1	unitless

[a] It is estimated using the 3 years of hourly surface data from Toledo Express Airport.

[b] The HHRAP recommends a range of values (0 - 100) cm/year. In this study, sine the site-specific data are not available, a default value of zero (0) cm/year was selected.

[c] The HHRAP recommends a default value of 0.1 for both grass and agricultural crops.

[d] The HHRAP recommends a range of values (50 – 300) $year^{-1}$.

3.6.4.3 Calculation of COPC Concentrations in Produce

Ingestion of produce that causes indirect exposure to COPCs generally depends on the COPCs concentrations in the leafy, fruit, and tuber portions of the plant. The following three possible mechanisms of contamination were considered in order to calculate chemical concentrations in locally grown produce [35]:

- The particle phase of COPCs is directed deposit onto exposed plant surface.
- The vapor phase of COPCs is up taken through plant foliage.
- Root uptake of COPCs in soil and transfer to belowground and aboveground portions of the plant.

The HHRAP [35] recommends and discusses (in Table B-2-7, Appendix B) the following equation to estimate the concentration of aboveground produce due to direct deposition (Pd):

$$Pd = \frac{1000 \times Q \times (1 - F_v) \times [Dydp + (Fw \times Dywy)] \times Rp \times [1.0 - exp(-Kp \times Tp)]}{Yp \times Kp} \quad 3.2$$

Where

Pd = The concentration of plant (aboveground produce) due to direct deposition (wet and dry), (mg COPC/ kg DW)

1000 = Units conversion factor (mg/g)

Q = The emission rate of mercury, (g/sec)

F_v = The mercury fraction in vapor phase (unitless).

Dydp = Unitized yearly wet deposition from particle phase (s/m^2.year)

Fw = 0.6 for cations & most organis, 0.2 for onions (unitless)

Dywp = Unitized yearly wet deposition from particle phase (s/m^2.year)

Rp = Interception fraction of the edible portion of plant (unitless)

Kp = Plant surface loss coefficient ($year^{-1}$)

Tp = The plant exposure length to deposition per harvest od the edible portion of the i^{th} plant group (year)

Yp = Yeild or standing crop biomass of the edible portion of the plant (productivity) ($kg\ DW/m^2$).

In addition, the HHRAP [35] recommends and discusses (in Table B-2-8, Appendix B) the following equation to estimate the concentration of aboveground produce to air-to-plant:

$$Pv = Q \times F_v \times \frac{Cy_v \times Bv_{ag} \times VG_{ag}}{\rho_a} \quad 3.3$$

Where

Pv = The mercury concentration in the plant resulting from air to plant transfer (µg COPC/g DW)

Q = The mercury emission rate (gr/sec)

F_v = The mercury fraction in vapor phase (unitless)

Cyv = Unitized yearly average air concentration from vapor phase ($\mu g.sec/g.m^3$)

Bv_{ag} = The air-to plant biotransfer factor of mercury ([mg COPC/g DW plant]/[mg COPC/g air]) (unitless)

VG_{ag} = The aboveground produce empirical correction factor (unitless)

ρ_a = Air density ($gram/m^3$)

In addition, The HHRAP [35] recommends and discusses (in Table B-2-9, Appendix B) the following equations to estimate the concentration of produce c in protected and exposed aboveground produce and belowground produce due to toot uptake (Pr):

Protected and exposed aboveground produce:

$$Pr = Cs \times Br \quad 3.4A$$

Belowground produce:

$$Pr = \frac{Cs \times RCF \times VG_{rootveg}}{Kd_s \times 1kg/L} \quad 3.4B$$

Where

Pr = Mercury concentration in produce due to root uptake (mg/kg)

Cs = Average concentration of soil over exposure duration (mg COPC/kg soil)

Br = The bioconcentration factor of plant-soil for produce (unitless)

RCF = The concentration factor of root (unitless)

$VG_{rootveg}$ = Empirical correction factor for belowground produce (unitless)

Kd_s = Partition coefficient of soil/water (L/kg).

In addition, The HHRAP [35] recommends and discusses (in Tables B-1-1 through B-1-6, Appendix B) the following equations to calculate cumulative soil concentration (Cs) with carcinogenic COPCs. Equation 3.5A was used for $T_2 \leq tD$ and equation 3.5B was used for $T_1 < tD < T_2$. Equation 3.5C was used for non-carcinogenic COPCs.

For Carcinogens:

For $T_2 \leq tD$

$$Cs = \frac{Ds}{Ks \times (tD - T_1)} \times \left[\left(tD + \frac{exp(-Ks \times tD)}{Ks}\right) - \left(T_1 + \frac{exp(-Ks \times T_1)}{Ks}\right)\right] \quad 3.5A$$

For $T_1 < tD < T_2$

$$Cs = \frac{\left(\frac{Ds \times tD - Cs_{tD}}{Ks}\right) + \left(\frac{Cs_{tD}}{Ks}\right) \times (1 - exp[-Ks \times (T_2 - tD)])}{T_2 - T_1} \quad 3.5B$$

For non-carcinogens:

$$Cs_{tD} = \frac{Ds \times [1 - exp(-Ks \times tD)]}{Ks} \quad 3.5C$$

Where

C_S = Average soil concentration over exposure duration (mg COPC/kg soil)

D_S = Deposition term (mg COPC/kg soil/year)

K_S = Soil loss constant of COPC due to all processes ($year^{-1}$)

t_D = Time period over which deposition occurs (time period of combustion) (year)

T_1 = Time period at the beginning of combustion (year)

$C_{S_{tD}}$ = Concentration of soil at time tD (mg/kg)

T_2 = Length of exposure duration (year)

3.6.4.4 Calculation of COPC Concentrations in Beef and Dairy products

The HHRAP [35] recommends that COPCs concentrations can be estimated in beef and dairy products depends on the COPCs cattle amount are predicted to consume through incidental ingestion of soil and their diet.

The HHRAP [35] recommends and discusses (in Table B-3-10, Appendix B) the following equation to estimate COPC concentration in beef:

$$A_{beef} = (\sum(F_i \times Qp_i \times P_i) + Q_S \times C_S \times B_S) \times Ba_{beef} \times MF \qquad 3.6$$

Where

A_{beef} = The mercury concentration in beef (mg COPC/kg FW tissue)

F_i = Plant type *i* fraction grown on contaminated soil and ingested by the animal (cattle) (unitless)

Qp_i = Plant type *i* quantity eaten by the animal (cattle) per day (kg DW plant/day)

P_i = The mercury concentration in each plant type *i* eaten by the animal (cattle) (mg/ kg DW)

Q_S = Soil quantity eaten by animal (cattle) each day (kg/day)

C_S = Average soil concentration over exposure duration (mg COPC/kg soil)

B_S = Bioavailability factor of soil (unitless)

Ba_{beef} = Biotransfer factor of COPC for beef (day/kg FW tissue)

MF = Metabolism factor (unitless)

In addition, the HHRAP [35] recommends and discusses (in Table B-3-11, Appendix B) the following equation to estimate COPC concentration in cow's milk:

$$A_{milk} = (\sum(F_i \times Qp_i \times P_i) + Q_S \times C_S \times B_S) \times Ba_{milk} \times MF \quad 3.7$$

Where

A_{beef} = The mercury concentration in milk (mg COPC/kg milk)

F_i = Plant type *i* fraction grown on contaminated soil and ingested by the animal (dairy cattle) (unitless)

Qp_i = Plant type *i* quantity eaten by the animal (cattle) each day (kg DW plant/day)

P_i = The mercury concentration in plant type *i* eaten by the animal (dairy cattle) (mg/ kg DW)

Qs = Soil quantity eaten by the animal (dairy cattle) each day (kg soil/day)

Cs = Average soil concentration over exposure duration (mg COPC/kg soil)

Bs = Bioavailability factor of soil (unitless)

Ba_{milk} = Biotransfer factor of COPC for milk (day/kg WW tissue)

MF = Metabolism factor (unitless)

3.6.4.5 Calculation of COPC Concentrations in Pork

The HHRAP [35] recommends that the concentrations of COPC in pork tissue can be calculated based on the COPC amount that swine consume through incidental ingestion of soil and through a diet consisting of grain silage.

The HHRAP [35] recommends and discusses (in Table B-3-12, Appendix B) the following equation to estimate COPC concentration in pork:

$$A_{pork} = (\sum(F_i \times Qp_i \times P_i) + Q_S \times C_S \times B_S) \times Ba_{pork} \times MF \quad 3.8$$

Where

A_{pork} = The mercury concentration in pork (mg COPC/kg FW tissue)

F_i = Plant type *i* fraction grown on contaminated soil and ingested by the animal (swine) (unitless)

Qp_i = Plant type *i* quantity eaten by the animal (swine) each day (kg DW plant/day)

P_i = The mercury concentration in plant type *i* eaten by the animal (swine) (mg/ kg DW)

Qs = Soil quantity eaten by the animal (swine) (kg /day)

Cs = Average soil concentration over exposure duration (mg COPC/kg soil)

Bs = Bioavailability factor of soil (unitless)

Ba_{pork} = Biotransfer factor of COPC for pork (day/kg WW tissue)

MF = Metabolism factor (unitless)

3.6.4.6 Calculation of COPC Concentrations in Chicken and Eggs

The COPC amounts that chickens consume through incidental ingestion of soil and through their diet was considered in order to calculate the concentration of chemicals in locally raised chicken and eggs.

The HHRAP [35] recommends and discusses (in Tables B.3.13 and B.3.14, Appendix B) the following equation to estimate COPC concentration in chicken and eggs:

$$A_{chicken}\ or\ A_{egg} = (\sum[F_i \times Qp_i \times P_i] + Q_S \times C_S \times B_S) \times \left(Ba_{egg}\ or\ Ba_{chicken}\right) \qquad 3.9$$

Where

$A_{chicken}$ = The concentration of mercury in chicken (mg COPC/kg FW tissue)

A_{egg} = The concentration of mercury in eggs (mg COPC/kg FW tissue)

F_i = Plant type i (grain) fraction grown on contaminated soil and ingested by the animal (chicken) (unitless)

Qp_i = Plant type i (grain) quantity eaten by the animal (chicken) each day(kg DW plant/day)

P_i = The concentration of mercury in plant type i (grain) eaten by the animal (chicken) (mg/kg DW)

Qs = Soil quantity eaten by animal (chicken) (kg/day)

Cs = Average concentration of soil over exposure duration (mg COPC/kg soil)

Bs = Bioavailability factor of soil (unitless)

$Ba_{chicken}$ = Biotransfer factor of COPC for chicken (day/kg FW tissue)

Ba_{egg} = Biotransfer factor of COPC for eggs (day/kg FW tissue)

The biotransfer is used to estimate concentrations of COPC in chicken or eggs. The approach presented in section 3.6.3.3 was used to calculate the concentration of COPC in grain. In addition, the equations referenced in section 3.6.3.2 were used to calculate COPC concentrations in soil.

3.6.4.7 Calculation of COPC Concentrations in Surface Water

The fish ingestion and drinking water exposure pathways were evaluated by calculating the concentration of COPC in surface water for water bodies. It uses a sediment delivery ratio and the Universal Soil Loss Equation (USEL) to estimate the soil erosion rate from the watershed. The equations recommended by [35] were used to calculate surface water concentrations including a sediment mass balance.

The water column COPC concentration can be defined as the sum of the concentration of COPC associated with suspended solids and the COPC concentration dissolved in water [35]. Table B-4.1 through Table B-4.28 in [35] present the equation recommended to calculate surface water concentrations.

3.6.4.8 Calculation of COPC Concentrations in Fish

According to [35], concentrations of COPC in fish can be calculated using a bioaccumulation factor (BAF), a bioconcentration factor (BCF), or a biotasediment accumulation factor (BSAF).

Generally, COPC concentrations in fish can be calculated using two methods. In the first method, it can be estimated by multiplying a chemical-specific bioaccumulation factor by the dissolved phase water concentration. In the second method, it can be estimated by multiplying a chemical-specific bioconcentration factor by the dissolved phase water concentration [35].

The COPC concentration sorbet to bed sediment (C_{sb}) used to estimate the concentration of COPC in fish can be calculated by using following equation [35]:

$$C_{sb} = f_{bs} \times C_{wtot} \times \left(\frac{Kd_{bs}}{\theta_{bs}+Kd_{bs}\times C_{BS}}\right) \times \left(\frac{d_{wc}+d_{bs}}{d_{bs}}\right) \quad 3.10$$

Where

C_{sb} = Concentration of mercury sorbed to bed sediment (mg COPC/ kg sediment)

f_{bs} = Fraction of total water body mercury concentration in benthic sediment (unitless)

C_{wtot} = Total water body mercury concentration (mg COPC/L water body)

Kd_{bs} = Bed sediment/sediment pore water partition coefficient (L COPC/kg water body).

θ_{bs} = Porosity of bed sediment.

C_{BS} = Concentration of bed sediment.

d_{wc} = Depth of water column (m)

d_{bs} = Depth of upper benthic sediment layer (m)

3.6.5 Inhalation Exposure Pathways

The potential impacts of chronic exposure through direct inhalation of vapor and particulate COPCs on human health as well as environment were considered for all receptors. The values of specific-toxicity chemicals were used for individual cancer risk and non-cancer hazard resulting from concentrations of COPC in air. This methodology does not account for time spent indoors where particulates are more likely not be inhaled and to settle out or for time spent away from the maximum air concentration point[35].

3.6.5.1 Ingestion Exposure Pathways

The chemical intakes through ingestion can be estimated by using following equation [35]:

$$I = \frac{C \times IR \times EF \times ED}{BW \times AT} \quad 3.11$$

Where

I = Intake (mg/kg.day)

C = The concentration of mercury in medium of concern.

IR = Ingestion rate.

EF = Exposure frequency (day/year)

ED = Exposure duration (years)

BW = Body weight (kg)

AT = Average time (days)

3.6.5.2 Food Ingestion Exposure Pathways

Animals and plants within the area of concern may deposit onto the earth's surface or take up COPCs in the air. The food ingestion pathways consider the potential for human exposure to COPCs. There are some factors, for example; food consumption rate, diet, the COPC media

concentrations, and the percentage of the diet, that have some effects on human exposure through food ingestion [35].

3.6.5.3 Soil Ingestion Exposure Pathways

The concentration of COPC in the soil will be varied with distance from the existing and proposed sources based on air dispersion modeling and deposition of COPCs. The potential for human exposure to COPCs which is primarily from hand-to-mouth behavior was considered for the soil ingestion pathway. Human exposure through soil ingestion was influenced by some factors [35]. These factors include: the rate of soil ingestion over the exposure time, soil COPC concentrations and the exposure frequency and duration.

3.6.5.4 Drinking Water Ingestion Exposure Pathways

A surface water body that may receive emissions deposition from existing and proposed plants was the main source of drinking water in this study.

Human exposure via surface water ingestion was influenced by some factors [35]. These factors including; the water consumption rate, the exposure frequency, and duration, and the estimated COPC concentrations in surface water.

3.6.5.5 Body Weight

The risk characterization equations used the choice of body weight presented in [35] Appendix C. The HHRAP [35] recommends that a weight of 15 kilograms for the child can be used in the human risk assessment.

In this study, an average adult and child body weights of 70 kg and 15 kg were used respectively.

3.6.5.6 Exposure Frequency

According to [35], the receptors in each exposure scenario were exposed to all of the exposure pathways of the scenario-specific 350 days per year. This means that the exposure frequency is 350 days/year).

3.6.5.7 Exposure Duration

Based on [35] recommendations, the assumed duration of exposure to the modeled concentrations of COPCs vary based on age and the exposure pathway. Additionally, the operating life of the facility being evaluated must be considered in risk calculations. The adult chronic exposure scenarios were based on the assumption that an adult is located at the location of maximum impact continuously for the entire exposure duration. For adult farmers, the direct exposure to emissions by inhalation occurs for the anticipated operating life of the facility, but indirect exposure from ingestion of home-grown produce and livestock continues for 40 years. Each exposure scenario receives indirect exposure through ingestion of contaminated homegrown food and direct contact with soil and water.

Chronic exposure scenarios for all children in the assessment area are based on the assumption that a child resides at the location of maximum impact from the second through the sixth year of life [35]. During this time, the child also receives indirect exposure to the same pathways as described for adults and contaminated homegrown food. The same considerations for exposure apply to infants for the first year of life. Infants in the assessment area are assumed to be exposed to COPCs through breast milk, inhalation pathway and consumption of home-grown food [35]. The HHRAP recommends the exposure duration values presented in Table 3.15.

Table 3.15: Values of exposure duration [35].

Recommended Exposure Scenario Receptor	Value	Source
Child Resident	6 years	[46], [47]
Adult Resident	30 years	[46], [47]
Fisher	30 years	[46], [47]
Fisher Child	6 years	Assumed to be the same as the Child Resident
Farmer	40 years	[48], [47]
Farmer Child	6 years	Assumed to be the same as the Child Resident

3.6.5.8 Quantification of Cancer Risk and Non-cancer Hazard

- **Cancer Risk**

The carcinogenic risk is estimated as the probability of an individual developing cancer over a lifetime as a result of exposure to specified emissions [35]. For this study, carcinogenic risk is estimated as an incremental probability of fatal cancer from exposure to emissions from each proposed plants.

The potential for cancer risk caused by inhalation exposure was calculated by multiplying a chemical-specific unit risk factor by the annual average air concentration. Individual ELCR from inhalation exposure was calculated by using following equation [35]:

$$\text{Cancer Risk} = Ca \times URF \qquad 3.12$$

Where

C_a = Annual average concentration of mercury in air (gram/m^3)

URF = Unit risk factor (gram/m^3)$^{-1}$

The potential for cancer risk caused by indirect exposure pathways was calculated by multiplying the chemical-specific cancer slop factor by the estimated lifetime average daily dose [35]. The potential for cancer risk can be calculated by using the following equation [35]:

$$\text{Cancer Risk} = \text{Lifetime average daily dose} \times \text{Cancer slop factor} \quad (3.13)$$

- **Non-cancer Hazard**

For COPCs with non-carcinogenic effects, the potential for non-carcinogenic toxic effects in an individual is evaluated by comparing the estimated exposure level over a specified time period with the appropriate non-cancer reference dose [35]. Both direct and indirect exposures are considered in the estimation of non-cancer health effects.

In this study, the annual average concentration of COPC in the air was compared to a chronic reference concentration and the maximum 1-hour concentration was also compared to an acute inhalation exposure criterion in order to evaluate the potential for non-cancer health effects associated with inhalation exposure to the COPCs.

The potential for non-cancer hazard from inhalation exposure can be calculated by using the following equation [35]:

$$Hazard\ quotient = \frac{C_a}{RfC\ or\ AIEC} \quad (3.14)$$

Where

C_a = Annual average concentration of mercury in air (mg/m^3)

RfC = Reference concentration (mg/m^3)

AIEC = Acute inhalation exposure criterion (mg/m^3)

The estimated average daily dose was compared to a reference dose derived for a similar exposure period in order to evaluate the potential for non-cancer health effects associated with

indirect exposure to the COPCs. The individual non-cancer hazards from ingestion exposures was calculated by using the following equation [35]:

$$Hazard\ quotient = \frac{Average\ daily\ dose\ (mg/kg.day)}{Reference\ dose\ (mg/kg.day)^{-1}} \quad 3.15$$

Chapter 4 : Risk Characterization

4.1 Introduction

The risk characterization for the proposed plant locations was performed in accordance with HHRAP guidelines. Air dispersion modeling results are combined with toxicity information, emissions estimates, and other site-specific information to generate risk and hazard values for individuals exposed to COPC emissions. The risk and hazard values for individuals can then be compared to acceptable benchmarks for human health. The magnitude and types of risks depend on the nature, duration, and frequency of exposure to the selected chemicals emitted from the process and the characteristics of the exposed human receptors.

Quantitative estimates of carcinogenic risks and non-carcinogenic hazards were calculated for direct inhalation exposures and indirect exposures to the COPC emissions. Estimated total carcinogenic risk was compared to an acceptable level of 1 case in one hundred thousand (1×10^{-5}).

The typical benchmark for evaluation of the estimated long-term, non-carcinogenic hazard from airborne unit emissions is 1.0. US EPA Region 6 recommended that a hazard index benchmark of 0.25 be utilized to take background concentrations of COPCs into consideration in areas where the significant industrial activity takes place. In addition, an acute hazard analysis was performed and the results were compared to an acceptable HI of 1.0.

4.2 Characterization of Carcinogenic Health Effects

The carcinogenic risk is estimated as the probability of an individual developing cancer over a lifetime as a result of exposure to specified emissions. In this study, carcinogenic risk is

estimated as an incremental probability of fatal cancer from exposure to emissions from each proposed plant for specific potential carcinogens (i.e., excess individual lifetime cancer risk).

According to the EPA website, environmental exposures to mercury are not likely to cause cancer in humans. As a result, carcinogenic health effects will not be discussed in this analysis.

4.3 Characterization of Non-Carcinogenic Health Effects

For COPCs with non-carcinogenic effects, the potential for non-carcinogenic toxic effects in an individual is evaluated by comparing the estimated exposure level over a specified time period with the appropriate non-cancer reference dose. The non-carcinogenic hazard quotient (HQ) is a unitless value that considers a threshold exposure limit that below which health effects are not expected to occur. Sensitive populations are considered in this benchmark. HQs represent a non-carcinogenic hazard associated with an individual COPC and a specific exposure pathway.

Both direct and indirect exposures are considered in the estimation of non-cancer health effects. HQs for direct exposures to COPCs are calculated by dividing the inhalation intake of a COPC by the inhalation reference dose (RfD) for that COPC. HQs for indirect exposures to COPCs are calculated similarly, and incorporate the averaging time for non-carcinogenic health effects. A Hazard Index (HI) is generated by summing HQ's for all selected COPCs for a given receptor.

4.4 Characterization of Acute Health Effects

Potential acute hazards associated with short-term emission release events were evaluated for the COPC. The acute HQ (HQA) represents the hazard associated with short-term direct exposure to the COPC in the air during a short-term emission release event. HQAs for the COPC were summed to calculate the overall acute HI.

4.5 Risk Characterization

Potential health risks associated with exposure to mercury emissions from the proposed industrial plants will be identified in following sections.

4.5.1 Proposed Plants Exposure Assessment

The total hazard quotients estimated by IRAP-h View, based on the air concentrations and depositions predicted by AERMOD for worst-case scenarios and maximum emissions from the proposed plant were calculated. The health risk assessment for all proposed plant locations will be discussed in the following sections. This risk assessment is based on the assumption that an individual living in the area surrounding the proposed locations would consume beef, milk, eggs, poultry, pork and vegetables produced from the farms in the surrounding areas.

As the results obtained from IRAP-h View model are in excess of 500 pages, excerpts for the worst-case scenarios will be discussed in the following sections.

Total Summary

The total non-cancer hazards estimated for each receptor population, for COPC, overall exposure pathways, and for all proposed locations are presented in following sections. U.S. EPA generally finds non-cancer hazard indices of less than 1 acceptable.

For the first proposed location, the total hazard indices are shown in Table 4.1. It can be seen that the highest identified hazard index is for a fisher adult and fisher child exposure pathways with predicted values of 1.87E+01 and 1.32E+01 respectively. These hazard indices are higher than the target hazard index of 1. Figure 4.1 shows the worst-case scenario for all exposure scenarios. It can be seen that the total non-cancer hazards are higher than the target hazard index of 1. In addition, we can note that the total non-cancer hazards vary over the area of concern. The

lowest identified hazard quotient is in the south-eastern area of proposed location. In contrast, the highest identified hazard quotient for all exposure scenarios is in the north area (Lake Erie area) of the proposed location with the predicted value of 1.87E+01 at receptors 136, 137, 138, 138, 139, 140, 141, 142, and 143 for the hazard quotient.

Table 4.1: The total non-cancer hazards predicted for each receptor and for COPC.

Resident		Farmer		Fisher	
Adult	Child	Adult	Child	Adult	Child
1.07E-02	3.12E-02	2.35E-02	4.86E-02	1.87E+01	1.32E+01

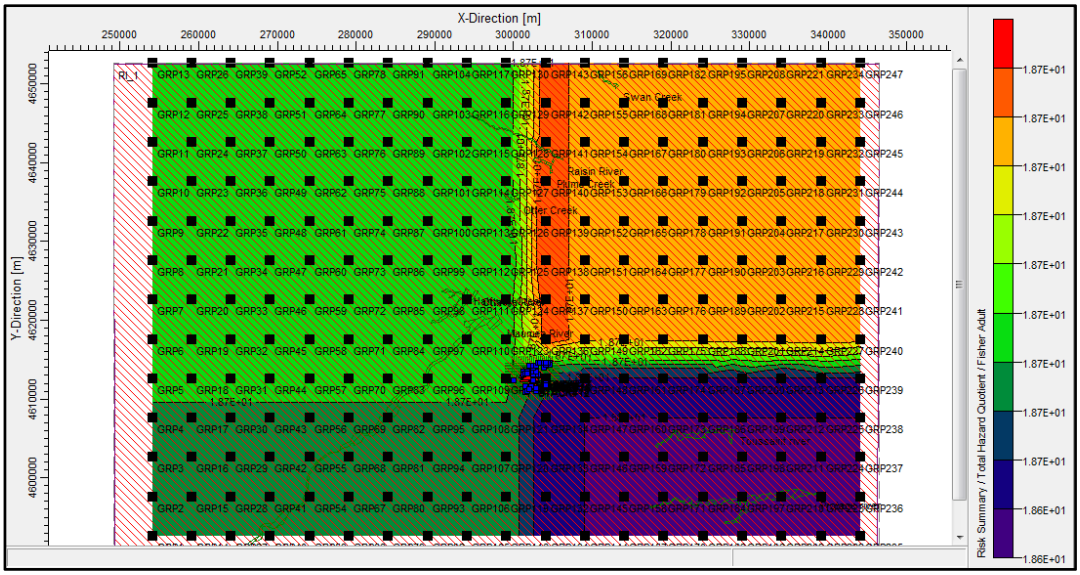

Figure 4.1: The contour plot of the total hazard quotient for the first proposed location.

For the second proposed location, Table 4.2 summarizes the total hazard indices for each receptor, for the COPC and aver all exposure pathways. It can be seen that the highest identified hazard index is for a fisher adult and fisher child exposure pathways with predicted values of 1.10E+02 and 7.78E+01 respectively. It can be seen that the total non-cancer hazards are higher

than the target hazard index of 1. Figure 4.2 shows the worst-case scenario for all exposure scenarios. It can be seen from the IRAP results that the total non-cancer hazards vary over the area of concern. The lowest identified hazard quotient is in the whole area of concern except the north-eastern area of the proposed location with the predicted value of 1.0991E+2. In contrast, the highest identified hazard quotient for all exposure scenarios is in the north-eastern area (Lake Erie area) of the proposed location with the predicted value of 1.10E+02 at receptor 136 for the hazard quotient.

Table 4.2: The total non-cancer hazards predicted for each receptor and for COPC.

Resident		**Farmer**		**Fisher**	
Adult	Child	Adult	Child	Adult	Child
1.58E-01	4.24E-01	3.54E-01	7.32E-01	1.10E+02	7.78E+01

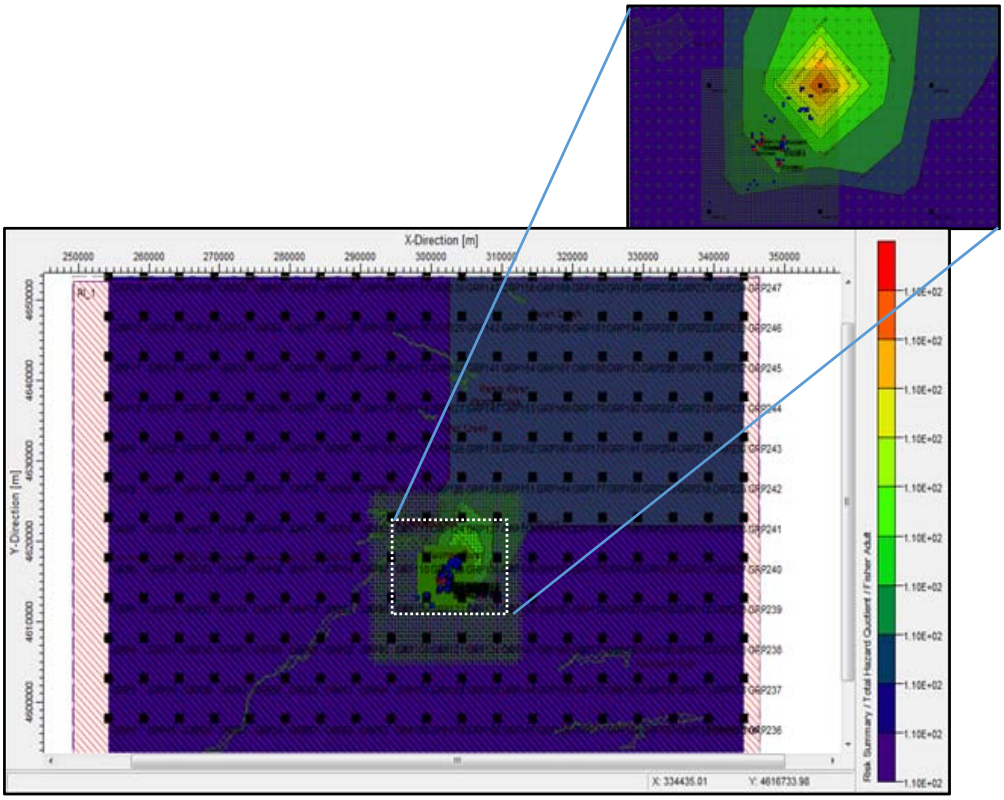

Figure 4.2: The contour plot of the total hazard quotient for the second proposed location.

For the third proposed location, Table 4.3 summarizes the total hazard indices for each receptor, for the COPC and over all exposure pathways. It can be seen that the highest identified hazard index is also for a fisher adult and fisher child exposure pathways with predicted values of 1.36E+01 and 9.58E+00 respectively. It can be seen that the total non-cancer hazards are higher than the target hazard index of 1. Figure 4.3 shows the worst-case scenario for all exposure scenarios. The lowest identified hazard quotient is in the whole area of concern except the north area of the proposed location with the predicted value of 9.58E+00. In contrast, the highest identified hazard quotient for all exposure scenarios is in the north-western area (Lake Erie area)

of the proposed location with the predicted value of 1.36E+01 at receptors 149, 150, 151, 152, 153, 154, 155, and 155 for the hazard quotient.

Table 4.3: The total non-cancer hazards predicted for each receptor and for COPC.

Resident		Farmer		Fisher	
Adult	Child	Adult	Child	Adult	Child
1.47E-02	3.94E-02	3.28E-02	6.78E-02	1.36E+01	9.58E+00

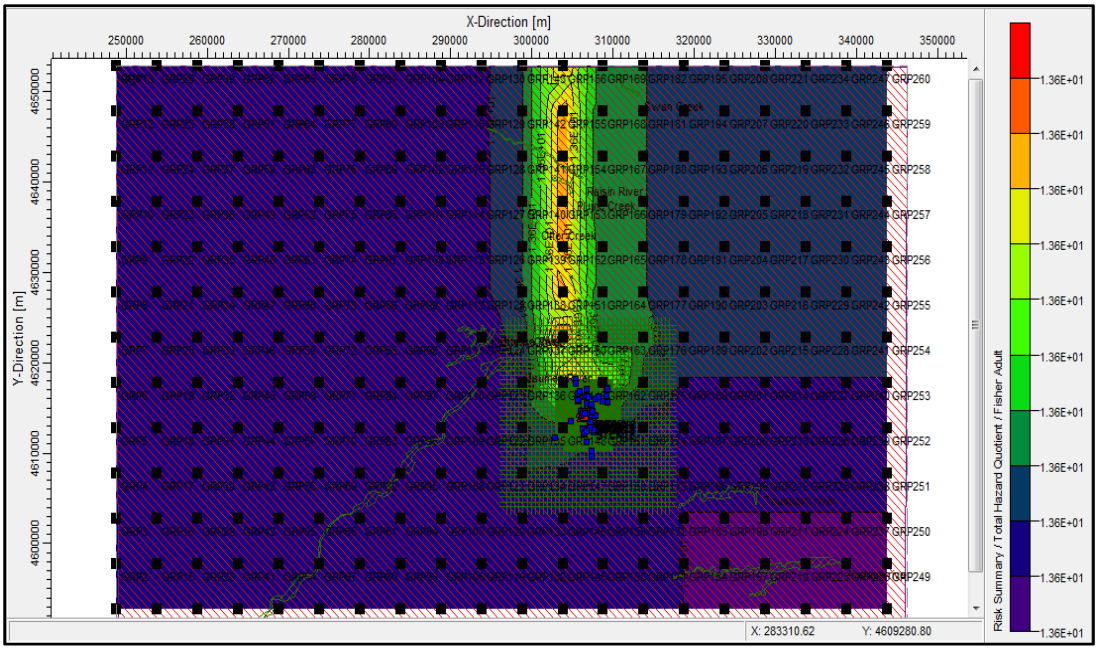

Figure 4.3: The contour plot of the total hazard quotient for the third proposed location.

For the fourth proposed location, Table 4.4 summarizes the total hazard indices for each receptor, for the COPC and overall exposure pathways. It can be seen that the highest identified hazard index is also for a fisher adult and fisher child exposure pathways with predicted values of 1.09E+01 and 7.70E+00 respectively. It can be seen that the total non-cancer hazards are higher

than the target hazard index of 1. Figure 4.4 shows the worst-case scenario for all exposure scenarios. The lowest identified hazard quotient is in the south-eastern area of the proposed location with the predicted value of 7.70E+00 at receptors 256, 243, 230, 217, 204, 191, 178, and 165. In contrast, the highest identified hazard quotient for all exposure scenarios is in the north-eastern area (Lake Erie area) of the proposed location with the predicted value of 1.09E+01 at receptor 141 for the hazard quotient.

Table 4.4: The total non-cancer hazards predicted for each receptor and for COPC.

Resident		**Farmer**		**Fisher**	
Adult	Child	Adult	Child	Adult	Child
9.83E-03	2.56E-02	2.11E-02	2.79E-03	1.09E+01	7.70E+00

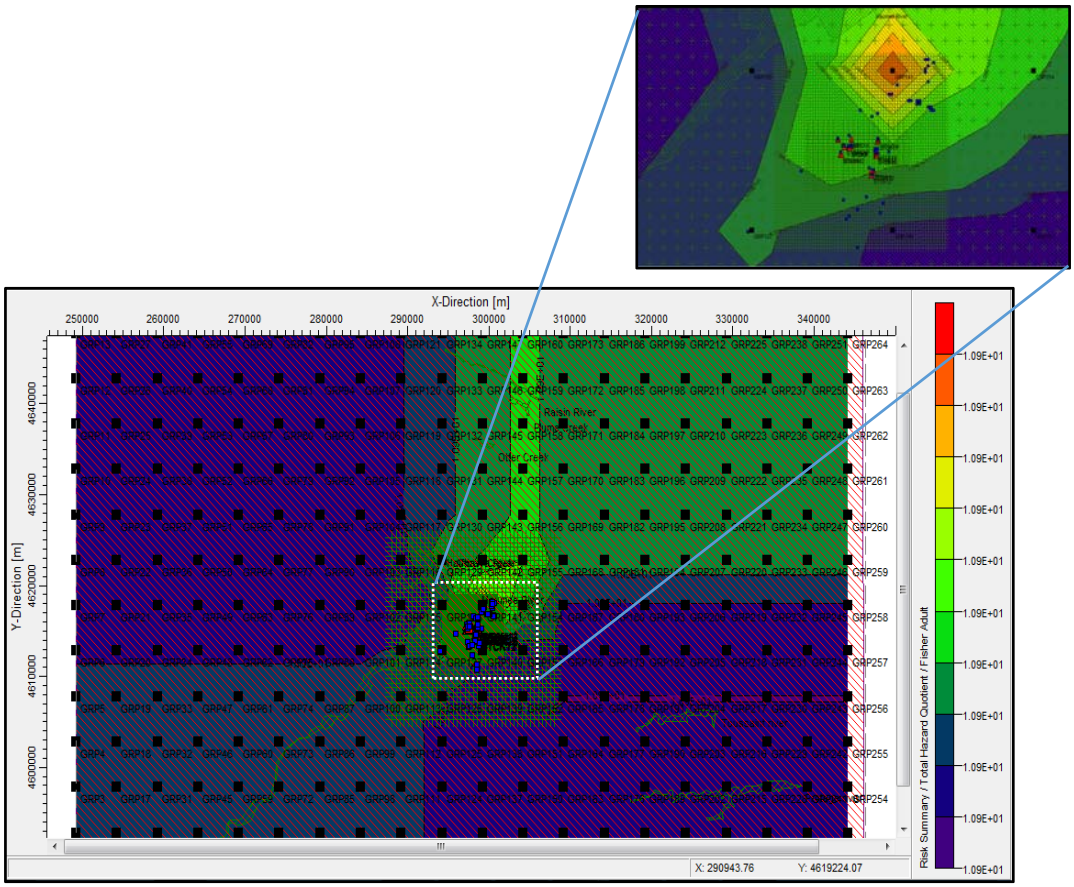

Figure 4.4: The contour plot of the total hazard quotient for the fourth proposed location.

In conclusion, we can see that the fourth proposed location has the lowest total hazard quotient. These total hazard quotients are higher than the benchmarks of 1. As a result, the hazard quotients from exposure to emissions from the fourth proposed location are expected especially for the fisher exposure pathways. As we mentioned before, the methyl-mercury is the primary form of mercury that poses health risks. Since the consumption of contaminated fish is the common pathway of human exposure to methyl-mercury, it is highly recommended that people, especially women who may become pregnant, pregnant women, nursing mothers, and young children, living in the area surrounding the proposed location do not eat fish or shellfish.

Acute Inhalation Risk

The ambient air concentration calculated by AERMOD were compared to non-cancer HQs for COPC to calculate the acute hazard quotient. The U.S. EPA-OSW recommendations are followed by IRAP in order to calculate the acute hazard quotient. The estimation of acute hazard quotient for all proposed location will be discussed in following sections.

For the first proposed location, the acute inhalation quotient risk ranges from 9.0747E-05 to 1.5050E-04 for all exposure scenarios and for all sources. Figure 4.5 shows the example of the worst-case scenario for all exposure scenarios and for source 1. It can be seen that the acute inhalation quotient risk is less than the than the target hazard index of 1. In addition, we can note that the acute inhalation quotient risks varies over the area of concern. The lowest identified hazard quotient is in the areas of Lake Erie and Toledo, and the areas in between. In contrast, the highest identified hazard quotient for all exposure scenarios is in the western area of the proposed plant location with a predicted value of 1.5050E-4 for the hazard quotient.

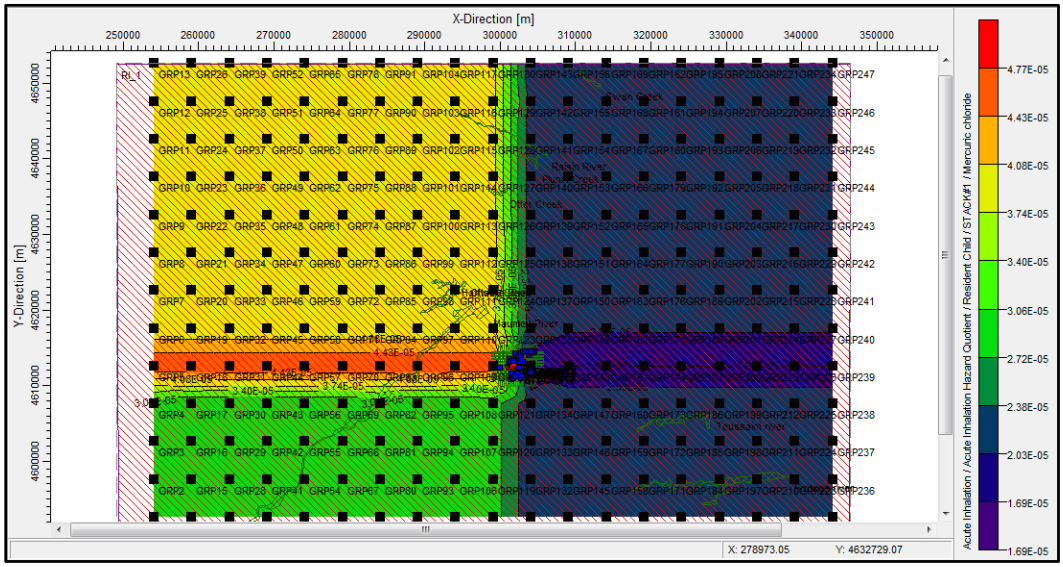

Figure 4.5: The contour plot of acute inhalation quotient risk for the first proposed location.

For the second proposed location, the acute inhalation quotient risk ranges from 4.0833E-05 to 1.7541E-04 for all exposure scenarios and for all sources. Figure 4.6 shows an example of the worst-case scenario for all exposure scenarios and for source 1. We can see that the all acute inhalation quotient risks are less than the target hazard index of 1. The lowest identified hazard quotient is in the areas of Lake Erie and Toledo. In contrast, the highest identified hazard quotient for all exposure scenarios is in the north-western area of the proposed location with a predicted value of 1.7541E-4 at receptor 123 for the hazard quotient.

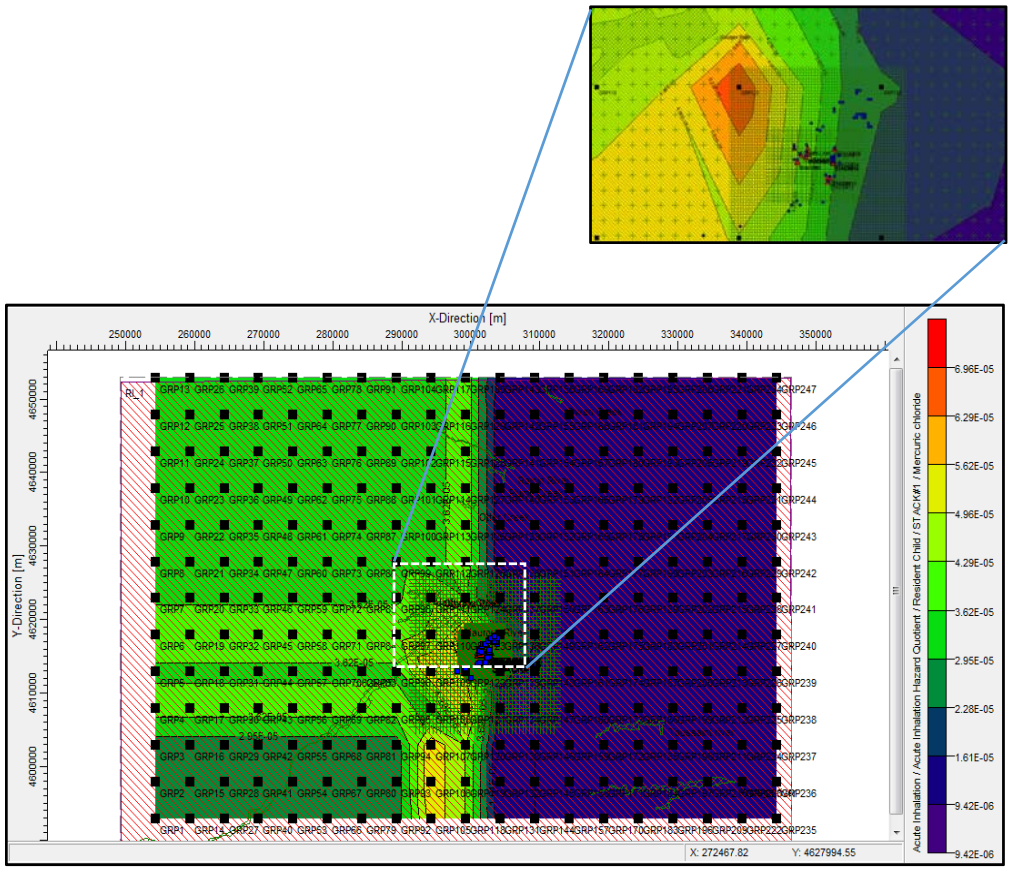

Figure 4.6: The contour plot of acute inhalation quotient risk for the second proposed location.

For the third proposed location, the acute inhalation hazard quotient for all exposure scenarios and for all sources ranges from 5.1711E-05 to 1.4770E-04. These acute inhalation hazard quotients are less than the target hazard index of 1. Figure 4.7 shows an example of the worst-case scenario for exposure scenarios and for source 1.It can be noted that the whole area of concern is still below the target hazard index of 1. The lowest identified hazard quotient is in the western area of Lake Erie. In contrast, the highest identified hazard quotient for all exposure scenarios is in the south-western area of the proposed location with a predicted value of 1.4770E-4 at receptor 148 for the hazard quotient.

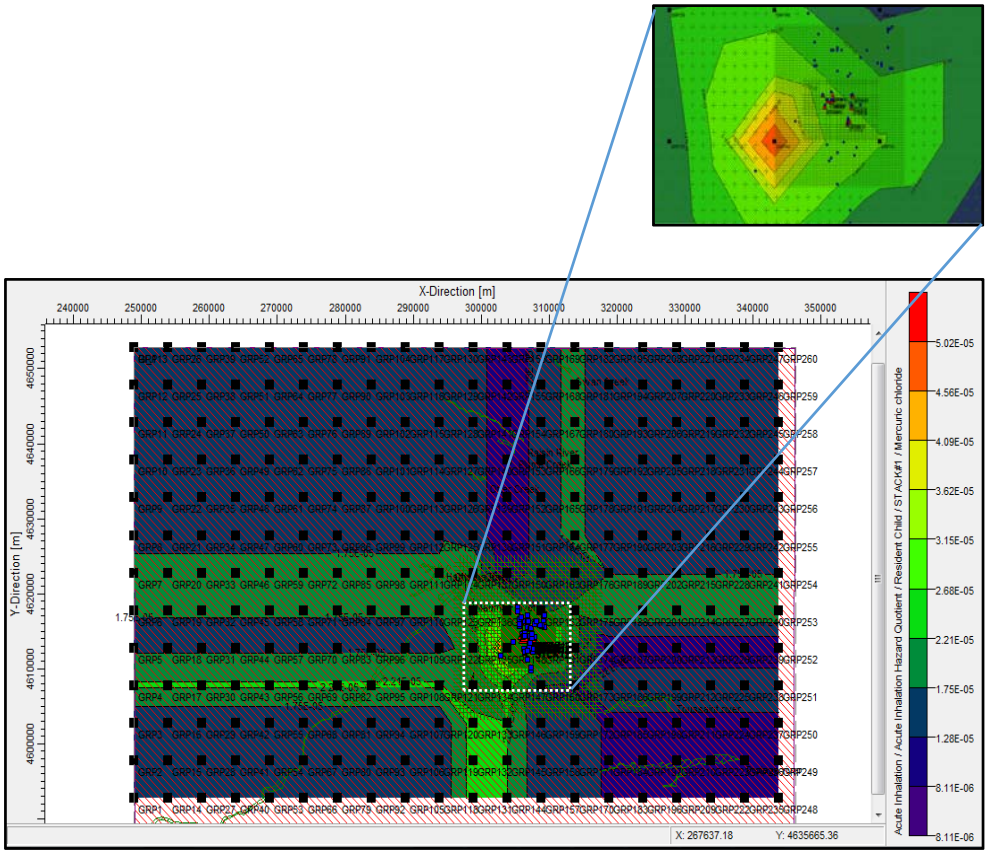

Figure 4.7: The contour plot of acute inhalation quotient risk for the third proposed location.

For the fourth proposed location, the acute inhalation hazard risk ranges from 7.4361E-05 to 1.5832E-04 for all exposure scenarios and for all sources. All these acute inhalation hazard risks are lower than the target hazard index of 1. Figure 4.8 shows the worst-case scenario for all exposure scenarios and for source 1. The lowest identified hazard quotient is in the north-eastern area of Lake Erie. In contrast, the highest identified hazard quotient for all exposure scenarios is in the south-western area of the proposed location with a predicted value of 1.5832E-04 at receptor 127 for the hazard quotient.

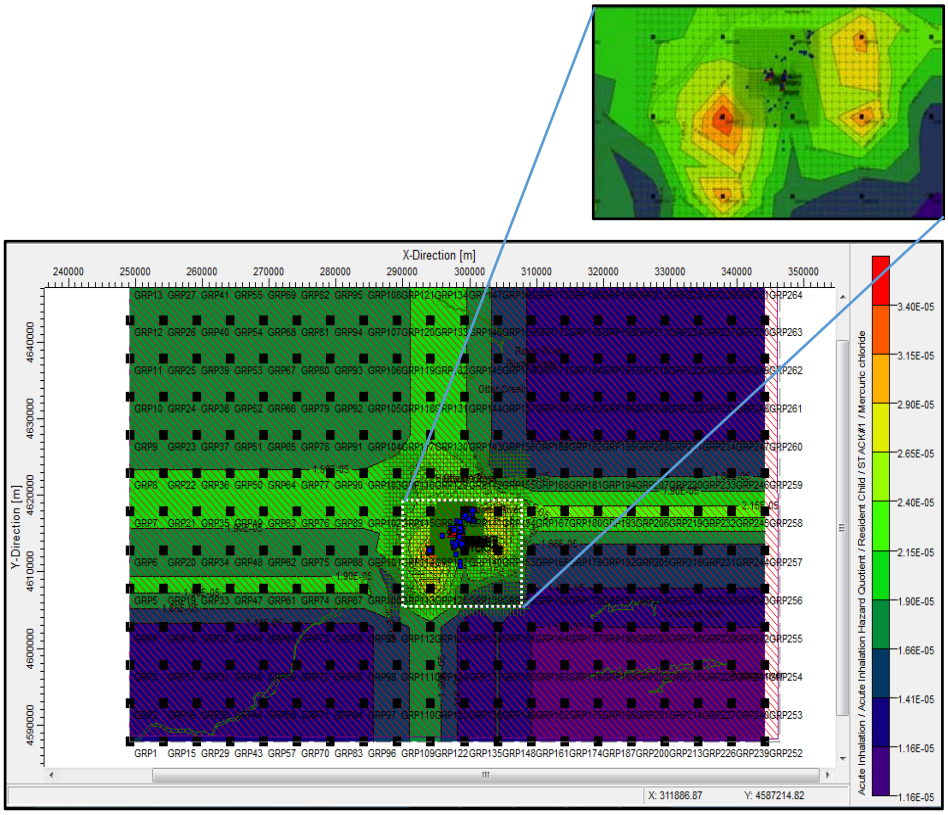

Figure 4.8: The contour plot of acute inhalation quotient risk for the fourth proposed location.

In conclusion, we can see that the second proposed location has the lowest acute inhalation hazard risk. These acute inhalation hazard risk are well within the benchmarks of 1 for the hazard quotient.

Soil Concentration

Average soil concentrations were calculated by IRAP-h View model. Table 4.3 presents the average estimated concentration of COPC in soil due to the all proposed plants.

For the first proposed location, average soil concentrations range between 2.4481E-04 to 1.2711E-01 mg COPC/kg soil for all exposure scenarios and all sources. Figure 4.9 shows the worst-case scenario for all exposure scenarios and for source 1. The lowest identified hazard quotient is in the south-eastern area of the Toledo area. In contrast, the highest identified hazard quotient for all exposure scenarios is in the north area of the proposed location with a predicted value of 1.2711E-01 mg COPC/kg soil at receptors 136,137,138,139,140,141,142 and 143 for the hazard quotient.

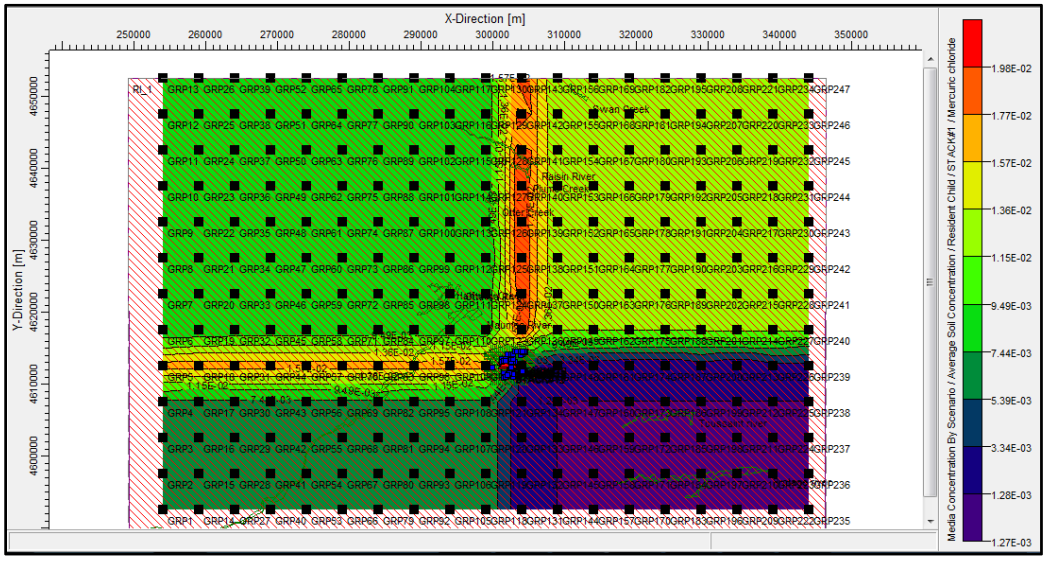

Figure 4.9: The contour plot of average soil concentration for the first proposed location.

For the second proposed location, the average soil concentrations for all exposure scenario and for all sources range from 1.7812E-4 to 2.0133E+00 mg COPC/kg soil. These concentration levels are higher and members of the local population are likely to be exposed to significant effects associated with the emission of COPC from the proposed location. Figure 4.10 shows the worst-case scenario for all exposure scenario and for source 1. We can note that the lowest identified hazard quotient is in the whole area of concern except the close area. In the close area, the highest identified hazard quotient for all exposure scenarios is predicted to be 2.0133E+00 mg COPC/kg soil at receptor 136 for the hazard quotient.

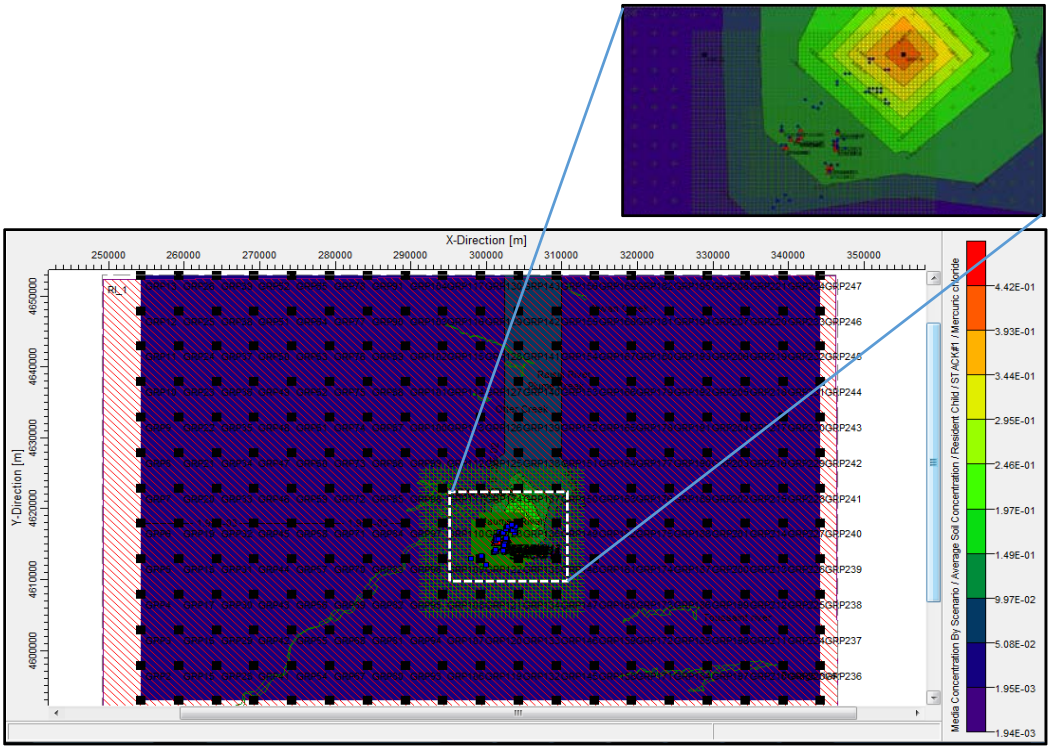

Figure 4.10: The contour plot of average soil concentration for the second proposed location.

For the third proposed location, the average soil concentrations for all exposure scenarios and for all sources range from 6.8108E-05 to 1.9279E-01 mg COPC/kg soil. Figure 4.11 shows the worst-case scenario for all exposure scenario and for source 1. We can note that the lowest

identified hazard quotient is in the whole area of concern except the north-western area. The highest identified hazard quotient for all exposure scenarios is in the area north-west of the proposed location with a predicted value 1.9279E-01 mg COPC/kg soil at receptor 149 for the hazard quotient.

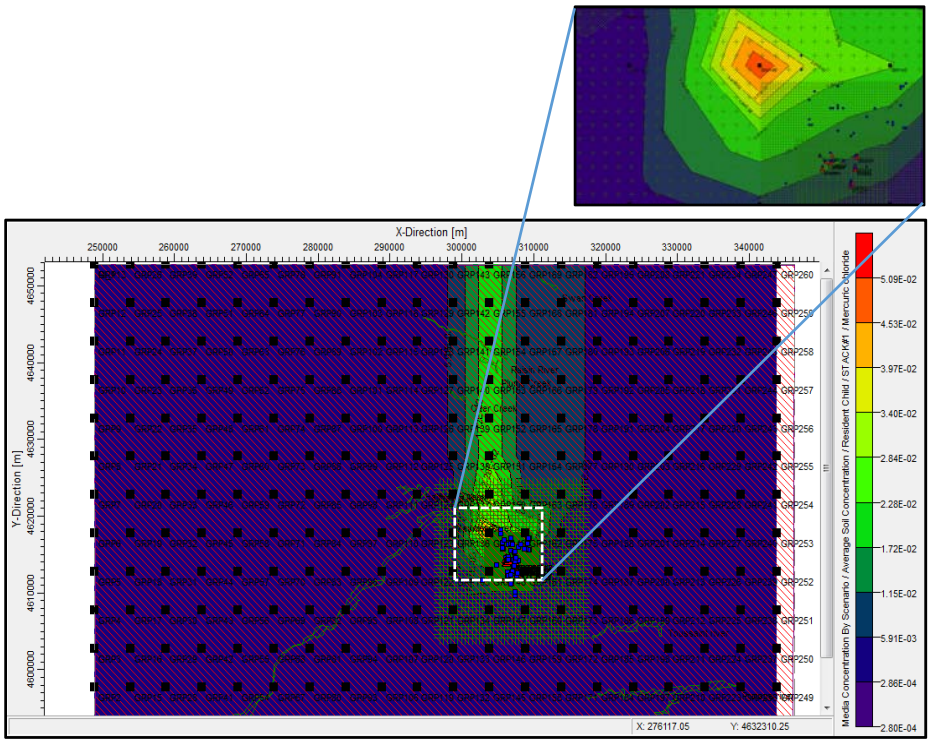

Figure 4.11: The contour plot of average soil concentration for the third proposed location.

For the fourth proposed location, the average soil concentrations for all exposure scenarios and for all sources range from 6.8266E-05 to 1.3595E-01 mg COPC/kg soil. Figure 4.12 shows the worst-case scenario for all exposure scenarios and for source 1. We can note that the lowest identified hazard quotient is in the whole area of concern except the north-eastern area. The highest identified hazard quotient for all exposure scenarios is in the north-eastern area of the proposed location with predicted value 1.3595E-01 mg COPC/kg soil at receptor 141 for the hazard quotient.

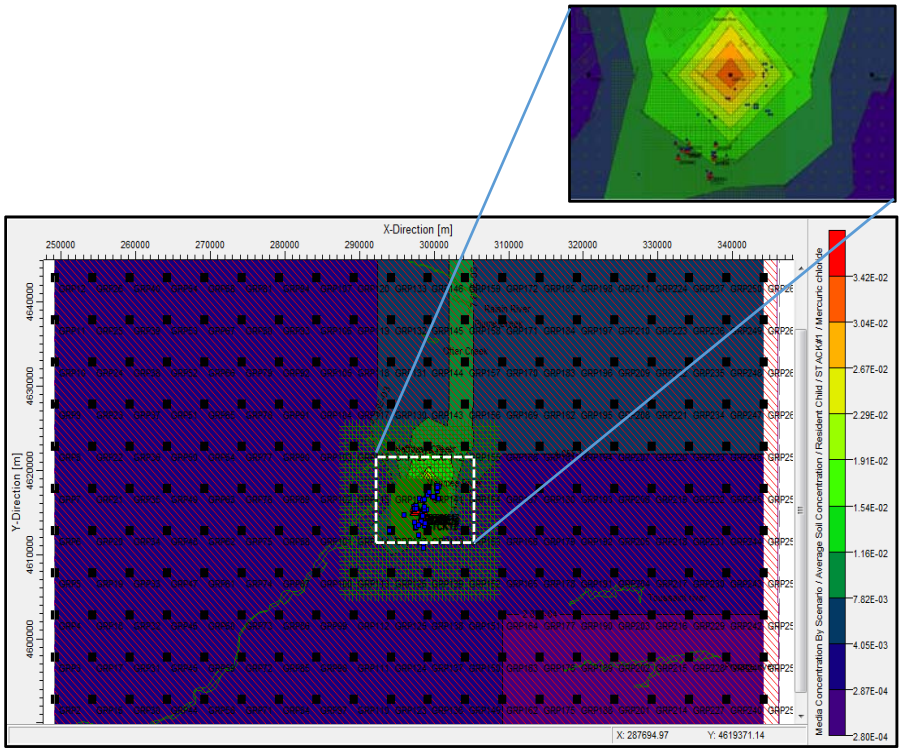

Figure 4.12: The contour plot of average soil concentration for the fourth proposed location.

In conclusion, we can note that the third proposed location has the lowest soil concentration levels. Although the estimated concentration of COPC in soil due to all proposed plants are acceptable, people working on the land in close proximity to the proposed plants may be exposed to, potentially, marginally higher levels of COPC are as a result of the operation of the proposed plants for the proportion of time they work there.

Produce Concentration

Produce concentrations for all exposure scenarios and for all sources were evaluated by IRAP-h View model. This evaluation is based on the assumption that the majority of people who are living in the area surrounding the proposed locations would consume fruits and vegetables grown in the vicinity of the proposed locations may be exposed to marginally higher levels of COPC.

For the first proposed location, the produce concentrations due to direct deposition range from 6.5395E+06 to 2.3740E-04 mg/kg. Figure 4.13 shows the worst-case scenario for all exposure scenarios and for all sources. We can note that the lowest identified hazard quotient is in the south-eastern area of the proposed location. In contrast, the highest identified hazard quotient for all exposure scenarios is in the area north of the proposed location with a predicted value 2.3740E-04 mg/kg at receptors 136, 137, 138, 139, 140, 141, 142, and 143 for the hazard quotient.

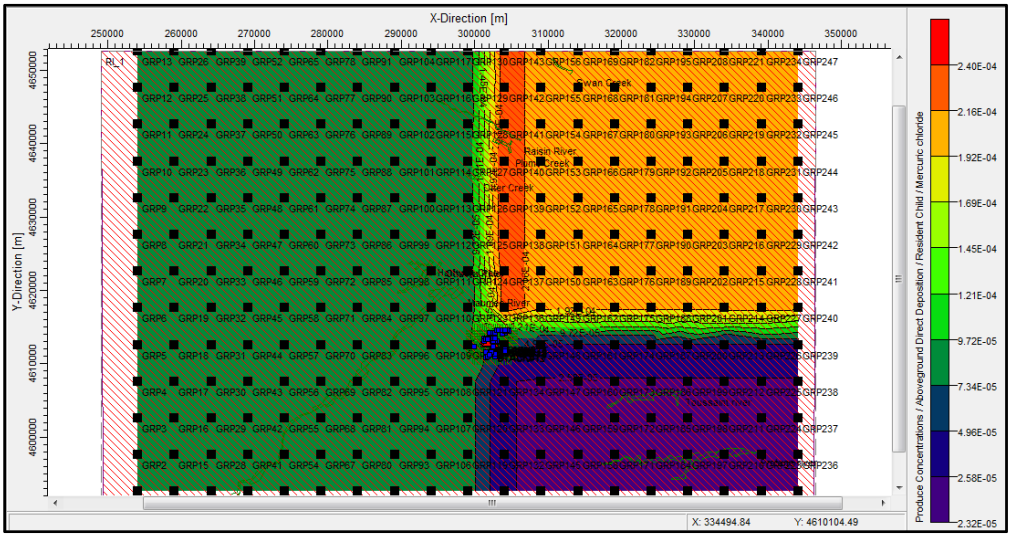

Figure 4.13: The contour plot of aboveground exposed produce concentration for the first proposed location.

For the second proposed location, the aboveground exposed produce concentration due to direct deposition for all exposure scenarios and all sources ranges from 4.4271E-06 to 4.3707E-03 mg/kg. Figure 4.14 shows the worst-case scenario for aboveground exposed produce concentration due to direct deposition for all exposure scenarios. We can note that the lowest identified hazard quotient is in the area west of the proposed location. In contrast, the highest identified hazard quotient for all exposure scenarios is in the area north east of the proposed location with a predicted value 4.3707E-03 mg/kg at receptor 136 for the hazard quotient.

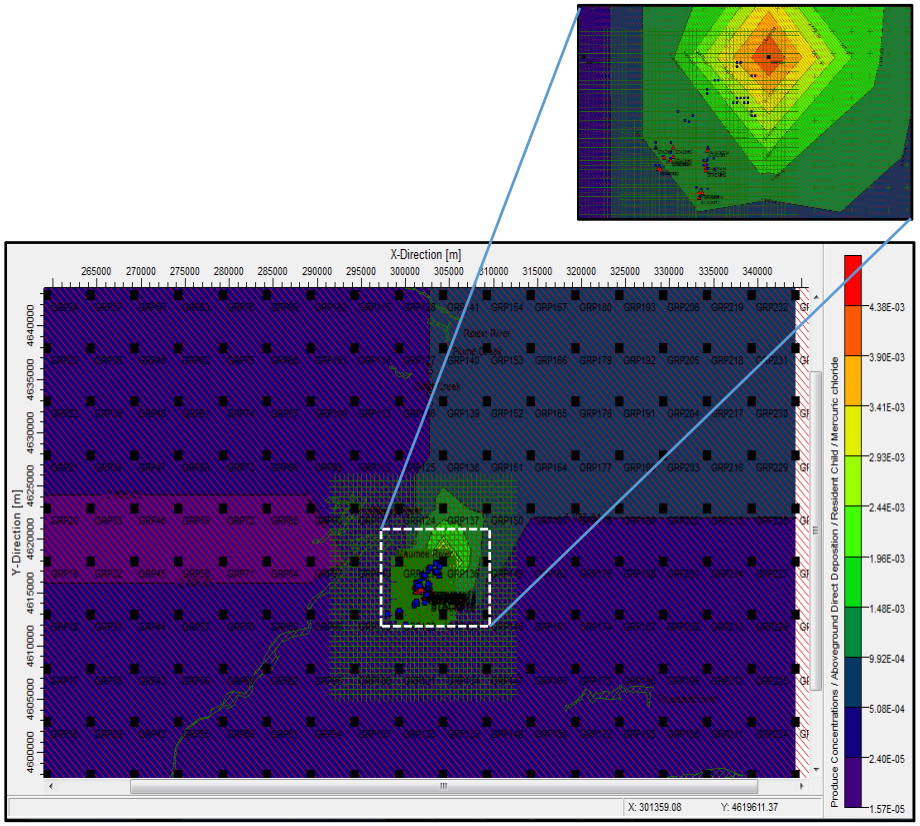

Figure 4.14: The contour plot of aboveground exposed produce concentration for the second proposed location.

For the third location, the aboveground exposed produce concentration due to direct for all exposure scenarios and for all sources ranges from 1.8472E-06 to 4.0755E-04 mg/kg. These concentration levels approaching the hazardous levels. Figure 4.15 shows the worst-case scenario for all exposure scenarios. We can note that the lowest identified hazard quotient is in the south-eastern area (Toledo area) of proposed location. In contrast, the highest identified hazard quotient for all exposure scenarios is in the area north of proposed location with a predicted value 4.0755E-04 mg/kg at receptor 150 for the hazard quotient.

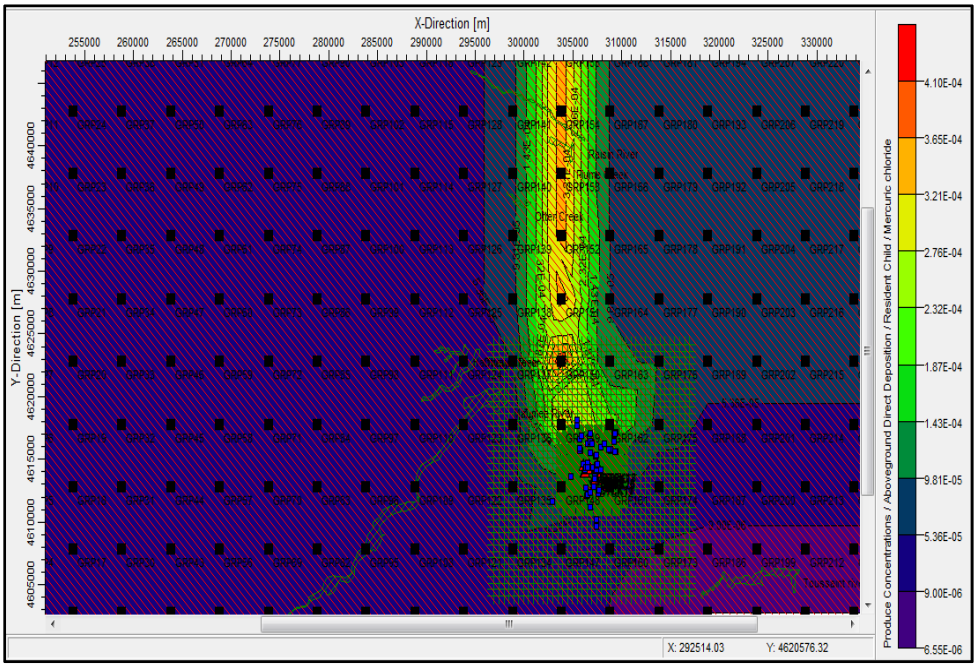

Figure 4.15: The contour plot of aboveground exposed produce concentration for the third location.

For the fourth location, the aboveground exposure produce concentration due to direct deposition for all exposure scenarios range 1.9313E-06 to 2.4649E-04 mg/kg. Figure 4.16 shows the worst- case scenario for all exposure scenarios. We can note that the lowest identified hazard quotient is in the south-eastern area of proposed location. In contrast, the highest identified hazard

quotient for all exposure scenarios is in the area north east of the proposed location with a predicted value 4.0755E-04 mg/kg at receptor 141 for the hazard quotient.

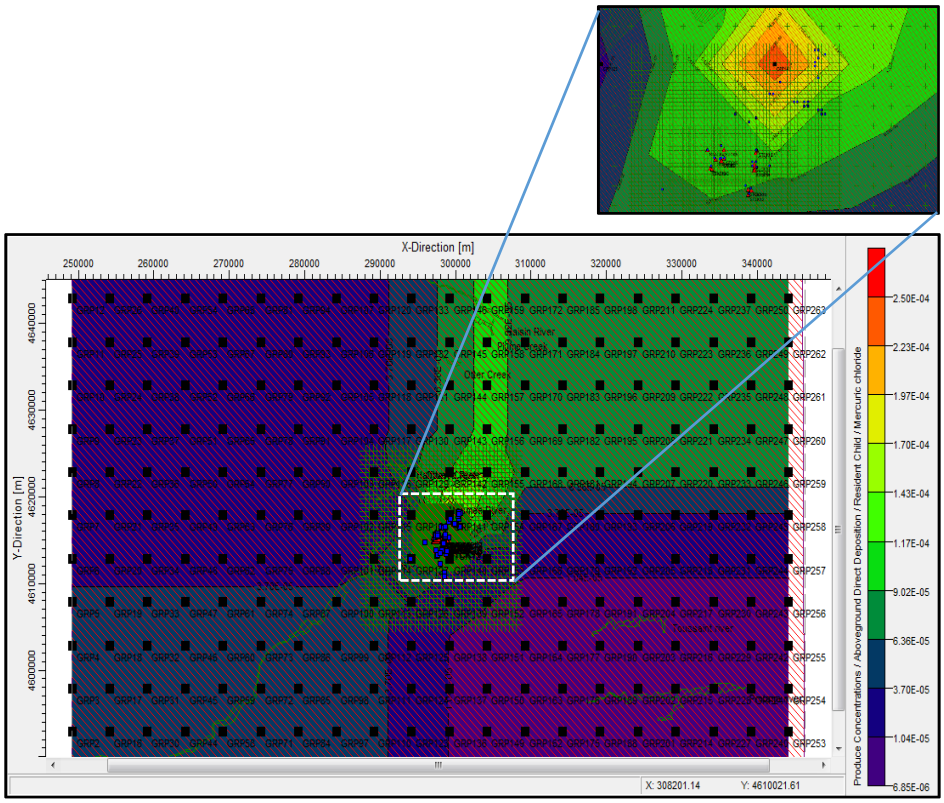

Figure 4.16: The contour plot of aboveground exposed produce concentration for the fourth proposed location.

In conclusion, we can note that the fourth proposed location has the lowest concentration levels. Although the fourth proposed location has the lowest concentration levels, people who consume fruit, vegetables and other produces grown in the vicinity of the proposed may, potentially, be exposed to marginally higher of COPC.

Beef Concentration

Beef concentrations were calculated by IRAP-h View model for all exposure scenarios and at all receptors. As with produces, beef may, potentially, be exposed to COPC through soil ingested with food picked up from the ground.

For the first proposed location, the hazard beef concentration for all exposure scenarios and for all sources ranges from 8.2718E-07 to 8.1237E-04 mg COPC/kg FW tissue. Figure 4.17 shows the worst-case scenario for all exposure scenarios and for source 7. We can note that the lowest identified hazard quotient is in the south-eastern area (Toledo area) of the proposed location. In contrast, the highest identified hazard quotient for all exposure scenarios is in the north area of proposed location with a predicted value 8.1237E-04 mg COPC/kg FW tissue at receptors 136, 137, 138, 139, 140, 141, 142 and 143 for the hazard quotient.

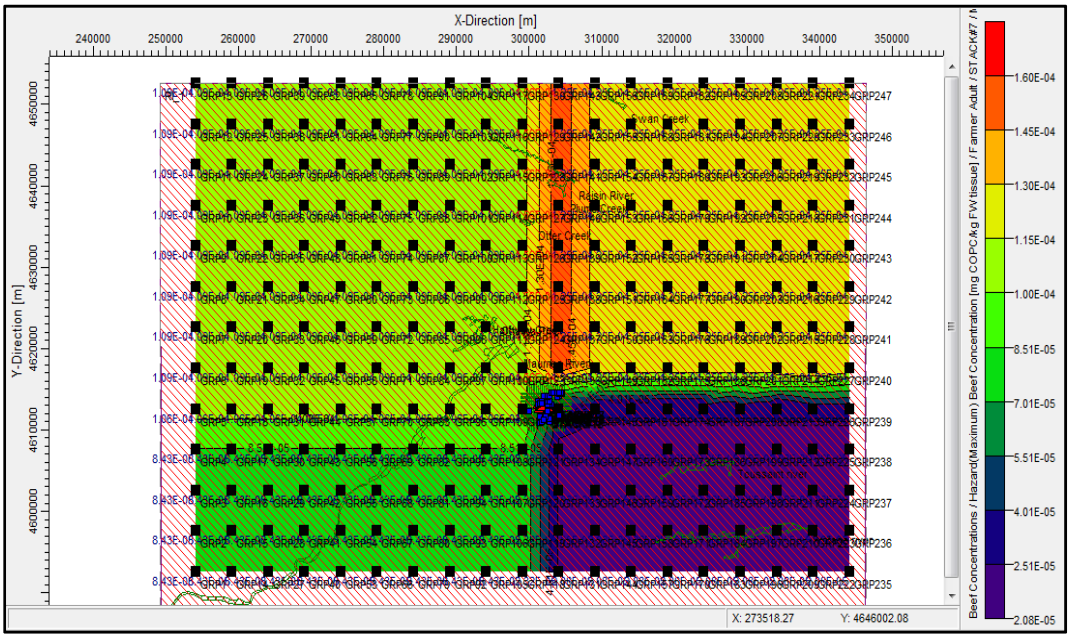

Figure 4.17: The contour plot of hazard (maximum) beef concentrations for the first proposed location.

For the second proposed location, the hazard beef concentration for all exposure scenarios and for all sources ranges from 6.0159E-07 to 1.3045E-02 mg COPC/kg FW tissue. Figure 4.18 shows the worst-case scenario for all exposure scenarios and for source 10. We can note that the lowest identified hazard quotient is at receptor 110 with predicted value 9.7216E-7 mg COPC/kg FW tissue. In contrast, the highest identified hazard quotient for all exposure scenarios is in the north-eastern area of the proposed location with a predicted value 1.3045E-02 mg COPC/kg FW tissue at receptors 136 for the hazard quotient.

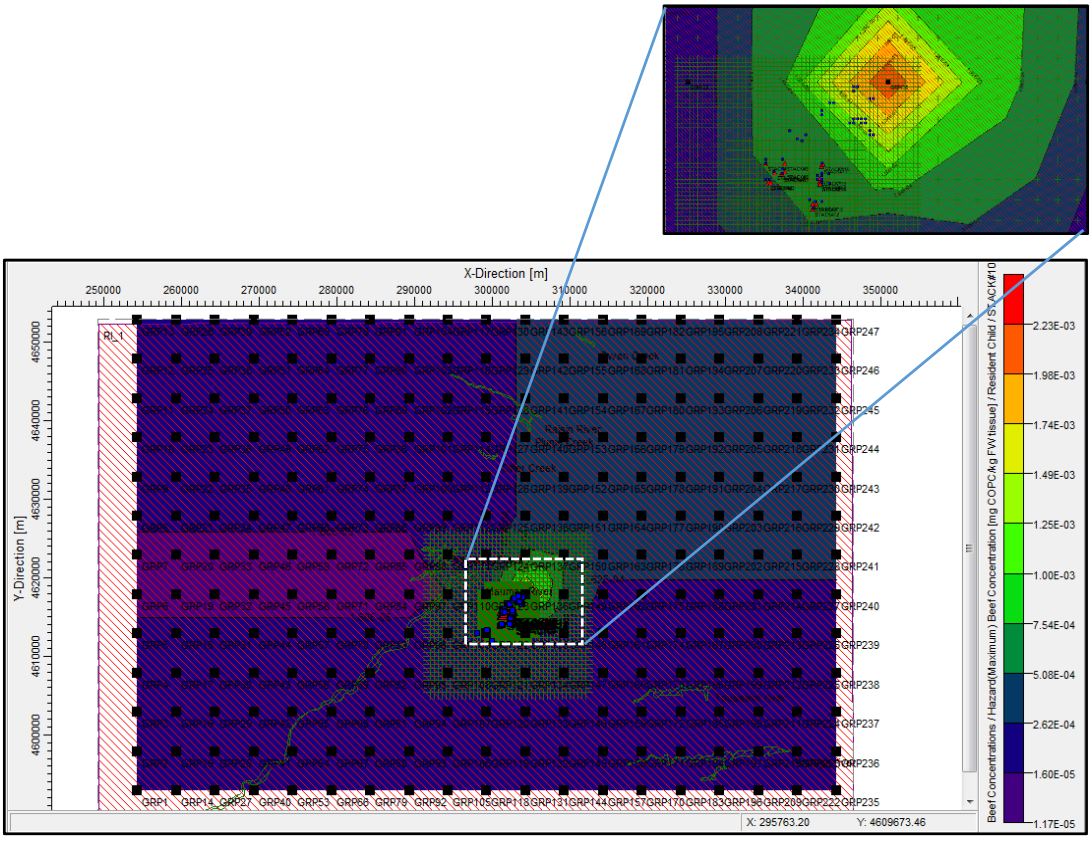

Figure 4.18: The contour plot of hazard (maximum) beef concentrations for the second proposed location.

For the third proposed location, the hazard beef concentration for all exposure scenarios and for all sources ranges from 2.4241E-07 to 1.2458E-03 mg COPC/kg FW tissue. Figure 4.19 shows the worst-case scenario for all exposure scenarios and for source 11. We can note that the

lowest identified hazard quotient is in the whole area of concern except the north-eastern area of the proposed location. In contrast, the highest identified hazard quotient for all exposure scenarios is in the north area of the proposed location with a predicted value 1.2458E-03 mg COPC/kg FW tissue at receptors 150, 151, 152, 153, 154, 155, and 156 for the hazard quotient.

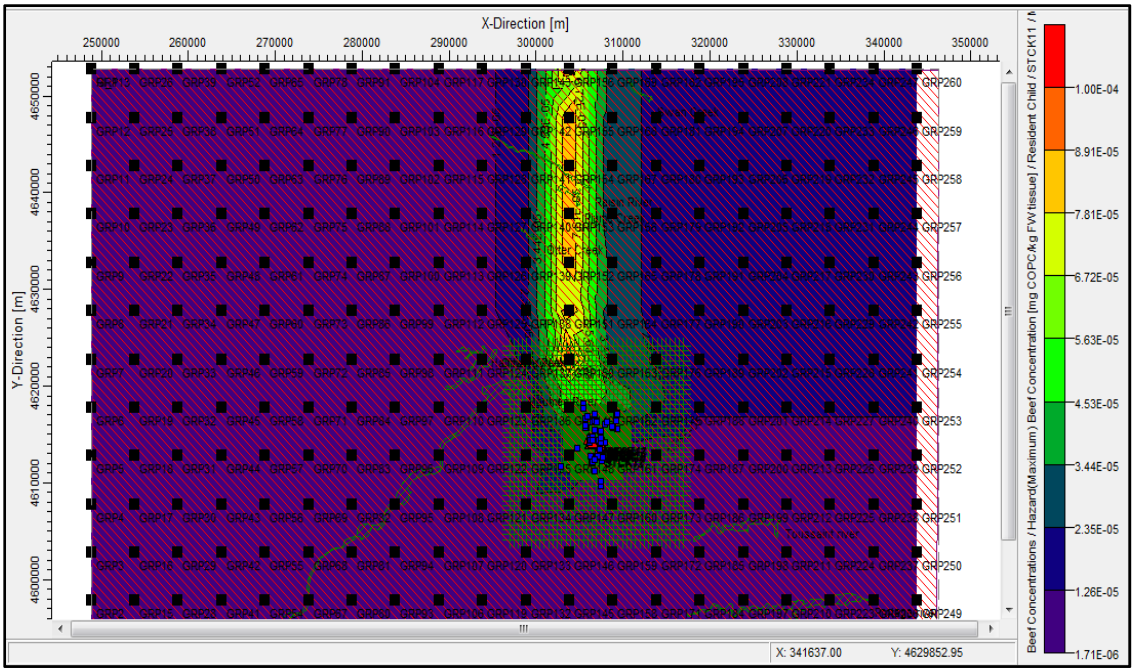

Figure 4.19: The contour plot of hazard (maximum) beef concentrations for the third proposed location.

For the fourth proposed location, the hazard beef concentration for all exposure scenarios and for all sources range from 2.6140E-07 to 8.6513E-04 mg COPC/kg FW tissue. Figure 4.20 shows the worst-case scenario for all exposure scenario and for source 3. We can note that the lowest identified hazard quotient is in the south-eastern area of proposed location. In contrast, the highest identified hazard quotient for all exposure scenarios is in the north area of the proposed location with a predicted value 8.6513E-04 mg COPC/kg FW tissue at receptor 141 for the hazard quotient.

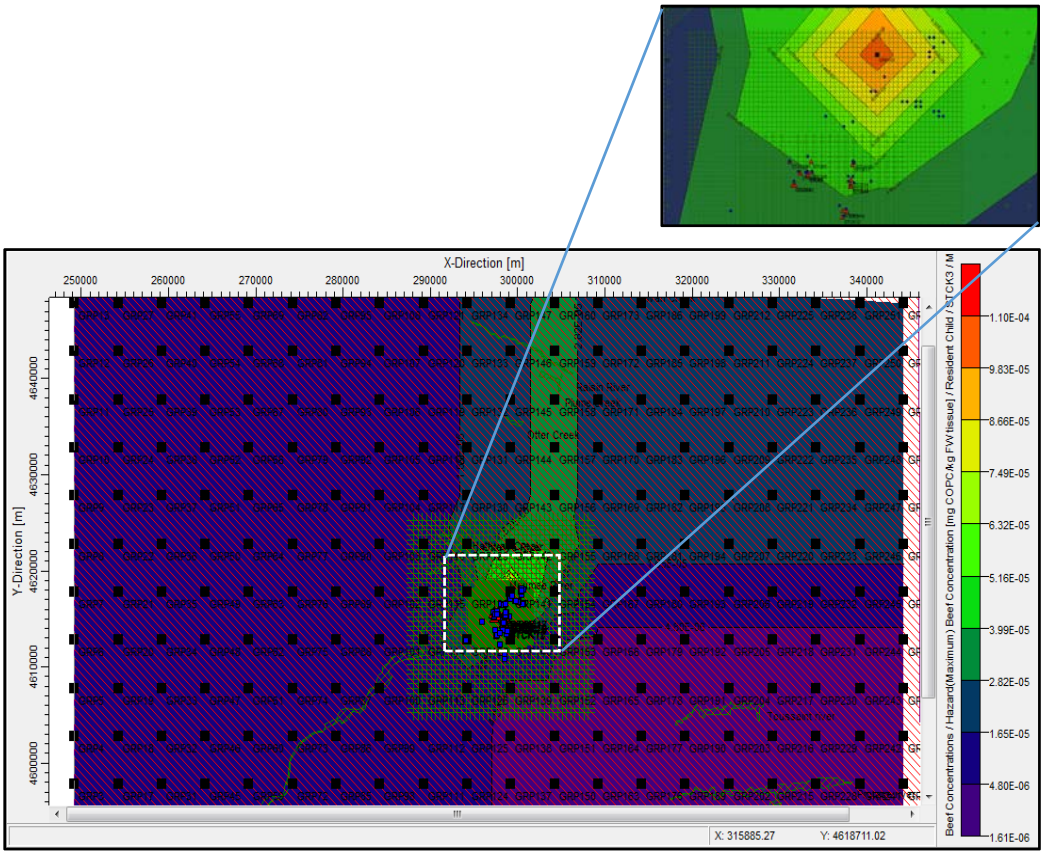

Figure 4.20: The contour plot of hazard (maximum) beef concentrations for the fourth proposed location.

In conclusion, we can note that the fourth proposed location have the lowest concentration levels. Although the fourth proposed location has the lowest beef concentration level, the beef may, potentially, be exposed to COPC through soil ingested with food picked up from the ground. It is not known if rearing of these animals occurs to a significant level in the vicinity of this proposed location, however, a future scenario might see a change in land use associated with the rearing of beef.

Chicken and egg Concentrations

The chicken and egg concentrations were calculated by IRAP-h View. As beef concentration, the chicken may, potentially, be exposed to COPC through soil ingested with food picked up from the ground. It is not known if rearing of chicken occurs to a significant level in the vicinity of the proposed location, however, a future scenario might see a change in land use that could be used for rearing chickens.

For the first proposed location, the hazard chicken and egg concentrations for all exposure scenarios and for all sources range from 4.4613E-08 to 1.4493E-04 mg COPC/kg FW tissue. Figure 4.21 shows the worst-case scenario for all exposure scenarios and for source 11. We can note that the lowest identified hazard quotient is in the area south east of the proposed location. In contrast, the highest identified hazard quotient for all exposure scenarios is in the north area of proposed location with a predicted value 1.4493E-04 mg COPC/kg FW tissue at receptors 136, 137, 138, 139, 140, 141, 142, and 143 for the hazard quotient.

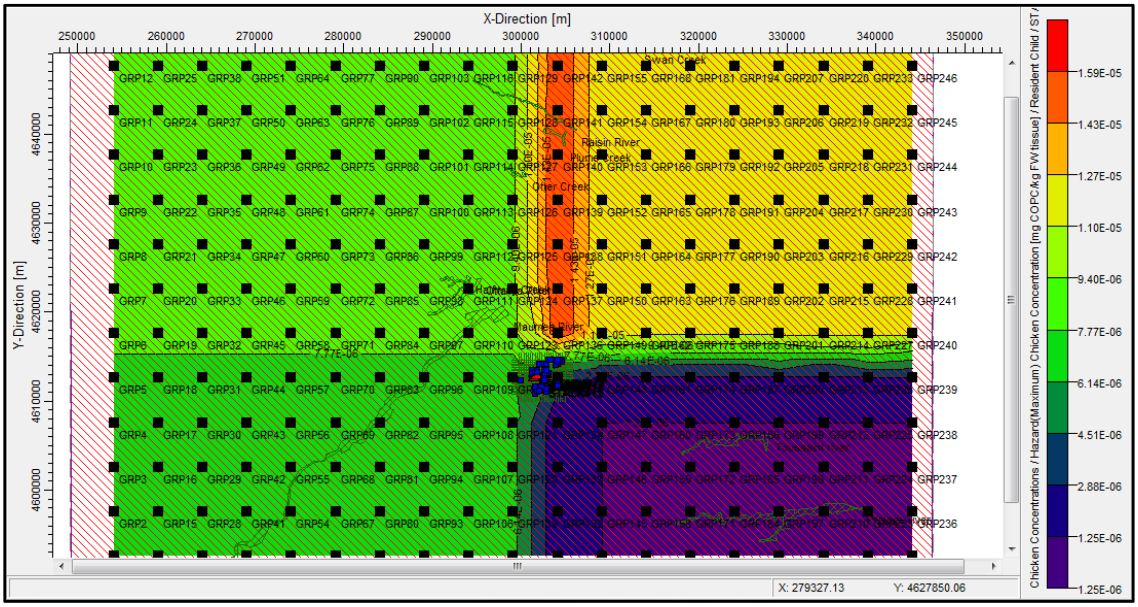

Figure 4.21: The contour plot of hazard (maximum) chicken and egg concentrations for the first proposed location.

For the second proposed location, the hazard chicken and egg concentrations for all exposure scenarios and for all sources range from 3.2265E-08 to 2.2937E-03 mg COPC/kg FW tissue. Figure 4.22 shows the worst-case scenario for all exposure scenarios and for source 14. We can note that the lowest identified hazard quotient is in the area west of the proposed location. In contrast, the highest identified hazard quotient for all exposure scenarios is in the north-eastern area of the proposed location with a predicted value 2.2937E-03 mg COPC/kg FW tissue at receptor 136 for the hazard quotient.

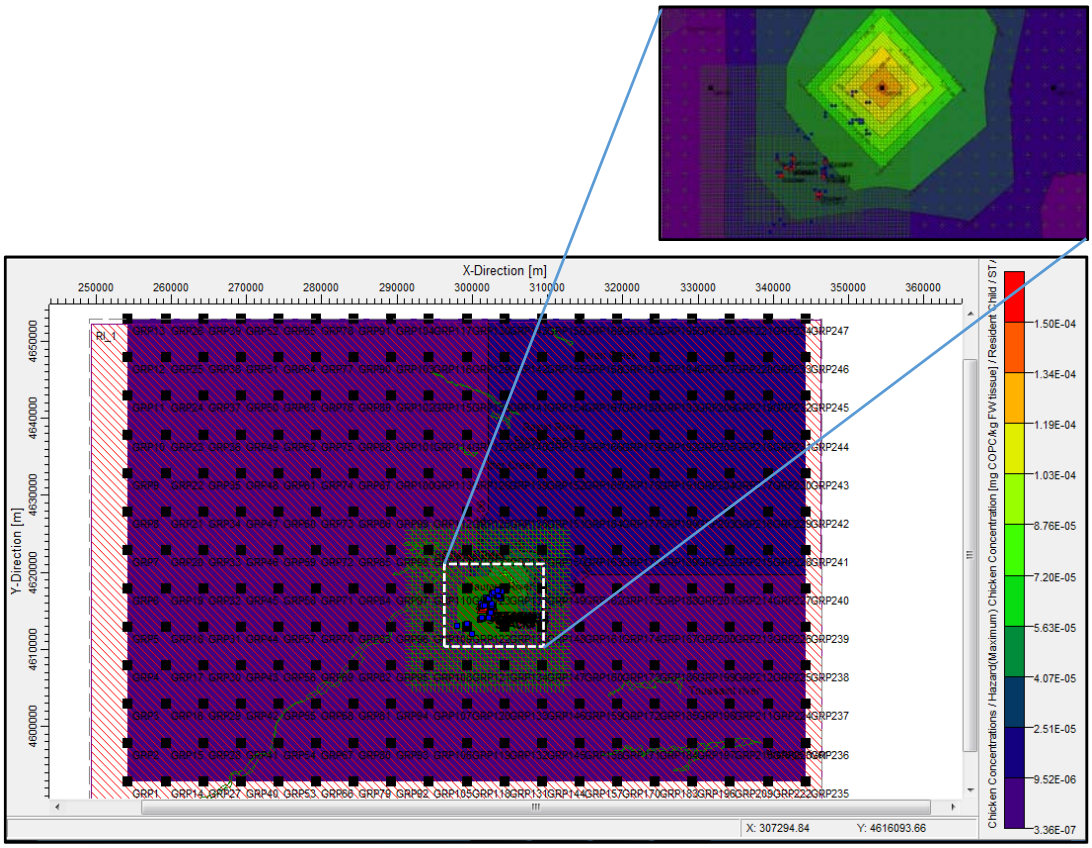

Figure 4.22: The contour plot of hazard (maximum) chicken and egg concentrations for the second proposed location.

For the third proposed location, the hazard chicken and egg concentrations for all exposure scenarios and for all sources range from 1.2337E-08 to 2.1964E-04 mg COPC/kg FW tissue. These

concentrations considered as accepted levels. Figure 4.23 shows the worst-case scenario for all exposure scenarios and for source 3. We can note that the lowest identified hazard quotient is in the area south east of the proposed location. In contrast, the highest identified hazard quotient for all exposure scenarios is in the area north west of the proposed location with a predicted value 2.1964E-04 mg COPC/kg FW tissue at receptor 149 for the hazard quotient.

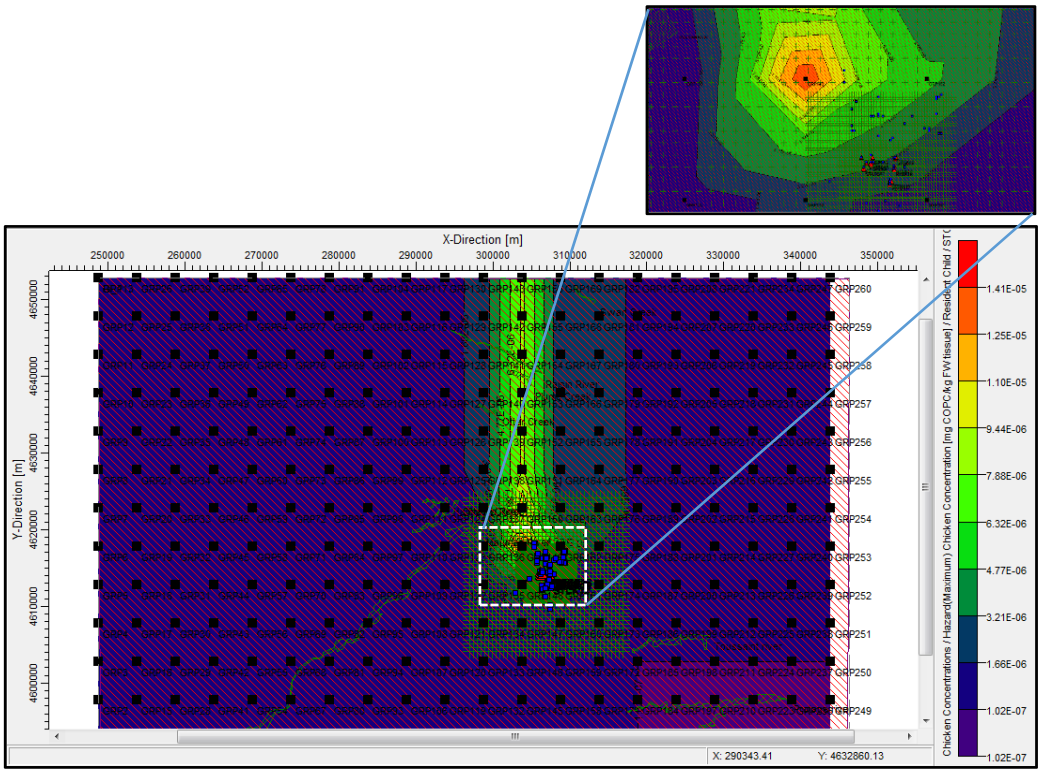

Figure 4.23: The contour plot of hazard (maximum) chicken and egg concentrations for the third proposed location.

For the fourth proposed location, the hazard chicken and eggs concentrations for all exposure scenarios and for all sources range from 1.2366E-08 to 1.5488E-04 mg COPC /kg FW tissue. Figure 4.24 the worst-case scenario for all exposure scenarios and for source 6. We can note that the lowest identified hazard quotient is in the area south east of the proposed location. In

contrast, the highest identified hazard quotient for all exposure scenarios is in the north-eastern area of the proposed location with a predicted value 1.5488E-04 mg COPC/kg FW tissue at receptor 141 for the hazard quotient.

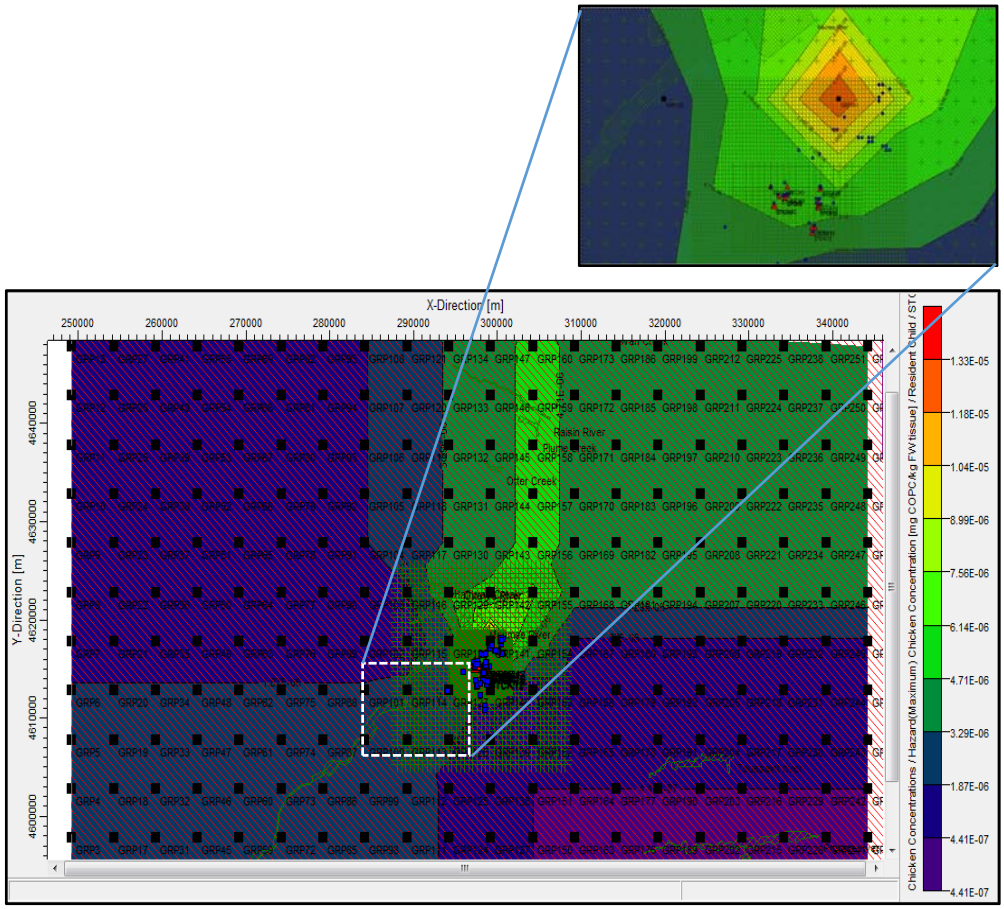

Figure 4.24: The contour plot of hazard (maximum) chicken and egg concentrations for the fourth proposed location.

In conclusion, we can see that the fourth proposed location has the lowest hazard chicken and egg concentrations. Although the fourth proposed location has the lowest health impact, the chicken may, potentially, be exposed to COPC through soil ingested with food picked up from the ground. A future scenario might see a change in land use that could be used for rearing chickens.

Therefore, the consumption of chicken and eggs could be a potential exposure scenario in the future.

Milk Concentration

Milk concentrations were calculated by the IRAP-h View model. Dairy herds may be exposed to COPC through soil ingested with their food. Babies also may be exposed to COPC via ingestion of contaminated breast milk.

For the first proposed location, the hazard milk concentration for all exposure scenarios and for all sources ranges from 4.9078E-07 to 3.4000E-04 mg COPC/kg FW tissue. Figure 4.25 shows the worst-case scenario for all exposure scenarios and for source 6. We can note that the lowest identified hazard quotient is in the area south east of the proposed location. In contrast, the highest identified hazard quotient for all exposure scenarios is in the north area of the proposed location with a predicted value 3.4000E-04 mg COPC/kg FW tissue at receptors 136, 137, 138, 139, 140, 141, 142, and 143 for the hazard quotient.

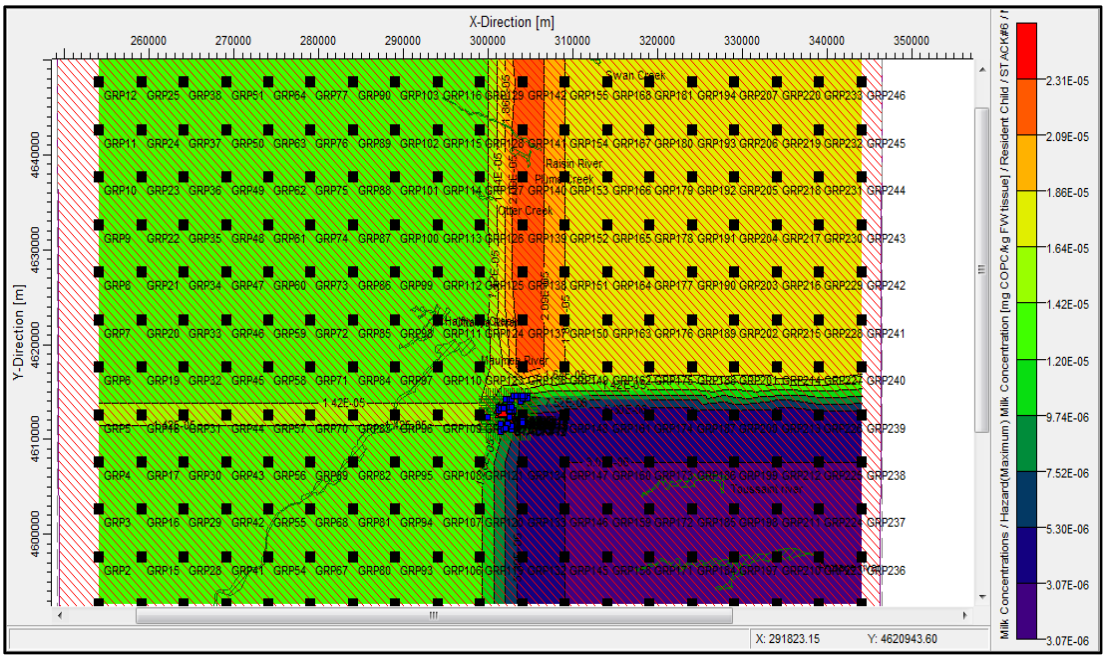

Figure 4.25: The contour plot of hazard (maximum) milk concentrations for the first proposed location.

For the second proposed location, the hazard milk concentration for all exposure scenarios and for all sources ranges from 3.5727E-07 to 5.5037E-03 mg COPC/kg FW tissue. Figure 4.26 shows the worst-case scenario for all exposure scenarios and for source 1. We can note that the lowest identified hazard quotient is in the whole area of concern except the north-eastern area of the proposed location. In contrast, the highest identified hazard quotient for all exposure scenarios is in the area north east of the proposed location with a predicted value 5.5037E-03 mg COPC/kg FW tissue at receptor 136 for the hazard quotient.

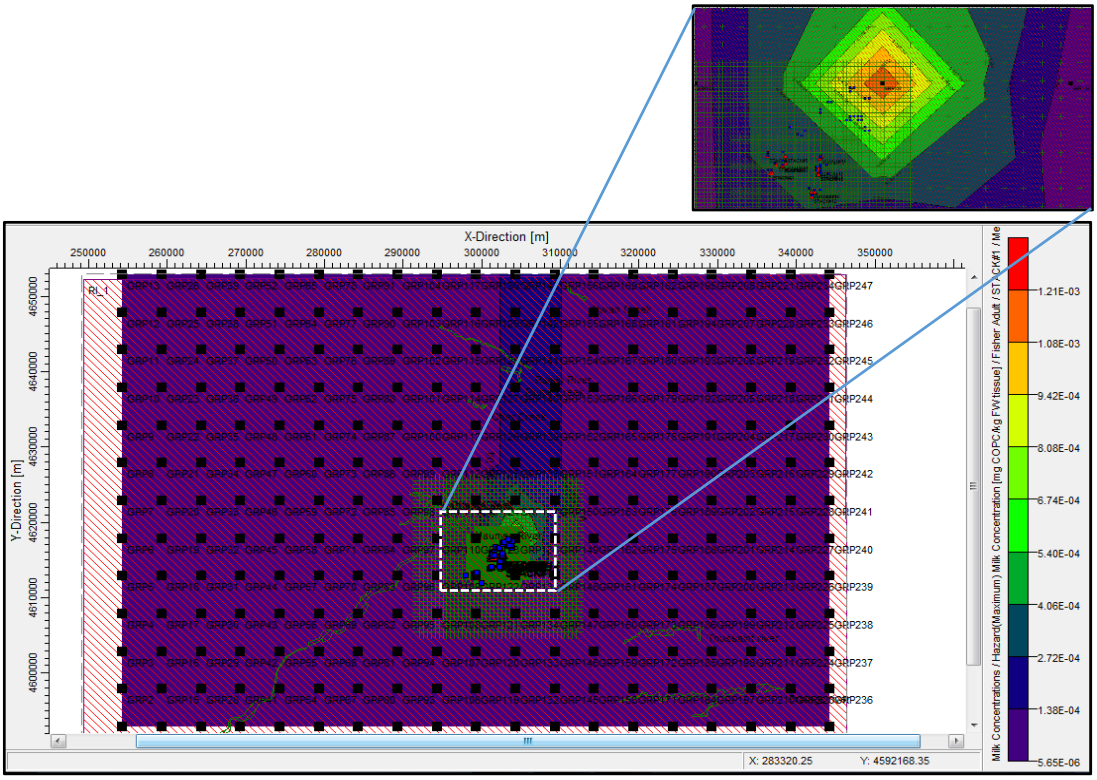

Figure 4.26: The contour plot of hazard (maximum) milk concentrations for the second proposed location.

For the third proposed location, the hazard milk concentration for all exposure scenarios and for all sources ranges from 1.4470E-07 to 5.2485E-04 mg COPC /kg FW tissue. Figure 4.27 shows the worst-case scenario for all exposure scenarios and for source 1. We can note that the lowest identified hazard quotient is in the whole area of concern except the north-western area of

the proposed location. In contrast, the highest identified hazard quotient for all exposure scenarios is in the north-western area of the proposed location with a predicted value 5.2485E-04 mg COPC/kg FW tissue at receptor 149 for the hazard quotient.

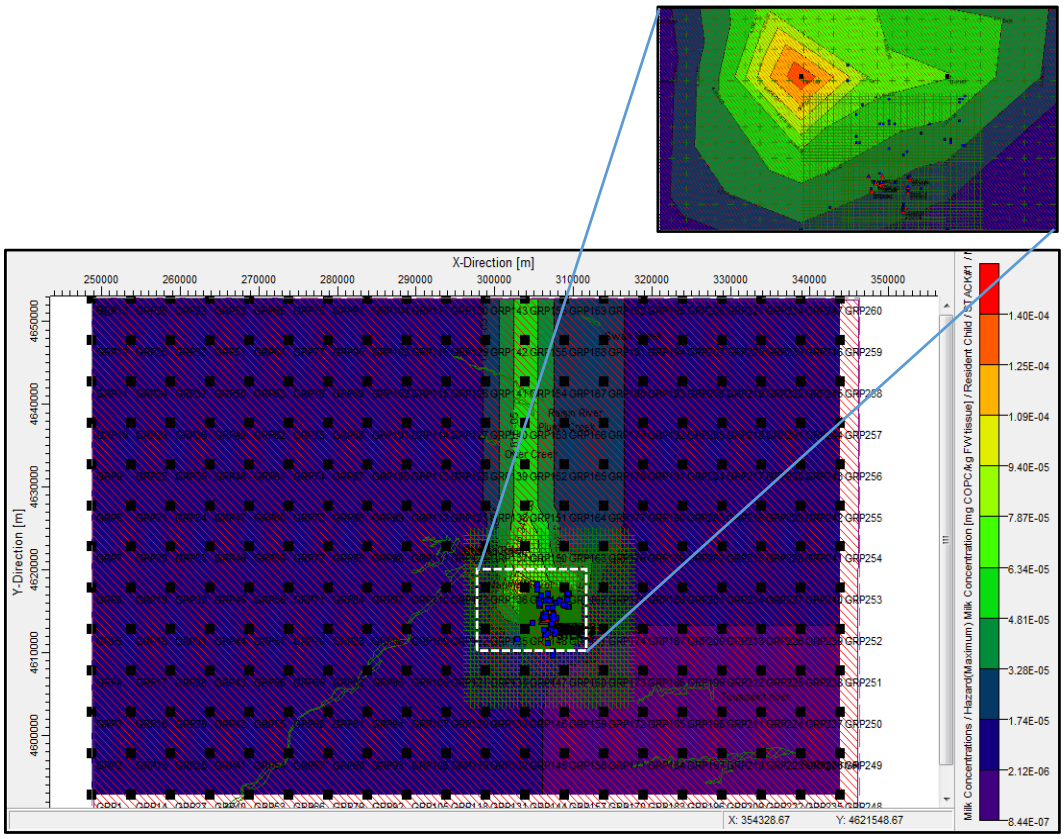

Figure 4.27: The contour plot of hazard (maximum) milk concentrations for the third proposed location.

For the fourth proposed location, the hazard milk concentration for all exposure scenarios and for all sources ranges from 1.5713E-07 to 3.6137E-04 mg COPC/kg FW tissue. Figure 4.28 shows the worst-case scenario for all exposure scenarios and for source 18. We can note that the lowest identified hazard quotient is in the whole area of concern except the north-eastern area of the proposed location. In contrast, the highest identified hazard quotient for all exposure scenarios is in the north-eastern area of the proposed location with a predicted value 3.6137E-04 mg COPC/kg FW tissue at receptor 141 for the hazard quotient.

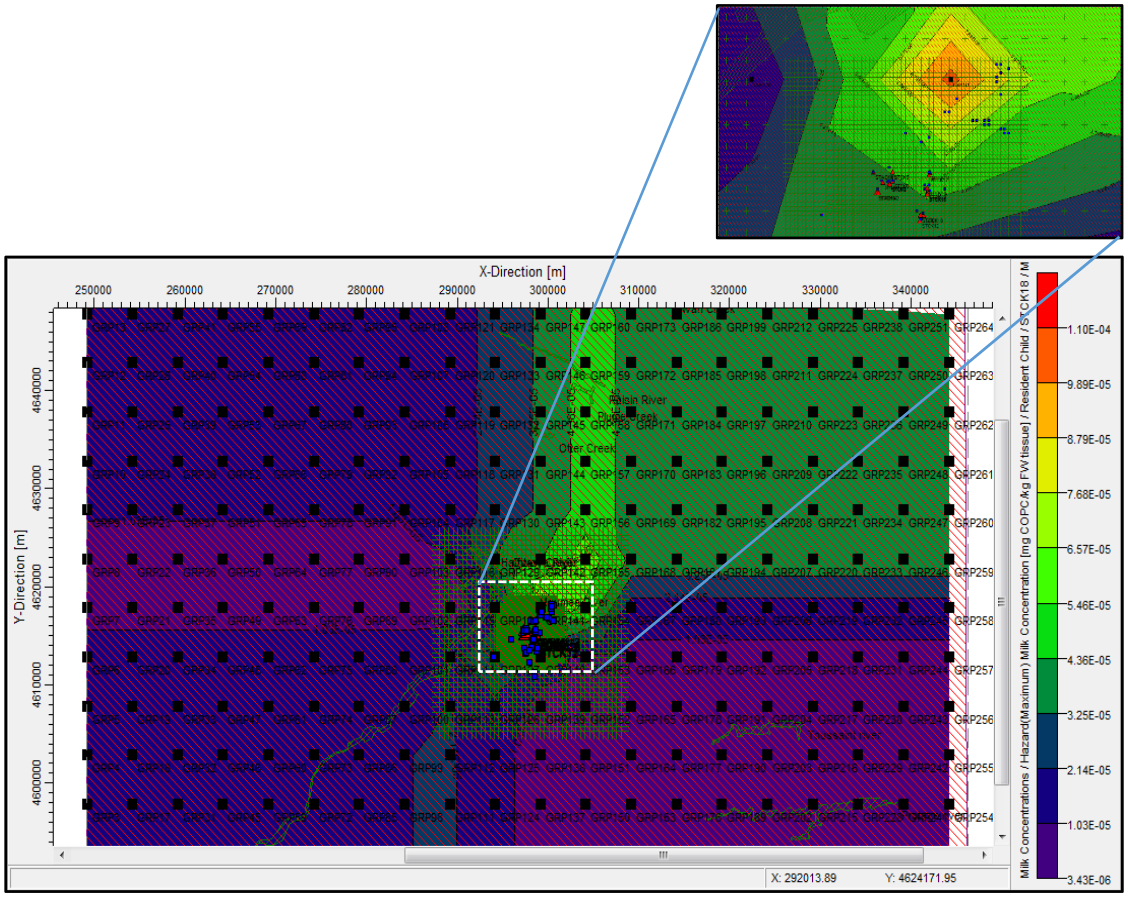

Figure 4.28: The contour plot of hazard (maximum) milk concentrations for the fourth proposed location.

In conclusion, it can be seen from IRAP-h View results that the third proposed location has the lowest milk concentration. Although the third proposed location has the lowest concentration levels, it is possible that dairy herds may, potentially, be exposed to COPC through soil ingested with their food. In addition, babies may, potentially, be exposed to COPC via ingestion of contaminated breast milk. The potential for contamination of breast milk is especially high for COPC which is likely to accumulate in breast milk. The mother may, potentially, be exposed to COPC via the inhalation or ingestion pathways.

Pork Concentration

The pork concentrations were calculated by IRAP-h View model. Pork may be exposed to COPC through soil ingested with food picked up from the ground.

For the first proposed location, the hazard pork concentration for all exposure scenarios and for all sources ranges from 1.2554E-09 to 3.4941E-06 mg COPC/kg FW tissue. Figure 4.29 shows the worst-case scenarios for all exposure scenarios and for source 6. We can note that the lowest identified hazard quotient is in the south-eastern area of the proposed location. In contrast, the highest identified hazard quotient for all exposure scenarios is in the north area of the proposed location with a predicted value 3.4941E-06 mg COPC/kg FW tissue at receptors 136, 137, 138, 139, 140, 141, 142, and 143 for the hazard quotient.

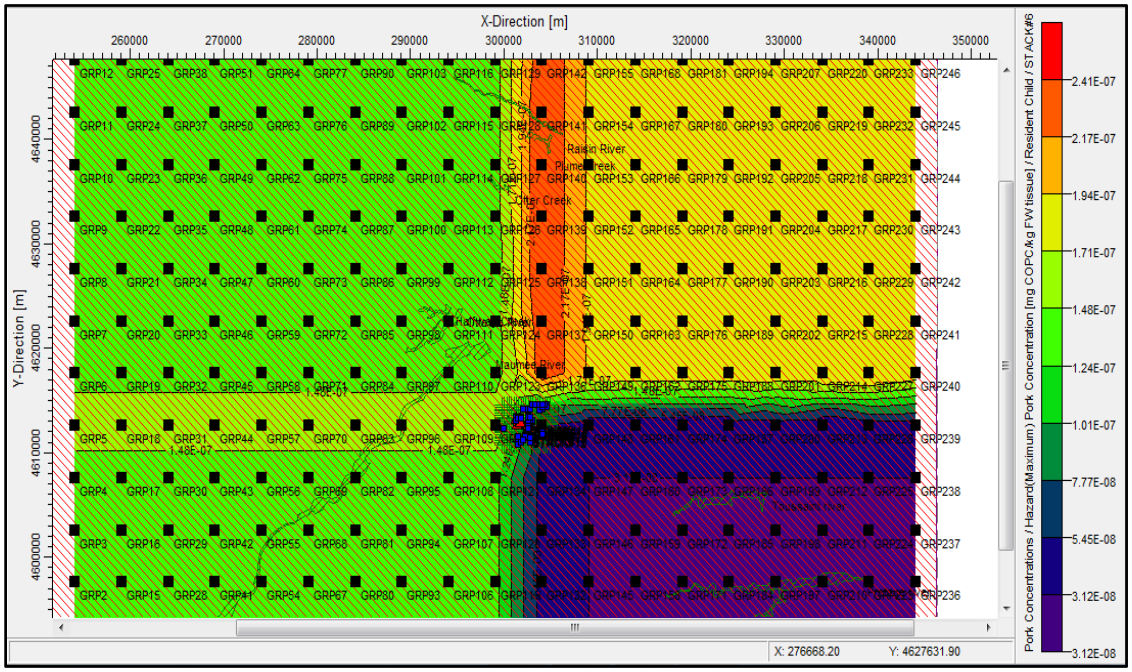

Figure 4.29: The contour plot of hazard (maximum) pork concentrations for the first proposed location.

For the second proposed location, the hazard pork concentration for all exposure scenarios and for all sources ranges from 9.1348E-10 to 5.5324E-05 mg COPC/kg FW tissue. Figure 4.30 shows the worst-case scenarios for all exposure scenarios and for source 1. We can note that the lowest identified hazard quotient is in the whole area of concern except the north-eastern area of the proposed location. In contrast, the highest identified hazard quotient for all exposure scenarios is in the area north east of the proposed location with a predicted value 5.5324E-05 mg COPC/kg FW tissue at receptor 136 for the hazard quotient.

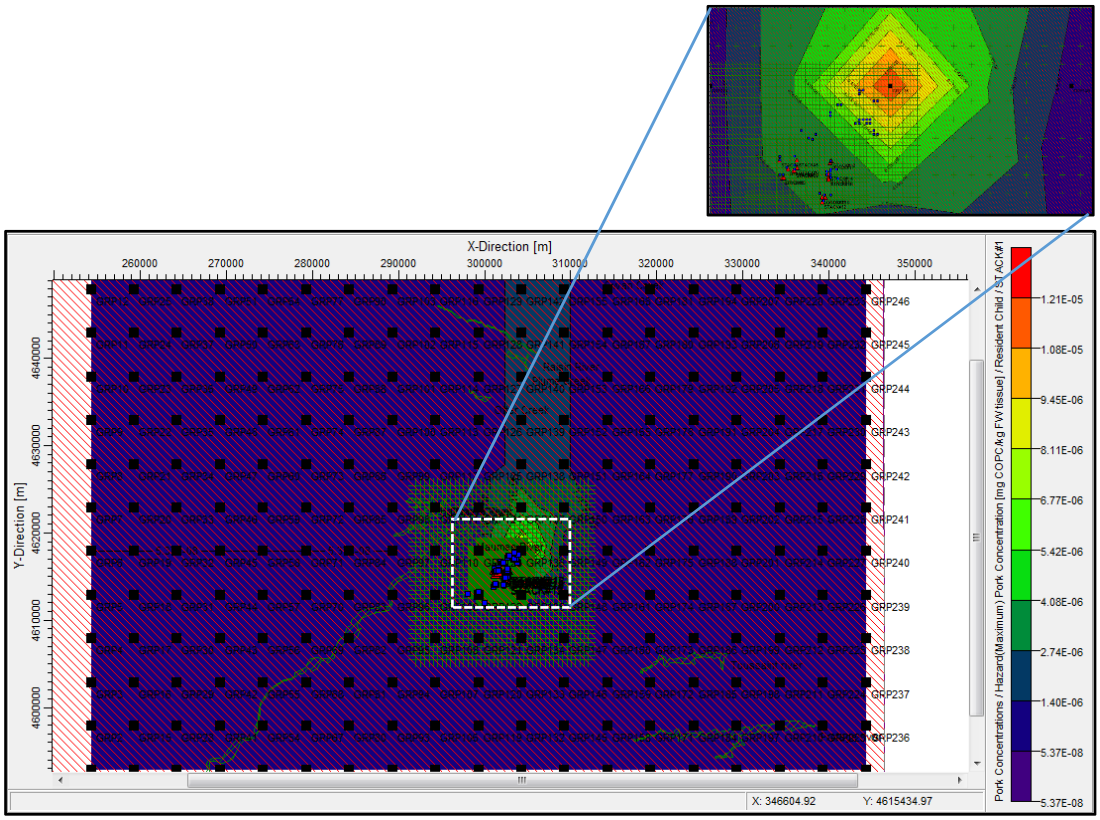

Figure 4.30: The contour plot of hazard (maximum) pork concentrations for the second proposed location.

For the third proposed location, the hazard pork concentration for all exposure scenarios and for all sources ranges from 3.5269E-10 to 5.2974E-06 mg COPC/kg FW tissue. Figure 4.31 shows the worst-case scenario for all exposure scenarios and for source 1. We can note that the

lowest identified hazard quotient is in the whole area of concern except the north-western area of the proposed location. In contrast, the highest identified hazard quotient for all exposure scenarios is in the area north west of the proposed location with a predicted value 5.2974E-06 mg COPC/kg FW tissue at receptor 149 for the hazard quotient.

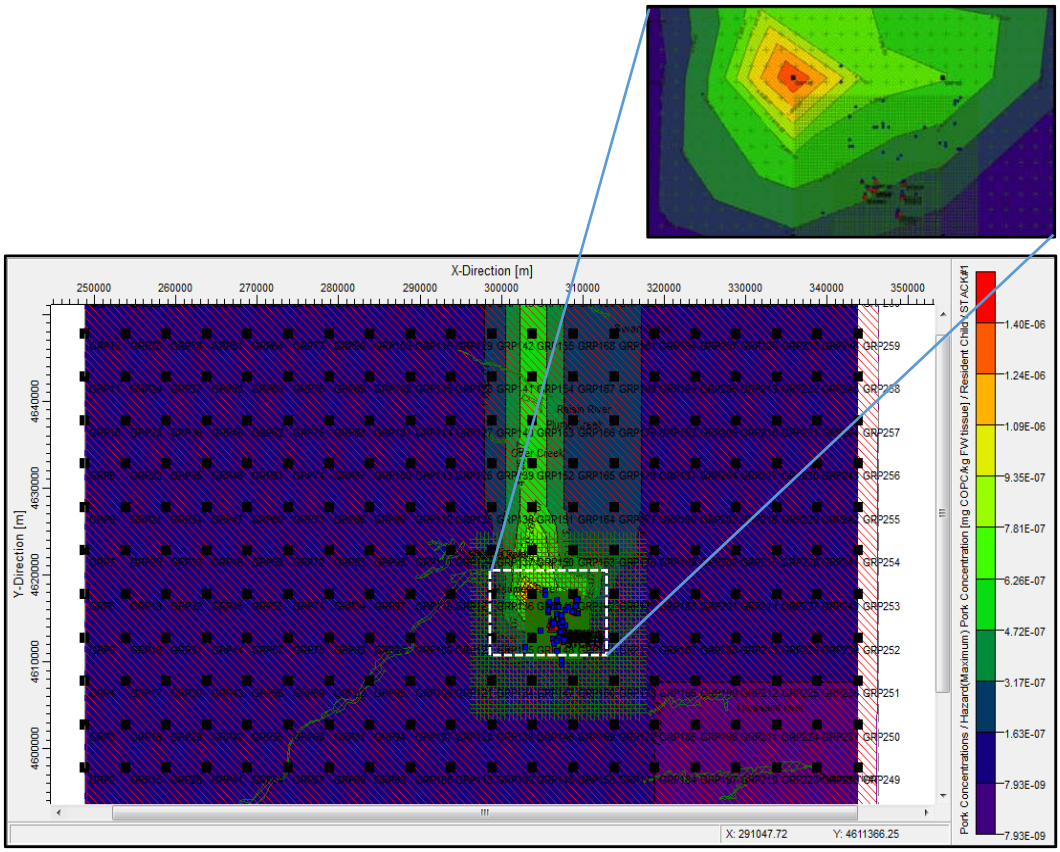

Figure 4.31: The contour plot of hazard (maximum) pork concentrations for the third proposed location.

For the fourth proposed location, the hazard pork concentration for all exposure scenarios and for all sources ranges from 3.6070E-10 to 3.7333E-06 mg COPC/kg FW tissue. Figure 4.32 shows the worst-case scenario for all exposure scenarios and for source 18. We can note that the lowest identified hazard quotient is in the whole area of concern except the north-eastern area of the proposed location. In contrast, the highest identified hazard quotient for all exposure scenarios

is in the area north east of the proposed location with a predicted value 3.7333E-06 mg COPC/kg FW tissue at receptor 141 for the hazard quotient.

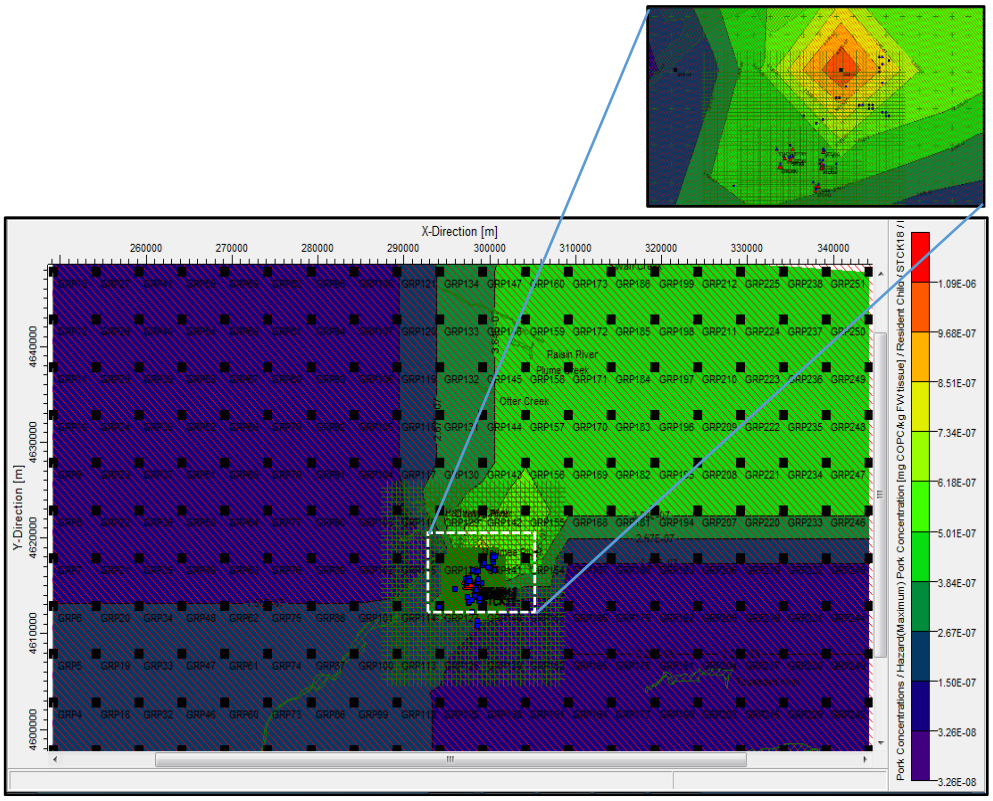

Figure 4.32: The contour plot of hazard (maximum) pork concentrations for the fourth proposed location.

In conclusion, it can be seen form IRAP-h View results that the first proposed location has the lowest concentration ranges. Although this is acceptable, pigs may, potentially, be exposed to COPC through soil ingested with food picked up from the ground. It is not known if rearing of pigs occurs to a significant level in the vicinity of the proposed location.

Air Concentration

For the first proposed location, the air concentration for all exposure scenarios and for all sources ranges from 1.6987E-07 to 2.1846E-04 µg/m^3. Figure 4.33 shows the worst-case scenario

for all exposure scenarios and for all sources. We can note that the lowest air concentration is in the south-eastern and north-western areas of the proposed location. In contrast, the highest air concentration for all exposure scenarios is in the north area of the proposed location with air concentration predicted value 2.1846E-04 mg COPC/kg FW tissue at receptors 136, 137, 138, 139, 140, 141, 142, 143.

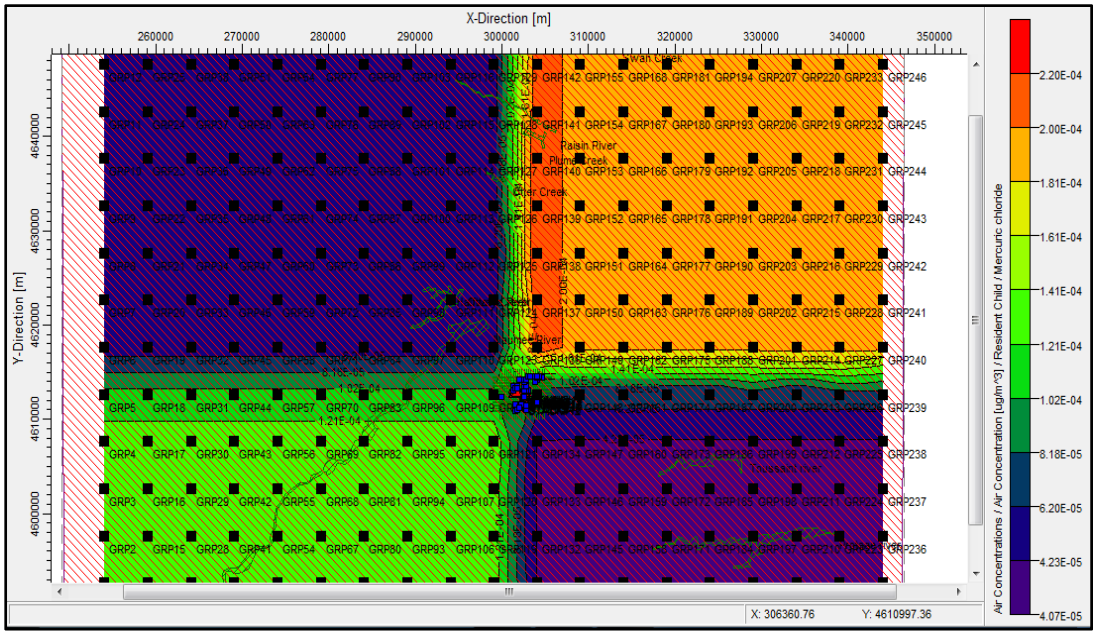

Figure 4.33: The contour plot of air concentration for the first proposed location.

For the second proposed location, the air concentration for all exposure scenarios and for all sources ranges from 5.4307E-08 to 1.1286E-04 µg/m^3. Figure 4.34 shows the worst-case scenario for all exposure scenarios and for all sources. We can note that the lowest air concentration is in the area south east of the proposed location. In contrast, the highest air concentration for all exposure scenarios is in the north-eastern area of the proposed location with air concentration predicted value 1.1286E-04 mg COPC/kg FW tissue at receptor 136.

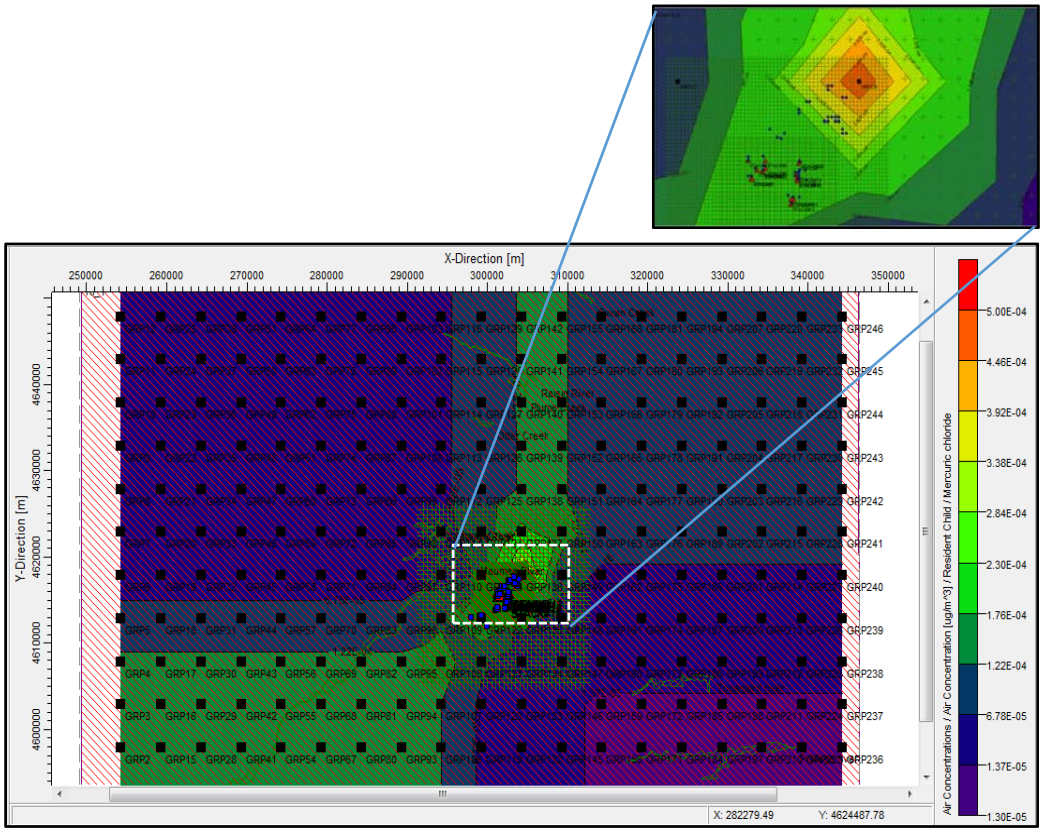

Figure 4.34: The contour plot of air concentration for the second proposed location.

For the third proposed location, the air concentration for all exposure scenarios and for all sources ranges from 6.6848E-08 to 1.9135E-04 µg/m^3. Figure 4.35 shows the worst-case scenario for all exposure scenarios. We can note that the lowest air concentration is in the south-eastern area of the proposed location. In contrast, the highest air concentration for all exposure scenarios is in the area north east of the proposed location with air concentration predicted value 1.9135E-04 mg COPC/kg FW tissue at receptor 162.

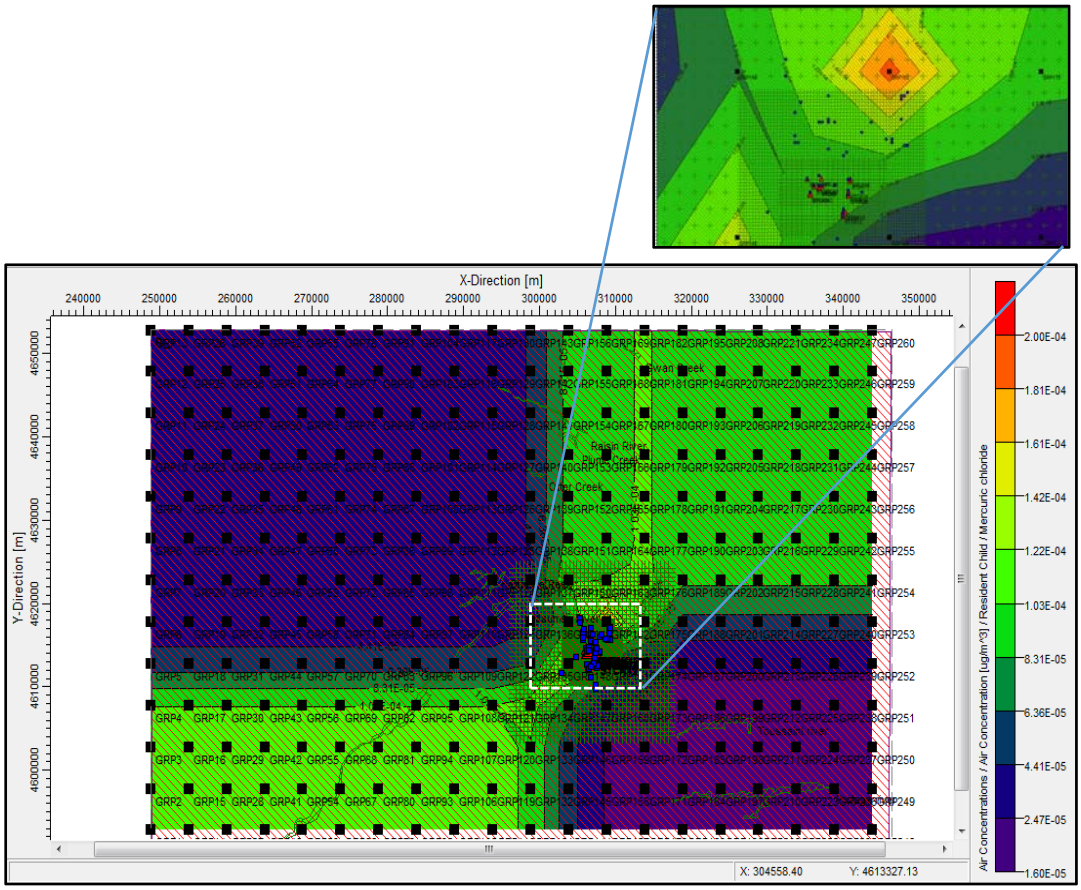

Figure 4.35: The contour plot of air concentration for the third proposed location.

For the fourth proposed location, the air concentration for all exposure scenarios and for all sources ranges from 8.4815E-08 to 2.5273E-04 µg/m^3. Figure 4.36 shows the worst-case scenario for all exposure scenarios. We can note that the lowest air concentration is in the south-eastern area of the proposed location. In contrast, the highest air concentration for all exposure scenarios is in the north-eastern area of the proposed location with air concentration predicted value 2.5273E-04 mg COPC/kg FW tissue at receptor 141.

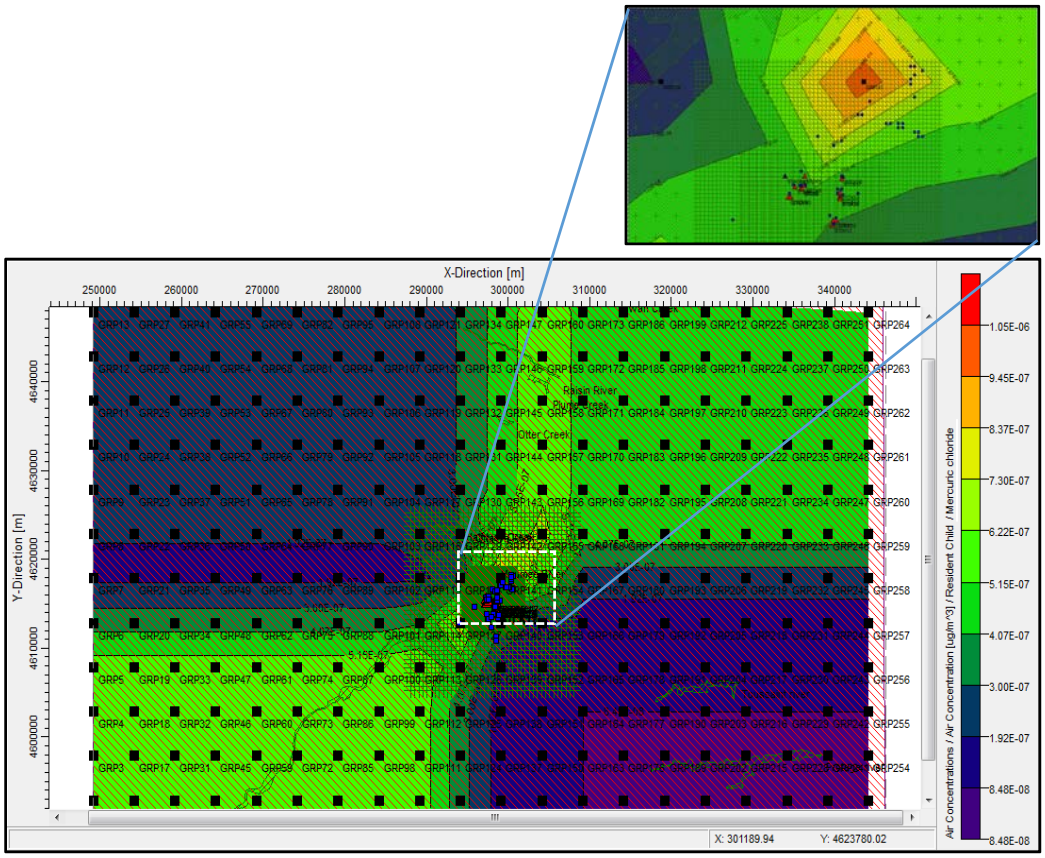

Figure 4.36: The contour plot of air concentration for the fourth proposed location.

In conclusion, it can be seen form IRAP-h View results that the fourth proposed location has the lowest air concentration levels. The air concentration for all proposed location has the lowest values at south-eastern areas of all proposed location. Although the fourth location has the lowest air concentration, the human and other ecosystems living in the Lake Erie area and south-western area of area of concern may, potentially, be exposed to COPC through breath.

4.5 Site Selection for New Industrial Plant

The emissions from all proposed locations and the potential for exposure to emissions were carefully analyzed in order to select the best location for a new industrial plant. The Analytic Hierarchy Process (AHP), which is developed by Saaty[49], was used to determine which

proposed plant is most important to help in selecting the best location for a new industrial plant. It is considered as a way of human decision-making, particularly in multi-criteria type problems. It is an effective technique for solving complex problems with multiple criteria (in our study, different proposed plant locations). The main benefits of using this technique include determining which criteria is the most important to risk assessment, and choosing the best proposed plant location among possible multiple proposed plant locations. The relative importance of each criterion should first be provided and preferences on each criterion for each proposed plant location should specified. Figure 4.37 shows the hierarchy for ranking the proposed plant locations.

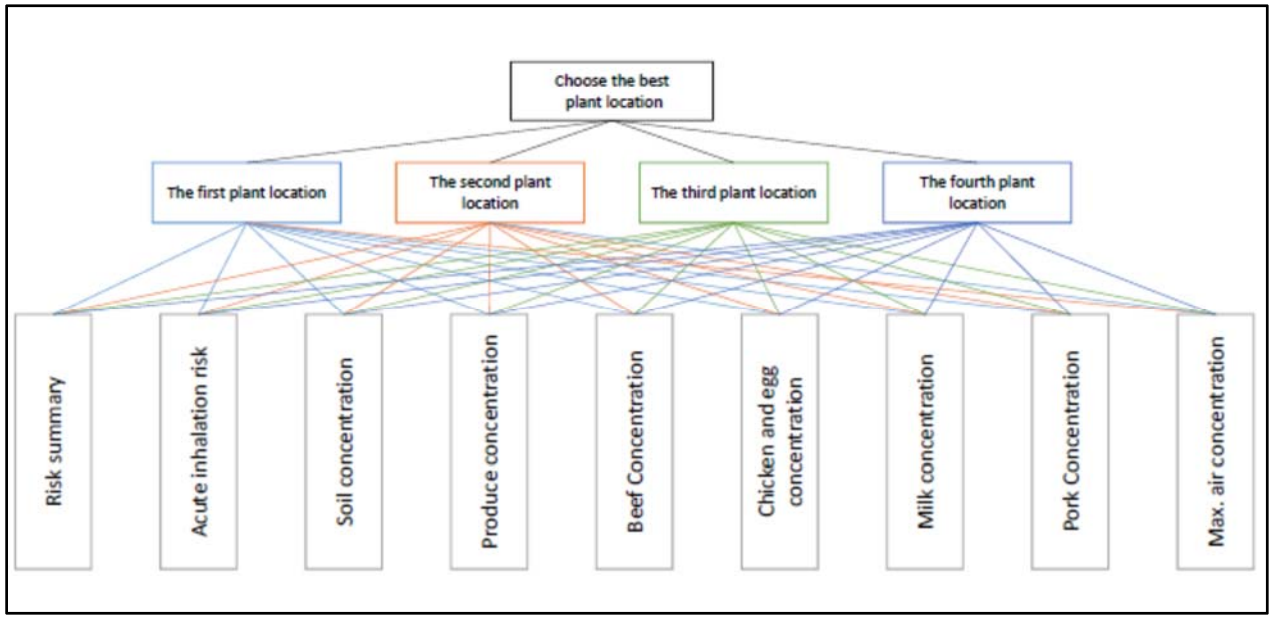

Figure 4.37: Hierarchy for ranking the proposed plant locations.

A square comparison matrix A with nine rows and nine columns is then generated on the basis of the pairwise preferences. The main diagonal of the comparison matrix will always be one (i.e. $a_{ii} = 1$) and the comparisons are made on the upper triangular matrix whereas the reciprocal of the upper triangular matrix are on the lower triangular matrix. Thus, matrix A takes the form

$$A = \begin{bmatrix} 1 & a_{12} & \cdots & a_{1n} \\ 1/a_{12} & 1 & \cdots & a_{2n} \\ \vdots & \vdots & 1 & \vdots \\ 1/a_{1n} & 1/a_{2n} & \cdots & 1 \end{bmatrix} \quad 5.1$$

Numerical rankings are related to verbal judgments of the preferences in order to rank the criteria against the objective. Table 4.5 shows verbal judgment of preferences.

Table 4.5: The Fundamental Scale of Pairwise Comparisons [49].

Verbal judgment of preference	**Numerical ranking**
Extreme importance	9
Very strong or demonstrated importance	7
Strong importance	5
Moderate importance	3
Equally importance	1
Intermediate	2, 4, 6, 8
Less importance	Reciprocal

In order to compare the alternatives, a ratio scale is used since numerical data are available for each of the criteria. Thus, the matrix A takes the following form where the w_i is the quantitative value for each of the criteria

$$A = \begin{bmatrix} w_1/w_1 & w_1/w_2 & \cdots & w_1/w_n \\ w_2/w_1 & w_2/w_2 & \cdots & w_2/w_n \\ \vdots & \vdots & & \vdots \\ w_n/w_1 & w_n/w_2 & \cdots & w_n/w_n \end{bmatrix} \quad 5.2$$

In this study, the criteria are compared against the objective, leading to one comparison matrix. Then each proposed plant location is compared against the nine criteria, leading to nine comparison matrices. Twelve comparison matrices in total are therefore generated. The inconsistency of the matrix was measured by using the maximum eigenvalue, λ_{max}, of a comparison matrix, the λ_{max} is obtained from:

$$\lambda_{max} = \sum_{i=1}^{n} y_i / p_i \qquad 5.3$$

Where

p_i = the priority vector which calculated by normalizing the matrix.

The inconsistency of a pairwise matrix can be calculated by comparing a random consistency indices (RI) with the consistency index (CI). CI can be calculated from following equation, and the values of the (RI) for our study are shown in Table 4.6.

$$CI = \frac{(\lambda_{max})}{n-1} \qquad 5.4$$

Table 4.6: Random Consistency Index (RI) [49].

Size of matrix (n)	1	2	3	4	5	6	7	8	9	10	11
RI	0.00	0.00	0.58	0.90	1.12	1.24	1.32	1.41	1.45	1.48	1.51

In order to decide whether the inconsistency of the matrix is acceptable, the consistency ratio (CR) was used. CR can be estimated from following equation.

$$CR = \frac{CI}{RI} \qquad 5.5$$

The inconsistency of the matrix is considered acceptable when CR is less than or equal to 0.1. The overall property ranking can be obtained when the above steps were conducted at all levels.

4.5.1 Ranking of Proposed Plant Locations

In this study, there are twelve pairwise comparison matrices in all: One for the criteria with respect to the objective, which is shown in Table 4.7, 15 comparison matrices for the four proposed plant locations with respect to the nine criteria. The nine criteria are risk summary, acute inhalation risk, soil concentration, produce concentration, beef concentration, chicken and egg concentration, milk concentration, pork concentration, maximum air concentration. We will only show one matrix as a sample comparing the alternatives (the proposed plant location) with respect to risk summary as shows in Table 4.8. We repeated these steps for all criteria and alternatives and the results are shown in appendix B.

The priorities for each matrix are obtained from the matrices of comparison for the ranking of proposed plant locations. The ranking of the alternatives is given against the 11 criteria. The final step is to combine all of the priority vectors for each criteria into another matrix (final rating matrix (F_R)) as shown in Table 4.9. Then we multiplied the transpose of the final rating matrix $[F_T]^T$ (as shown in Table 4.10) by the priority vector[W] in order to find the best proposed location.

$$\text{Alternative value} = [F_R]^T.[W] \qquad 5.6$$

Finally, it can be noted from the results showed in Table 4.12 that the relative importance of criteria. We can conclude that the first proposed plant location should be the best location for a new plant with respect to all the criteria that we analyzed.

Table 4.7: Pairwise comparison matrix of the main criteria with respect to the objective.

	Risk Summary	Acute inhalation	Soil Conc.	Produce Conc.	Beef Conc.	Chicken Conc.	Milk Conc.	Pork Conc.	Air Conc.	Priorities
Risk Summary	1	5	9	9	9	9	9	9	7	0.393489
Acute inhalation	0.2	1	5	5	5	5	5	5	7	0.193844
Soil Conc.	0.111111111	0.2	1	1	1	1	1	1	0.142857143	0.033892
Produce Conc.	0.111111111	0.2	1	1	1	1	1	1	0.142857143	0.033892
Beef Conc.	0.111111111	0.2	1	1	1	3	3	3	0.142857143	0.055984
Chicken Conc.	0.111111111	0.2	1	1	0.333333333	1	3	3	0.142857143	0.044989
Milk Conc.	0.111111111	0.2	1	1	0.333333333	0.333333333	1	3	0.142857143	0.034986
Pork Conc.	0.111111111	0.2	1	1	0.333333333	0.333333333	0.333333333	1	0.142857143	0.02581
Air Conc.	0.142857143	0.142857143	7	7	7	7	7	7	1	0.183114

Table 4.8: Pairwise comparison matrix for the alternatives with respect to risk summary.

	Location #1	Location #2	Location #3	Location #4	Priorities
Location #1	1	7	5	3	0.530275178
Location #2	0.142857143	1	5	5	0.265529507
Location #3	0.2	0.2	1	3	0.12034075
Location #4	0.333333333	0.2	0.333333333	1	0.083854565

Table 4.9: The ranking of the alternatives to obtain the final results.

Criteria	Location #1	Location #2	Location #3	Location #4	Priority
Risk summary	0.561538462	0.298076923	0.094230769	0.046153846	0.01936
Acute inhalation risk	0.54440054	0.213527544	0.165872818	0.076199099	0.03667
Soil concentration	0.4902788	0.308996596	0.127767298	0.072957306	0.05613
Produce concentration	0.541029911	0.260586935	0.126003726	0.072379429	0.07047
Beef Concentration	0.4718249	0.317405686	0.137180404	0.07358901	0.08694
Chicken Concentration	0.519103438	0.289521515	0.139782226	0.051592821	0.1063
Milk Concentration	0.494652406	0.299966578	0.150122549	0.055258467	0.12979
Pork Concentration	0.496260126	0.32333441	0.103070706	0.077334758	0.15967
Air Concentration	0.33579244	0.339273873	0.217257958	0.107675729	0.33466

Table 4.10: The transpose of final rating matrix.

0.561538462	0.54440054	0.4902788	0.541029911	0.4718249	0.519103438	0.494652406	0.496260126	0.33579244
0.298076923	0.213527544	0.308996596	0.260586935	0.317405686	0.289521515	0.299966578	0.32333441	0.339273873
0.094230769	0.165872818	0.127767298	0.126003726	0.137180404	0.139782226	0.150122549	0.103070706	0.217257958
0.046153846	0.076199099	0.072957306	0.072379429	0.07358901	0.051592821	0.055258467	0.077334758	0.107675729

Table 4.11: The alternative values for all the proposed plant locations

The proposed plant location	Alternative value
The first proposed plant location	0.44849652
The second proposed plant location	0.311780614
The third proposed plant location	0.159392493
The fourth proposed plant location	0.080320373

Chapter 5 : Conclusion and Recommendations

5.1 Conclusion

The main objective of this thesis was to assess the potential impacts associated with the emissions of toxic air contaminants from new industrial plants in order to select the best location based on human health risk assessment. The effects of human exposure from emissions to air from the proposed locations are considered in this study. This study has been carried out in accordance with Human Health Risk Assessment Protocol (HHRAP) for hazardous waste combustion facilities published by the U.S. Environmental Protection Agency (EPA). Exposure assessment incorporates the results of dispersion and deposition modeling with health effects known to be associated with COPC and potential exposure pathways to produce an estimate health risk.

The industrial Risk Assessment Program – Human Health (IRAP-h View Version 4.5.5), which is based on the U.S. EPA HHRAP, has been used to calculate the transport and fate of mercury from all proposed industrial plants. The geographical area considered in this study, together with the locations of the various sources, is located in Toledo City, Ohio State, USA. The total hazard quotient estimated by the IRAP-h View model, based on the air dispersion modeling estimation of air concentrations and depositions by AERMOD model for the worst-case scenarios maximum emissions from all proposed plants were calculated.

After a deep analysis and understanding of all results estimated by IRAP-h View model and using AHP method, we can conclude that the potential exposure to emission from the first proposed location has the lowest risk levels and it is, therefore, the best location for the new industrial plant.

5.2 Recommendations

For future selection of best location for a new industrial plant based on human health risk assessment, it is recommended to:

1. Avoid the human health risk associated with mercury emissions from the proposed industrial plant. The new industrial plant should be operated in a high conversion regime, preferably with the hydro-processing (severe hydro-treating, hydrocracking) suitable for converting refractory.
2. Complete conservative and extensive multi-pathway risk assessment should be provided in order to predict the potential hazards the emissions may pose on the nearby environment and population.
3. Select the new industrial plant location away from the residential area to protect people from the effects of mercury emissions and serious health effects.

Appendix A

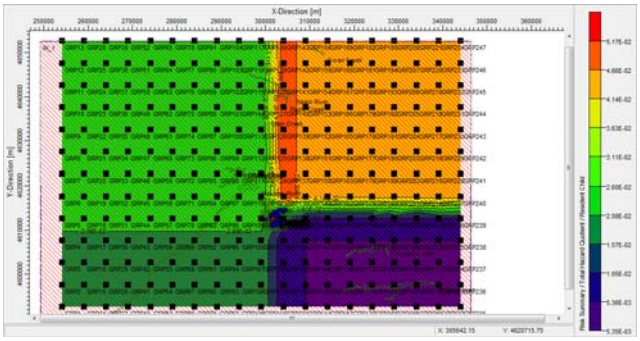

Resident child scenario

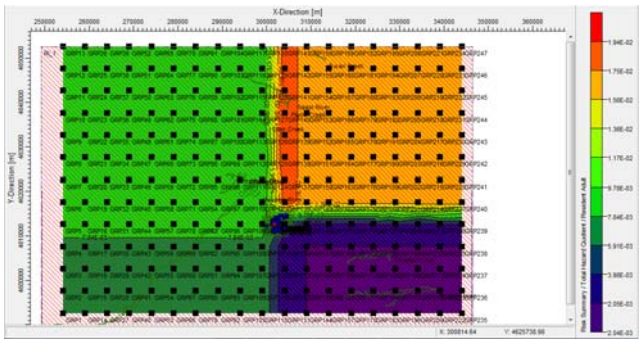

Resident adult scenario

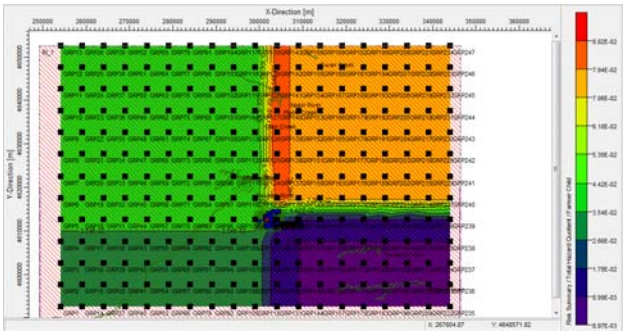

Farmer child scenario

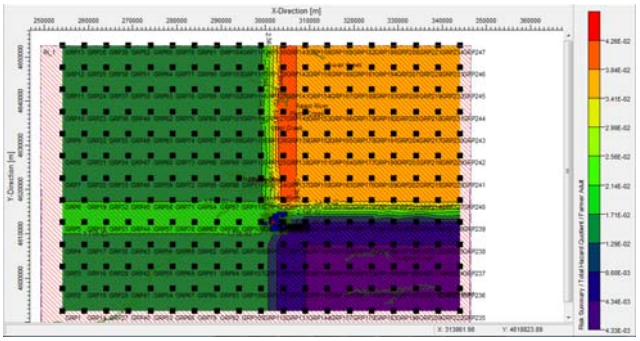

Farmer adult scenario

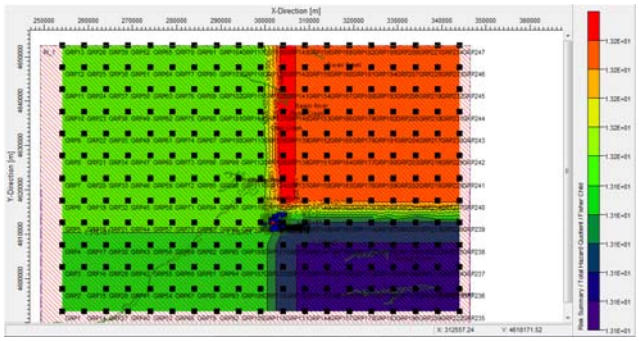

Fisher child scenario

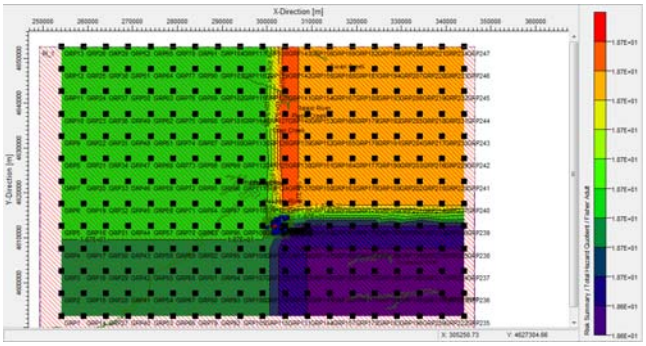

Fisher adult scenario

Figure A.1: The contour plots of total hazard quotient for the first proposed location.

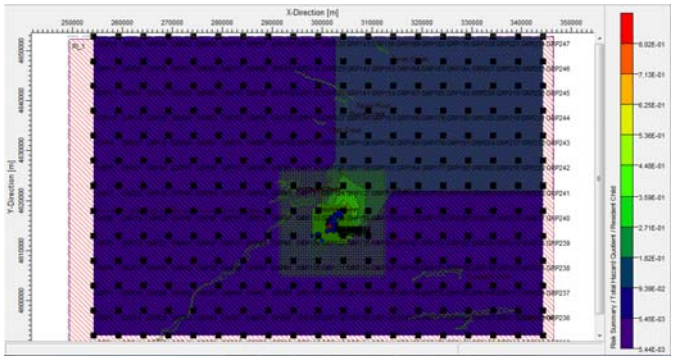

Resident child scenario

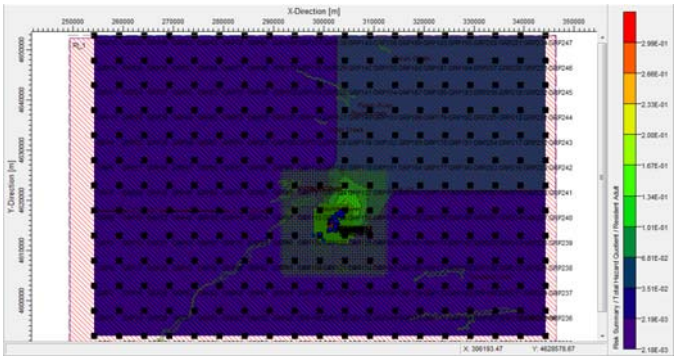

Resident adult scenario

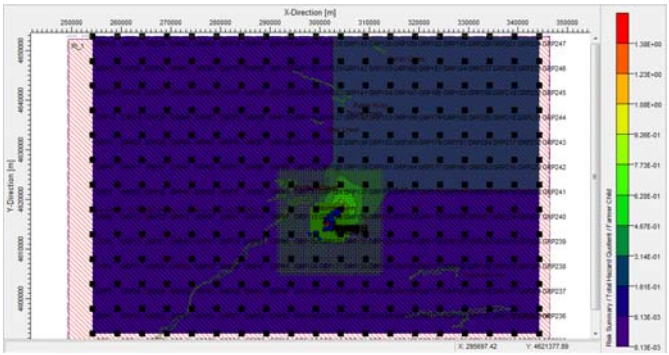

Farmer child scenario

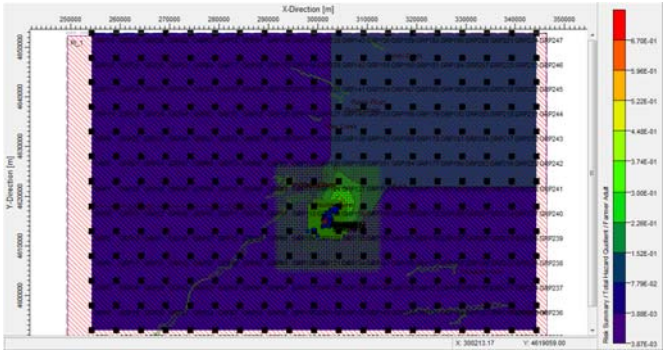

Farmer adult scenario

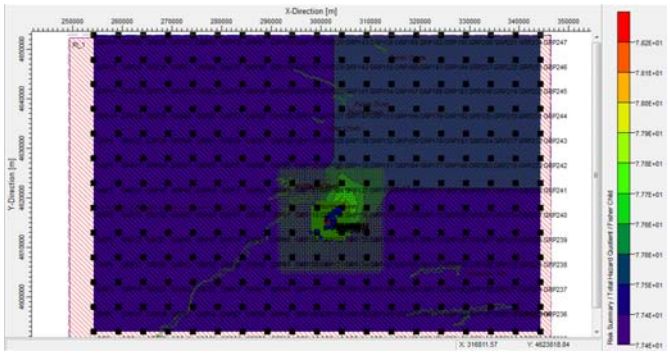

Fisher child scenario

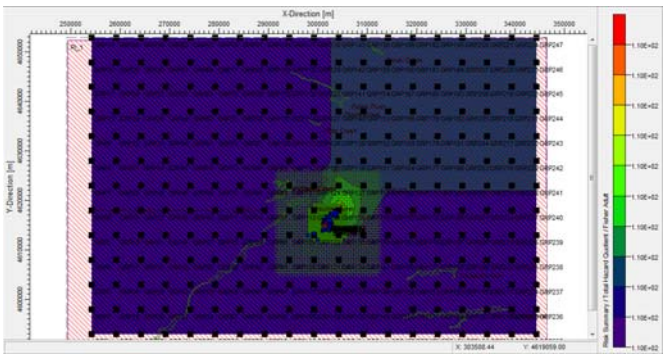

Fisher adult scenario

Figure A.2: The contour plots of the total hazard quotient for the second proposed location.

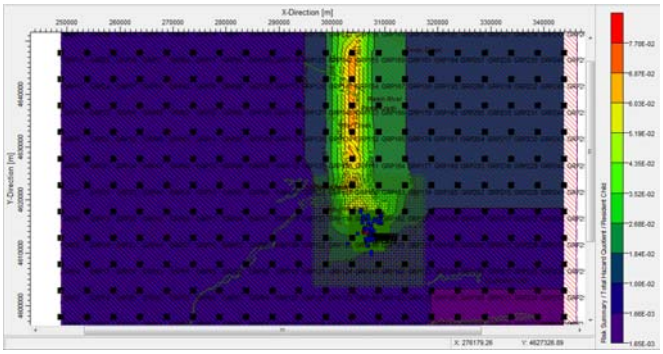

Resident child scenario

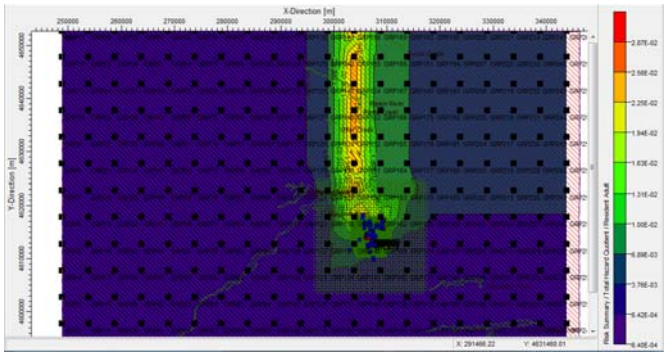

Resident adult scenario

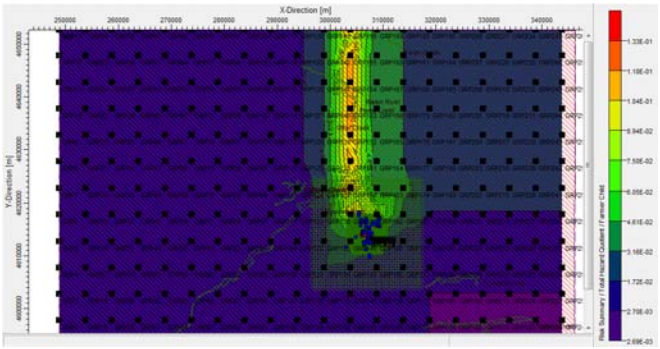

Farmer child scenario

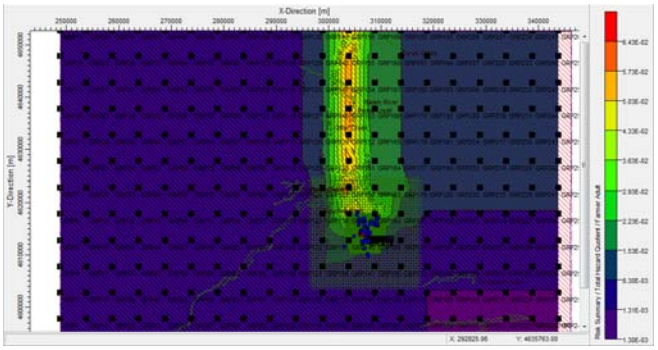

Farmer adult scenario

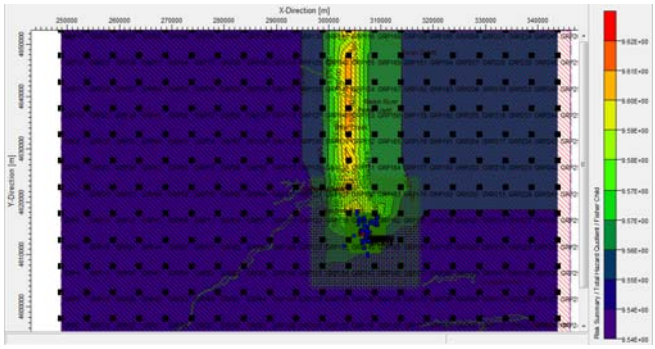

Fisher child scenario

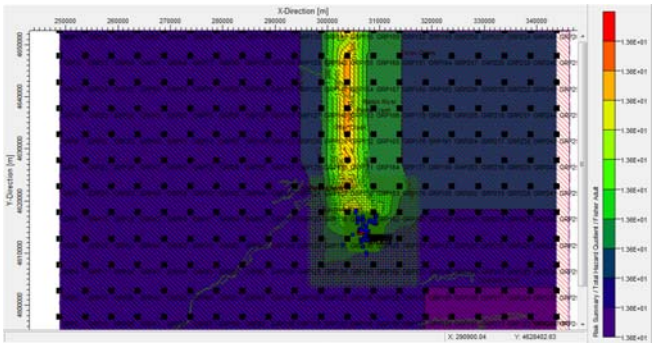

Fisher adult scenario

Figure 5A.3: The contour plots of total hazard quotient for the third proposed location.

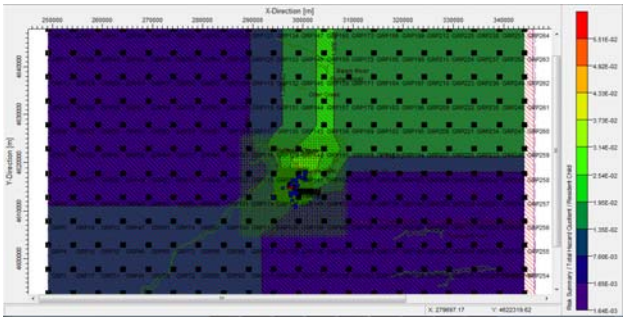

Resident child scenario

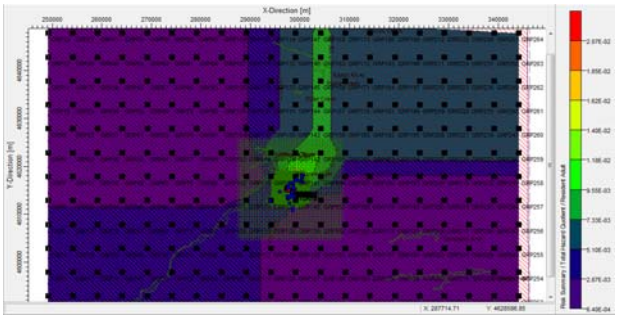

Resident adult scenario

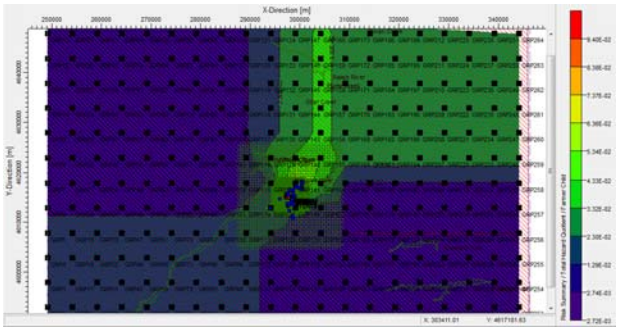

Farmer child scenario

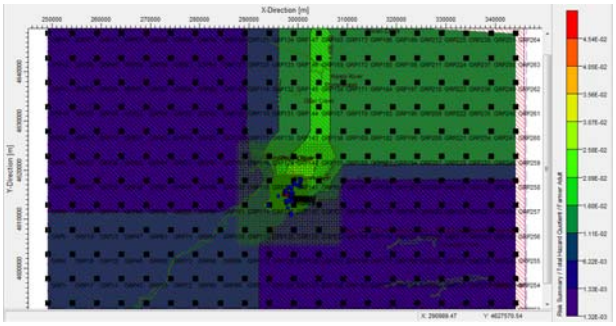

Farmer adult scenario

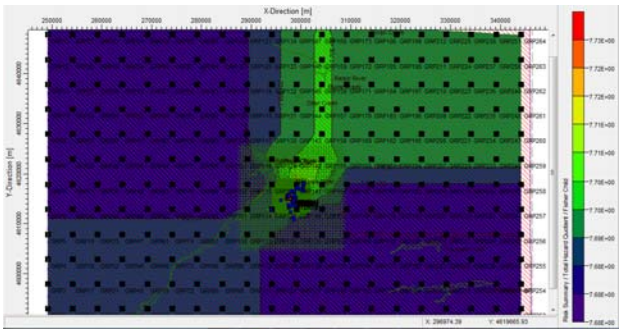

Fisher child scenario

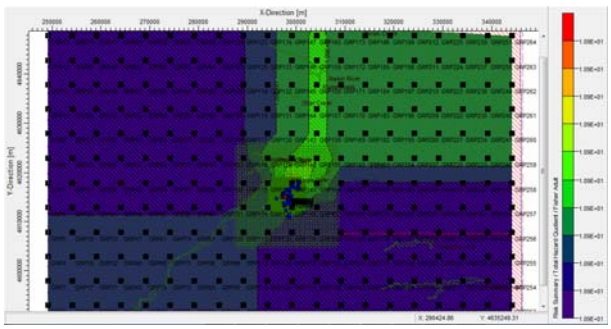

Fisher adult scenario

Figure A.4: The contour plots of total hazard quotient for the fourth proposed location.

Appendix B

For acute inhalation risk:

Table 0B.1: Pairwise comparison matrix [C] for the alternatives with respect to acute inhalation risk.

	Location #1	Location #2	Location #3	Location #4	Priority
Location #1	1	5	7	3	0.54440054
Location #2	0.2	1	3	5	0.213527544
Location #3	0.142857143	0.333333333	1	7	0.165872818
Location #4	0.333333333	0.2	0.142857143	1	0.076199099

- Normalizing the matrix [C] by dividing each element in every column by the sum of that column.

Table B.2: Normalizing the pairwise comparison matrix[C].

	Location #1	Location #2	Location #3	Location #4
Location #1	0.596590909	0.765306122	0.628205128	0.1875
Location #2	0.119318182	0.153061224	0.269230769	0.3125
Location #3	0.085227273	0.051020408	0.08974359	0.4375
Location #4	0.198863636	0.030612245	0.012820513	0.0625

- Checking for consistency:

$\lambda =$ 0.4592

CI = -1.180266667

RI = 0.9

CR = -1.31141 less than 0.1, the consistency of the matrix is considered acceptable

For soil concentration:

Table 0B.3: Pairwise comparison matrix [C] for the alternatives with respect to soil concentration.

	Location #1	Location #2	Location #3	Location #4	Priority
Location #1	1	7	5	3	0.4902788
Location #2	0.142857143	1	9	7	0.308996596
Location #3	0.2	0.111111111	1	5	0.127767298
Location #4	0.333333333	0.142857143	0.2	1	0.072957306

- Normalizing the matrix [C] by dividing each element in every column by the sum of that column.

Table B.4: Normalizing of the pairwise comparison matrix[C].

	Location #1	Location #2	Location #3	Location #4
Location #1	0.596590909	0.848076923	0.328947368	0.1875
Location #2	0.085227273	0.121153846	0.592105263	0.4375
Location #3	0.119318182	0.013461538	0.065789474	0.3125
Location #4	0.198863636	0.017307692	0.013157895	0.0625

- Checking for consistency:

$\lambda =$ 0.5099

CI = -1.163366667

RI = 0.9

CR = -1.29263 less than 0.1, the consistency of the matrix is considered acceptable

For produce concentration:

Table B.5: Pairwise comparison matrix [C] for the alternatives with respect to produce concentration.

	Location #1	Location #2	Location #3	Location #4	Priority
Location #1	1	5	7	3	0.541029911
Location #2	0.2	1	3	9	0.260586935
Location #3	0.142857143	0.333333333	1	5	0.126003726
Location #4	0.333333333	0.111111111	0.2	1	0.072379429

- Normalizing the matrix [C] by dividing each element in every column by the sum of that column.

Table 0B.6: Normalizing of the pairwise comparison matrix[C].

	Location #1	Location #2	Location #3	Location #4
Location #1	0.596590909	0.775862069	0.625	0.166666667
Location #2	0.119318182	0.155172414	0.267857143	0.5
Location #3	0.085227273	0.051724138	0.089285714	0.277777778
Location #4	0.198863636	0.017241379	0.017857143	0.055555556

- Checking for consistency:

λ = 0.462075

CI = -1.179308333

RI = 0.9

CR = -1.31034 less than 0.1, the consistency of the matrix is considered acceptable

For beef concentration:

Table 0B.7: Pairwise comparison matrix [C] for the alternatives with respect to beef concentration.

	Location #1	Location #2	Location #3	Location #4	Priority
Location #1	1	3	3	5	0.4718249
Location #2	0.333333333	1	7	3	0.317405686
Location #3	0.333333333	0.142857143	1	3	0.137180404
Location #4	0.2	0.333333333	0.333333333	1	0.07358901

- Normalizing the matrix [C] by dividing each element in every column by the sum of that column.

Table B.8: Normalizing of the pairwise comparison matrix[C].

	Location #1	Location #2	Location #3	Location #4
Location #1	0.535714286	0.670212766	0.264705882	0.416666667
Location #2	0.178571429	0.223404255	0.617647059	0.25
Location #3	0.178571429	0.031914894	0.088235294	0.25
Location #4	0.107142857	0.074468085	0.029411765	0.083333333

- Checking for consistency:

λ = 0.52985

CI = -1.156716667

RI = 0.9

CR = -1.28524 less than 0.1, the consistency of the matrix is considered acceptable

For chicken and egg concentration:

Table 0B.9: Pairwise comparison matrix [C] for the alternatives with respect to chicken and egg concentration.

	Location #1	Location #2	Location #3	Location #4	Priority
Location #1	1	7	5	5	0.519103438
Location #2	0.142857143	1	9	7	0.289521515
Location #3	0.2	0.111111111	1	7	0.139782226
Location #4	0.2	0.142857143	0.142857143	1	0.051592821

- Normalizing the matrix [C] by dividing each element in every column by the sum of that column.

Table 0B.10: Normalizing of the pairwise comparison matrix[C].

	Location #1	Location #2	Location #3	Location #4
Location #1	0.648148148	0.848076923	0.330188679	0.25
Location #2	0.092592593	0.121153846	0.594339623	0.35
Location #3	0.12962963	0.013461538	0.066037736	0.35
Location #4	0.12962963	0.017307692	0.009433962	0.05

- Checking for consistency:

λ = 0.4816

CI = -1.1728

RI = 0.9

CR = -1.30311 less than 0.1, the consistency of the matrix is considered acceptable

For milk concentration:

Table B.11: Pairwise comparison matrix [C] for the alternatives with respect to milk concentration.

	Location #1	Location #2	Location #3	Location #4	Priority
Location #1	1	7	3	5	0.494652406
Location #2	0.142857143	1	9	5	0.299966578
Location #3	0.333333333	0.111111111	1	5	0.150122549
Location #4	0.2	0.2	0.2	1	0.055258467

- Normalizing the matrix [C] by dividing each element in every column by the sum of that column.

Table 0B.12: Normalizing of the pairwise comparison matrix[C].

	Location #1	Location #2	Location #3	Location #4
Location #1	0.596590909	0.842245989	0.227272727	0.3125
Location #2	0.085227273	0.120320856	0.681818182	0.3125
Location #3	0.198863636	0.013368984	0.075757576	0.3125
Location #4	0.119318182	0.024064171	0.015151515	0.0625

- Checking for consistency:

λ = 0.5054

CI = -1.164866667

RI = 0.9

CR = -1.2943 less than 0.1, the consistency of the matrix is considered acceptable

For pork concentration:

Table B.13: Pairwise comparison matrix [C] for the alternatives with respect to pork concentration.

	Location #1	Location #2	Location #3	Location #4	Priority
Location #1	1	7	5	3	0.496260126
Location #2	0.142857143	1	9	7	0.32333441
Location #3	0.2	0.111111111	1	3	0.103070706
Location #4	0.333333333	0.142857143	0.333333333	1	0.077334758

- Normalizing the matrix [C] by dividing each element in every column by the sum of that column.

Table 0B.14: Normalizing of the pairwise comparison matrix[C].

	Location #1	Location #2	Location #3	Location #4
Location #1	0.596590909	0.848076923	0.326086957	0.214285714
Location #2	0.085227273	0.121153846	0.586956522	0.5
Location #3	0.119318182	0.013461538	0.065217391	0.214285714
Location #4	0.198863636	0.017307692	0.02173913	0.071428571

- Checking for consistency:

λ = 0.503775

CI = -1.165408333

RI = 0.9

CR = -1.2949 less than 0.1, the consistency of the matrix is considered acceptable

For air concentration:

Table 0B.15: Pairwise comparison matrix [C] for the alternatives with respect to air concentration.

	Location #1	Location #2	Location #3	Location #4	Priority
Location #1	1	5	1	1	0.33579244
Location #2	0.2	1	3	9	0.339273873
Location #3	1	0.333333333	1	5	0.217257958
Location #4	1	0.111111111	0.2	1	0.107675729

- Normalizing the matrix [C] by dividing each element in every column by the sum of that column.

Table 0B.16: Normalizing of the pairwise comparison matrix[C].

	Location #1	Location #2	Location #3	Location #4
Location #1	0.3125	0.775862069	0.192307692	0.0625
Location #2	0.0625	0.155172414	0.576923077	0.5625
Location #3	0.3125	0.051724138	0.192307692	0.3125
Location #4	0.3125	0.017241379	0.038461538	0.0625

- Checking for consistency:

λ = 0.73685

CI = -1.087716667

RI = 0.9

CR = -1.20857 less than 0.1, the consistency of the matrix is considered acceptable

References

[1] A. D. Visscher, *Air Dispersion Modeling: Foundations and Applications*. Hoboken, New Jersey: Wiley, 2013.

[2] J.-M. Guldmann and D. Shefer, *Industrial Location and Air Quality Control: A Planning Approach*. New York: John Wiley & Sons Inc, 1980.

[3] T. Cai, S. Wang, and Q. Xu, "Monte Carlo optimization for site selection of new chemical plants," *J. Environ. Manage.*, vol. 163, pp. 28–38, Nov. 2015.

[4] D. H. F. Liu and B. G. Liptak, Eds., *Air Pollution*. Boca Raton: CRC Press, 1999.

[5] K. Wark, C. F. Warner, and W. T. Davis, *Air Pollution: Its Origin and Control*, 3 edition. Menlo Park, Calif: Prentice Hall, 1997.

[6] F. Mehdizadeh and H. S. Rifai, "Modeling point source plumes at high altitudes using a modified Gaussian model," *Atmos. Environ.*, vol. 38, no. 6, pp. 821–831, Feb. 2004.

[7] K. J. James, M. Cherry, and M. A. Stack, "Assessment of chemical plant emissions on an urban environment: A new approach to air quality measurements," *Chemosphere*, vol. 31, no. 7, pp. 3741–3751, Oct. 1995.

[8] Y. Zhou, J. I. Levy, J. K. Hammitt, and J. S. Evans, "Estimating population exposure to power plant emissions using CALPUFF: a case study in Beijing, China," *Atmos. Environ.*, vol. 37, no. 6, pp. 815–826, Feb. 2003.

[9] U. E. N. C. for E. Assessment, "Good practice guide for atmospheric dispersion modelling: 2. Which dispersion model to use?," 15-Mar-2009. [Online]. Available: https://hero.epa.gov/hero/index.cfm/reference/details/reference_id/2325113. [Accessed: 26-Feb-2016].

[10] A. Okubo and S. A. Levin, “A Theoretical Framework for Data Analysis of Wind Dispersal of Seeds and Pollen,” *Ecology*, vol. 70, no. 2, pp. 329–338, 1989.

[11] J. M. Stockie, “The Mathematics of Atmospheric Dispersion Modeling.,” *SIAM Rev.*, vol. 53, no. 2, pp. 349–372, 2011.

[12] J. J. Peirce, P. A. Vesilind, and R. Weiner, *Environmental Pollution and Control*, 4 edition. Butterworth-Heinemann, 1998.

[13] D. B. Turner, *Workbook of Atmospheric Dispersion Estimates: Second Edition*, 2nd ed. edition. Boca Raton: CRC Press, 1994.

[14] D. G. Steyn and S. Trini Castelli, Eds., *Air Pollution Modeling and its Application XXI*. Dordrecht: Springer Netherlands, 2012.

[15] S. Shewchuk, H. Guo, and Xing, “The use of air quality dispersion models for validation of operational setback distances near intensive livestock operations,” Confidential Report for Environment Canada, 2006.

[16] M. El-Harbawi, “Air quality modelling, simulation, and computational methods: a review,” *Environ. Rev.*, vol. 21, no. 3, pp. 149–179, May 2013.

[17] *User’s Guide for the AMS/EPA Regulatory Model--AERMOD.* U.S. Environmental Protection Agency, Office of Air Quality Planning and Standards, Emissions, Monitoring, and Analysis Division, 2004.

[18] K. S. Bhardwaj, “Examination of Sensitivity of Land Use Parameters and Population on the Performance of the AERMOD Model for an Urban Area,” University of Toledo, 2005.

[19] Y. Xing, H. Guo, J. Feddes, Z. Yu, S. Shewchuck, and B. Predicala, “Sensitivities of Four Air Dispersion Models to Climatic Parameters for Swine Odor Dispersion,” *Trans. ASABE*, vol. 50, no. 3, pp. 1007–1017, 2007.

[20] O. US EPA, “National Ambient Air Quality Standards (NAAQS) | Technology Transfer Network | US EPA.” [Online]. Available: http://www3.epa.gov/ttn/naaqs/criteria.html. [Accessed: 26-Feb-2016].

[21] R. Becker and V. Henderson, “Effects of Air Quality Regulations on Polluting Industries,” *J. Polit. Econ.*, vol. 108, no. 2, pp. 379–421, 2000.

[22] W. B. Gray, “Manufacturing Plant Location: Does State Pollution Regulation Matter?,” National Bureau of Economic Research, Working Paper 5880, Jan. 1997.

[23] L. F. Lira-Barragán, J. M. Ponce-Ortega, M. Serna-González, and M. M. El-Halwagi, “An MINLP Model for the Optimal Location of a New Industrial Plant with Simultaneous Consideration of Economic and Environmental Criteria,” *Ind. Eng. Chem. Res.*, vol. 50, no. 2, pp. 953–964, Jan. 2011.

[24] J. Fliege, “OLAF – A general modeling system to evaluate and optimize the location of an air polluting facility,” -*Spektrum*, vol. 23, no. 1, pp. 117–136, Feb. 2001.

[25] N. García-Chan, L. J. Alvarez-Vázquez, A. Martínez, and M. E. Vázquez-Méndez, “On optimal location and management of a new industrial plant: Numerical simulation and control,” *J. Frankl. Inst.*, vol. 351, no. 3, pp. 1356–1371, Mar. 2014.

[26] H. A. Stafford, “Environmental Protection and Industrial Location,” *Ann. Assoc. Am. Geogr.*, vol. 75, no. 2, pp. 227–240, 1985.

[27] J.-M. Guldmann and D. Shefer, “Optimal plant location and air quality management under indivisibilities and economies of scale,” *Socioecon. Plann. Sci.*, vol. 11, no. 2, pp. 77–93, 1977.

[28] P. E. Murillo-Alvarado, J. M. Ponce-Ortega, M. M. El-Halwagi, and J. G. Segovia-Hernandez, “Optimal integration of gaseous emissions from new industrial plants with the surroundings,” *Clean Technol. Environ. Policy*, vol. 15, no. 1, pp. 93–110, May 2012.

[29] R. E. Kohn, “Industrial Location and Air Pollution Abatement*,” *J. Reg. Sci.*, vol. 14, no. 1, pp. 55–63, Apr. 1974.

[30] J. R. Taylor, A. Hasegawa, and L. A. Chambers, “Control of air pollution by site selection and zoning,” *Monogr. Ser. World Health Organ.*, vol. 46, pp. 293–306, 1961.

[31] T. Jeppesen, J. A. List, and H. Folmer, “Environmental Regulations and New Plant Location Decisions: Evidence from a Meta-Analysis,” *J. Reg. Sci.*, vol. 42, no. 1, pp. 19–49, Feb. 2002.

[32] A. Levinson, “Environmental regulations and manufacturers’ location choices: Evidence from the Census of Manufactures,” *J. Public Econ.*, vol. 62, no. 1–2, pp. 5–29, Oct. 1996.

[33] V. D. McConnell and R. M. Schwab, “The Impact of Environmental Regulation on Industry Location Decisions: The Motor Vehicle Industry,” *Land Econ.*, vol. 66, no. 1, pp. 67–81, 1990.

[34] J. A. List, W. W. McHone, and D. L. Millimet, “Effects of air quality regulation on the destination choice of relocating plants,” *Oxf. Econ. Pap.*, vol. 55, no. 4, pp. 657–678, Oct. 2003.

[35] USEPA. 2005, “Human Health Risk Assessment Protocol for Hazardous Waste Combustion Facilities.” Office of Solid Waste and Emergency Response (5305W), September.

[36] [Online]. Available: https://www3.epa.gov/air/tribal/WETG/wetg2014/indian-policy_1984.pdf. [Accessed: 26-Mar-2016].

[37] M. Cashmore, “The role of science in environmental impact assessment: process and procedure versus purpose in the development of theory,” *Environ. Impact Assess. Rev.*, vol. 24, no. 4, pp. 403–426, May 2004.

[38] O. Timothy and W. R. D. Sewell, “Project appraisal and policy review / edited by Timothy O’Riordan and W. R. Derrick Sewell,” *ResearchGate*.

[39] J. Petts, *Handbook of Environmental Impact Assessment: Volume 2: Impact and Limitations*. John Wiley & Sons, 2009.

[40] R. T. Burnett, J. Brook, T. Dann, C. Delocla, O. Philips, S. Cakmak, R. Vincent, M. S. Goldberg, and D. Krewski, “Association between particulate- and gas-phase components of urban air pollution and daily mortality in eight Canadian cities,” *Inhal. Toxicol.*, vol. 12 Suppl 4, pp. 15–39, 2000.

[41] G. C. Pratt, M. Dymond, K. Ellickson, and J. Thé, “Validation of a novel air toxic risk model with air monitoring,” *Risk Anal. Off. Publ. Soc. Risk Anal.*, vol. 32, no. 1, pp. 96–112, Jan. 2012.

[42] “Law Document English View,” *Ontario.ca*. [Online]. Available: http://www.ontario.ca/laws/view. [Accessed: 27-Feb-2016].

[43] A. Masuraha, “Evaluation of the AERMOD Model and Examination of Required Length of Meteorological Data for Computing Concentrations in Urban Areas,” University of Toledo, 2006.

[44] US. EPA, *User’s guide for the AMS/EPA regulatory modelAERMOD*. Office of Air Quality Planning and Standards Emissions, Monitoring, and Analysis Division.

[45] O. US EPA, “Mercury Study Report to Congress.” [Online]. Available: http://www.epa.gov/mercury/mercury-study-report-congress. [Accessed: 27-Feb-2016].

[46] U.S. EPA, “Exposure Factors Handbook. OHEA. Exposure Assessment Group.,” 1990. .

[47] U.S. EPA, “Revised Draft Guidance for Performing Screening Level Risk Analyses at Combustion Facilities Burning Hazardous Wastes. Attachment C, Draft Exposure Assessment Guidance for RCRA Hazardous Waste Combustion Facilities.,” 1994. [Online]. Available: http://nepis.epa.gov/Exe/ZyNET.exe/10000TC3.TXT?ZyActionD=ZyDocument&Client=EPA&Index=1991+Thru+1994&Docs=&Query=&Time=&EndTime=&SearchMethod=1&TocRestrict=n&Toc=&TocEntry=&QField=&QFieldYear=&QFieldMonth=&QFieldDay=&IntQFieldOp=0&ExtQFieldOp=0&XmlQuery=&File=D%3A%5Czyfiles%5CIndex%20Data%5C91thru94%5CTxt%5C00000010%5C10000TC3.txt&User=ANONYMOUS&Password=anonymous&SortMethod=h%7C-&MaximumDocuments=1&FuzzyDegree=0&ImageQuality=r75g8/r75g8/x150y150g16/i425&Display=p%7Cf&DefSeekPage=x&SearchBack=ZyActionL&Back=ZyActionS&BackDesc=Results%20page&MaximumPages=1&ZyEntry=1&SeekPage=x&ZyPURL. [Accessed: 31-Mar-2016].

[48] *Estimating Exposure to Dioxin-like Compounds: Review Draft*. U.S. Environmental Protection Agency, Office of Health and Environmental Assessment, Exposure Assessment Group, 1994.

[49] T. L. Saaty, *The Analytic Hierarchy Process: Planning, Priority Setting, Resource Allocation*. McGraw-Hill, 1980.